The Pennsylvania State University
The Graduate School

DATA ANALYSIS AND SYSTEM IDENTIFICATION ALGORITHMS FOR BEHAVIORAL DYNAMICAL MODELING

A Dissertation in
Electrical Engineering and Computer Science
by
Sahar Hojjatinia

Submitted in Partial Fulfillment
of the Requirements
for the Degree of

Doctor of Philosophy

December 2022

The dissertation of Sahar Hojjatinia was reviewed and approved by the following:

Constantino M. Lagoa
Professor of Electrical Engineering
Dissertation Advisor
Chair of Committee

David E. Conroy
Professor of Kinesiology and Human Development & Family Studies and Public Health Sciences

Vishal Monga
Professor of Electrical Engineering

Minghui Zhu
Associate Professor of Electrical Engineering

Tom La Porta
Professor and Department Head of Electrical Engineering

Abstract

In the past few years, the development and advancements in new sensing technologies and wearable activity monitors have enabled the collection of high frequency individual data. This opens the exciting opportunity of identifying the relation between different variables and modeling the dynamic responses of the output to input variables. Such models then can be used in designing and developing targeted adaptive micro-treatments that use collected data to determine which is the best treatment option and when it should be delivered.

However, there are significant challenges in the analysis of this type of data. First, due to the high rate of data collection, it can no longer be assumed that the input or the micro-intervention only has an instantaneous effect on the output; there are also some delayed effects. Moreover, such data frequently suffers from data fragmentation, i.e., poor placement of sensors, non-wear of the data collecting device and/or external disturbances that can lead to intervals of time where the data collected is not reliable, that is missing or corrupted.

Literature in behavioral medicine, a multidisciplinary field focusing on health aspects of biological, behavioral, psychological, and social sciences have shown that a variety of medical and mental health conditions can be prevented or treated if intervened before or in early stages of the condition. For example, studies have shown a relationship between physical inactivity and a large range of diseases such as cardiovascular and metabolic diseases, etc. As another example, cigarette smoking is the leading preventable cause of death in the United States, responsible for about one in five deaths annually, with the yearly medical and economic burden of more than $300 billion.

The availability of large amounts of intensive longitudinal data and the limitation of currently used methods for analyzing such data has been the motivation behind this work. The main objective of this dissertation has been to deal with such challenges by leveraging concepts from the areas of control systems engineering, dynamical models, machine learning, and signal processing, and the application of these tools and techniques in modeling the human behavior. To achieve this goal, the main focus was to develop different algorithms and tools to identify models that consider the delayed effects of inputs and output and are capable of handling the fragmented data. Finally, the standard algorithms used and the developed ones were implemented and applied to identify the models describing the relation between different variables and analyze health problems in behavioral medicine.

The drawbacks of system identification methods mostly used in literature and the efficiency of the atomic norm minimization technique in identifying parsimonious models

from experimental data have motivated us to develop novel identification algorithms that consider sparsity using the atomic norm concept, in addition to using and implementing some of the standard algorithms. That is, by developing parsimonious model identification algorithms, we seek to identify models that provide a desired explanation of the data with as few parameters as possible.

As an application of the algorithms used or developed in this dissertation, we identified personalized dynamic models of physical activity in response to digital messaging interventions to promote physical activity and reduce sedentary behavior. Identified switched system parameters provide the basis to tailor decision rules that can be used for future just-in-time adaptive interventions. Additionally, we proposed a new methodology to identify relation between stress and smoking considering sparsity. This is most important at the moments preceding and following the smoking episodes since it provides the basis for designing person-specific, tailored smoking cessation interventions from the parameters linking vulnerable moments to intervention decisions in the future works. As another project, a time-varying version of logistic regression model in combination with regularized l1-norm, to induce sparsity, is developed to identify the models that best describe the dynamics of the data and can predict the future outcomes.

Table of Contents

List of Figures

List of Tables

List of Symbols

Variables

y	Output variable
u	Input variable
$\hat{y}$	Predicted output variable
r	Residual which is the difference between the true and predicted outputs
h	Impulse response
y_{input}	Output of the system related to the input response (zero state)
y_{int}	Output of the system related to the intrinsic response (zero input)
c_{input}	Constants related to the input response
c_{int}	Constants related to the intrinsic response
p	Poles of the system
p^*	Complex conjugate of p

Operations

$h * u$	Convolution of h and u

Norm

$\|t\|_0$	0-pseudo norm of a vector t
$\|t\|_1$	1-norm of a vector t

Miscellaneous

$\mathbb{R}$	Set of the real numbers
ϵ	Noise

CI	Confidence interval
μ	Mean
σ	Standard Deviation, Sigmoid function
$p(y\|x)$	Conditional probability of $y = 1$ given x
η^2	Effect sizes for the two-way repeated measures ANOVA and Kendall's W for the Friedman's Test
α	Scaling factor
δ	Error term
Σ	Covariance matrix

Abbreviated terms

SS	Steady state that is defined as the ultimate amount of the cumulative step response
RT	Rise time; time that it takes for the cumulative step response to advance from 10% to 90% of the steady state
ST	Settling time; time that the step response enters a boundary around the steady state with the upper- and lower bounds being 95% and 105% of the steady state
EfT	Effective time; the duration that the system response is above the noise level (outside the error bounds)
$InDel$	Initial delay; latency to initiate a momentary response
$PMag$	Peak magnitude; time that it takes for an input to start having a momentary effect
$PDel$	Peak delay; maximum momentary effect
M	Mean
SD	Standard Deviation
Mdn	Median
GED	General Educational Development
SE	Standard Error

Acknowledgments

It is with great gratitude to thank my advisor, Dr. Constantino Lagoa for his support and help. It was my pleasure and honor to work with him. He has inspired and motivated me to go through the unknowns and find my way. I deeply thank him for the continuous support of my PhD study and research.

I would like to thank members of my dissertation committee, Dr. David Conroy, Dr. Vishal Monga and Dr. Minghui Zhu for their time, support, and reviewing my dissertation. I would especially like to thank Dr. David Conroy for his support in our collaborative projects.

I would like to thank our collaborators in Sense2Stop study whom acquired the data and provided some of the software. Specifically, I would like to thank Dr. Bonnie Spring, Dr. Inbal Nahum-Shani, Dr. Santosh Kumar, Dr. Timothy Hnat, Dr. Syed Monowar Hossain, Shahin Alan Samiei, and Elyse Daly. I would also like to thank Dr. David Conroy and Deborah Brunke-Reese for data acquisition and Dr. Sarah Hojjatinia for developing some software for the Random AIM project.

My sincere thanks also goes to my family for their always support, encouragement, and love both from close and apart; my amazing parents, Zahra and Reza who did anything and everything for me just to be happy, fulfilled, and successful, my wonderful sisters Setareh and Sarah who this journey and achievement would have been impossible without them, and my best friend Samira who is like a sister to me. Thank you for being so supportive, considerate, encouraging, loving and always by my side. My special thanks goes to the most precious person in my life, Sarah, who went above and beyond to support me with her strength, passion, insight, and love.

Funding Acknowledgment and Disclaimer The project described was supported by the National Center for Advancing Translational Sciences, National Institutes of Health, through Grant UL1 TR002014 and Grant UL1 TR00045, the National Heart, Lung and Blood Institute, National Institutes of Health, through Grant R01 HL142732, the National Institute of Biomedical Imaging and Bioengineering, National Institutes of Health, through Grant U54 EB020404, and the National Science Foundation through Grant ECCS 1808266. The content is solely the responsibility of the authors and does not necessarily represent the official views of the NIH or the NSF.

Dedication

To my wonderful sisters Sarah and Setareh.

Chapter 1
Introduction

This dissertation presents techniques and methodologies extended or developed using tools from control systems engineering for identifying dynamical models and investigating the connection between different variables in behavioral medicine applications. In this regard, system identification approaches are modified to incorporate the time-varying effects of the variables on person-specific level. In the following, a general background and motivation for this work, a brief description of each chapter, and the contribution and outline of each is provided.

1.1 Intensive longitudinal data

Techniques used by clinical and behavioral scientists for designing treatments and interventions have been mostly based on static models since the behavioral data available has been usually not intensive. Behavioral data has been usually non-intensive because patients have been contacted infrequently and/or the data collection has been limited to the clinical visit intervals.

In the past few years, the development of new technologies such as cameras and cell phones, and advances in sensing and wearable devices such as activity trackers and health monitors have enabled the collection of large amounts of intensive longitudinal personal data. This opens the exciting opportunity of identifying the relation between the variables and modeling the dynamic responses of the output to input variables. Such models then can be used in designing and developing targeted adaptive micro-treatments that use collected data to determine which is the best treatment option and when it should be delivered.

This revolution in technology means that high frequency data can now be passively collected on many aspects of the status of an individual. One can collect data on

health behaviors such as physical activity [1, 2], eating [3], alcohol consumption and smoking [4–7], biological quantities such as heart rate, ECG, blood oxygen, respiration rate, and glucose [8], mood and stress [9, 10], location, social environment and social contacts [11–14]. Having access to such data, and using powerful tools that can extract information from them can provide valuable insight on the responses of individuals under different conditions or to interventions. Such insights then can be used for tailoring treatments that can be instantly delivered using devices such as cell phones.

Human behavior is a dynamic concept. As a matter of fact, even traditional clinicians/behavioral scientists consider the current state of the patient/participant and their responses to the past treatments in order to choose a proper treatment. That is, they practically incorporate the dynamics of the behavior change into the current treatment decision. Although they use non-intensive data for such treatment decisions, this represents the importance of considering dynamics of the behavior change and past treatment effects into current decision. At this time, the ability to collect intensive longitudinal data provides the opportunity to incorporate the dynamics of behavior change into the models describing the behavior that is one of the main focuses in this dissertation.

Intensive longitudinal data, like the ones mentioned above, are very different from the data collected in "traditional studies" and cannot, in our view, be fully exploited and analyzed using the tools that are currently available to behavioral scientists. First, data on an individual can now be collected every day, every hour or even every minute. Therefore, the traditional assumption that the input at time t only has a possible effect on the output at time t is now testable. But, to do that, a framework is needed that allows for modeling "memory effect"; i.e., a framework that can model the fact that an input can have a delayed (shifted in time or lagged) effect, where it might have an immediate influence on the output as well as an effect on future outputs. For example, a stress event might not only have an immediate effect on increasing the probability of smoking, but it can also have a lingering effect that increases the smoking odds for some time instances following that stress event [15].

Moreover, such a framework should not impose predetermined values for the lags in the effects of the inputs. In literature, there has been some attempts to extend existing approaches in order to deal with these delayed effects such as use of lags in multilevel models [16–18]. However, these approaches only consider models with a "rigid structure" like fixed lags and do not allow for complex input responses. Moreover, there is limited interpretation of the dynamic characteristics of the models obtained.

Second, intensive longitudinal data is often fragmented; i.e., it is common to have many time instants with no measurements or unreliable ones. For example, in the study [19], events such as physical activity or incorrect placement of sensors confound estimates of stress resulting in fragmented information across the day on its probability estimates. Moreover, in studies using wearable devices, data fragmentation can occur due to non-wear, sensor malfunction, syncing errors, etc. [20].

1.2 Dynamical System Modeling

1.2.1 System Identification

System identification is a central concept in control systems engineering that identifies the mathematical model describing how the inputs affect the output given some a priori information. Common system identification approaches are *parametric methods* and *non-parametric methods* [21–23]. Parametric methods identify systems with underlying mathematical structure associated with the model coefficients or parameters while non-parametric methods rely directly of system's response to model it.

For example, for linear systems, a method to obtain the transfer function of a system is a parametric method where the parameters are the coefficients of numerator and denominator of the transfer function and the system's order has to be predefined. On the other hand, a method to obtain the impulse response, step response, or the frequency response of a system with no specific parameter structure, belongs to non-parametric methods [24, 25].

Set membership and *subspace identification* methods are two widely used categories of the non-parametric methods. Although set membership methods provide a bound on the worst-case identification error, they often lead to high order models and the potential model order reduction step might not always work well. Subspace identification is a more recent, computationally attractive method that can handle unknown initial conditions and force a bound on the model order [26]. However, these methods require large datasets to identify accurate models and deal with the whole dataset at once which makes it hard to design recursive algorithms. Moreover, they are not suitable for enforcing model consistency with a priori information such as bounds on the time constants, approximate pole locations, etc.

More recent methods tend to promote low complexity as an a priori to solve the optimization problem. Taking advantage of both set membership and subspace identi-

fication methods, the new methods tend to find the most parsimonious model from a set of potential models that meet the problem criteria [27–29]. Identifying parsimonious (lower order) models has been a non-convex problem (with the existence of local minima) and led to investigating potential relaxations. Although these methods usually work well in practice, they might not be computationally efficient and there is no guarantee that they provide the simplest model.

1.2.2 Sparse Models

Solving the problem of identifying parsimonious models (estimating the model coefficients describing the dynamics of input and output) from experimental data has led to much recent work. The non-convex nature of this problem has directed the proceeding approaches to consider relaxations such as Group Lasso or nuclear norm minimization [30, 31]. The difficulty of computational complexity and no guarantee for identifying simplest model representing the data in these methods has led to a new approach called atomic norm minimization [32].

This technique represents the response of a linear time-invariant system as a linear combination of suitably chosen objects or atoms [33, 34]. Atomic norm minimization results in efficient identification of sparse models from experimental data, avoids the regularization steps, and incorporates stability constraints automatically [35, 36].

The drawbacks of the system identification methods mentioned above and the efficiency of the atomic norm minimization technique have motivated us to develop a novel identification algorithm that considers sparsity using the atomic norm concept, and this method would belong to non-parametric identification methods [37]. Therefore, to identify the dynamical models, we use concepts from control systems engineering and sparse signal reconstruction to develop tools for parsimonious modeling of interactions between intensive longitudinal data streams. In other words, by developing a new parsimonious model identification algorithm, we seek to identify models that provide a desired explanation of the data with as few parameters as possible.

1.2.3 State of the Art in Behavioral Medicine and Sciences

High frequency data, which is also defined by volume, velocity, and variety [38], makes it possible (a) identify the mathematical model representing the relation between different variable over time (b) to detect and predict the moments of vulnerability, opportunity, and receptivity and (c) to design efficient intervention programs in order to promote a

good habit or activity and reduce a risk or negative effect when it is needed.

It has been suggested that vulnerable states are dynamic processes that incorporate static and episodic factors; i.e., influences that can change over time [39]. Just-in-Time Adaptive interventions (JITAIs) are an emerging type of adaptive interventions capable of administering adaptive treatments in terms of type, timing, and intensity by monitoring individual's behavior changes using intensive longitudinal data including ecological momentary assessments (EMAs).

Behavioral JITAIs have three key features including providing the support in real time when the individuals are at risk of engaging in a negative health behavior or have the opportunity to engage in a positive one, adapting the timing and content of the support according to collected data like location of the user, and triggering the support by the system, not necessarily based on users' feedback [39]. The third feature is the one that distinguishes JITAIs from "just-in-time" interventions. That is, using sensors in the system to collect person-level data in addition to the EMAs provides the opportunity for adaptation and triggering the support dynamically [40]. These three features that represent the ability of JITAIs to detect and deliver support at the right "moment" has led them to be implemented in various health related concerns such as physical activity [41], stress management [42], fluid consumption [43], weight loss [44], sun protection [45], addiction [46], and smoking cessation [47] among others.

As a specific example, [48] developed a smartphone behavioral intervention called FOCUS that can provide illness management support to individuals with schizophrenia. In this platform, four components of a JITAI that are decision points, intervention options, tailoring variables, and decision rules are as follows: (1) intervention decisions were made after each random prompt for self-report (if the individual did not respond to a prompt, it was interpreted as being not receptive and no decision was made); (2) intervention options consisted of recommendation on self-management techniques, and feedback and positive reinforcements; (3) tailoring variables were obtained via active assessments or EMAs by sending prompts three times a day to self-report; and (4) each decision point corresponds to a decision rule and the value of the tailoring variables determined the intervention options.

Although JITAIs use longitudinal data, decision rules for an intervention are mostly tailored on less frequent data from, for example, self-reports. This leads to making specific assumptions about the change between assessments or the latency of predictions. Furthermore, JITAIs require large amounts of data, usually aggregated from all the participants to be able to develop a decision rule. Moreover, to the best of our knowledge,

they do not take into account the "memory effect" of the tailoring variables.

In this dissertation, we address these limitations by identifying dynamical models that are person-specific algorithms developed using high frequency sensor data. Applying these methods, "memory effect" is considered to provide decision rules considering not only the present moment of the tailoring variables but also their past moments that might lead to an event. As an example, if we want to investigate the effect of stress, our aim is to identify person-specific dynamic models of smoking responses to stress. In this context, the tailoring variable is stress collected by high frequency sensors and decision points are the moments that stress level leads to smoking (considering the past and present moments of stress).

One method used in literature to analyze the time-varying relations between longitudinal variables is multilevel modeling of time-varying relations [49]. Multilevel modeling (MLM) is an analytical method for analyzing intensive longitudinal data with time-varying and time-invariant covariates and an extension of traditional regression models that can handle within- and between-individual effects in the same model [50–52]. MLM addresses the limitation of traditional analysis techniques like analysis of covariance that aggregate data over time (e.g. repeated measures analysis of variance) and explores the effect of time-varying covariates as within- and between-person effects [50]. Computation of the within-person effect can be done by creating a series of deviation scores from a personal average on the covariate. Therefore, the average amount of changes in an output associated with momentary deviation from a personal mean is represented by the effect of a time-varying covariate. While multilevel modeling provides a basis and is extendable to analyze time-varying effects (see [49] for time-varying association between physical activity and affect), it is limited to simple change patterns that can be modeled with a relatively few parameters; e.g., linear or quadratic trends, or it becomes complicated in terms of implementation and interpretation.

In general, although multilevel modeling is useful for studying developmental processes, they are not ideal in modeling longitudinal data concerning daily affective, symptom measurements, or affective ratings in an observational study [16]. For such data, there is an interest in the dynamics of a stationary process, i.e., changes in the process over time but not as a function of time. Multilevel autoregressive model can be used to handle this kind of data. Using this approach, the individual- and population-level autoregressive coefficients provide an overall description of the dynamic process for an individual and the average dynamic pattern, respectively [53]. Even though multilevel autoregressive model considers the effect of previous data points on the later data points to model the process,

the first- and second-order models (i.e., considering only one or two lags) have usually been used in the studies [17, 18]. Additionally, when using this technique, the order of the model has to be predetermined. The dynamical system modeling approach developed in later chapters of this dissertation is capable of identifying how far to look back in time automatically. Moreover, multilevel modeling cannot leverage the interpretation tools that are provided via dynamical system modeling.

Time-varying effect model (TVEM) can address the limitation of MLM model on the simplicity of change patterns, since the shape of modeled relation does not require an a priori constraint and it only assumes a smooth pattern of change [54, 55]. TVEMs are statistical approaches and extensions of linear regression models with the main difference being the model coefficients. That is, TVEMs estimate regression coefficients (i.e., intercepts and slopes) as flexible, nonparametric functions of time [56]. Success of TVEM in handling the challenges of EMA data and determining the time-varying effects has led it to be used in variety of behavioral and psychological science researches to explore the relation between smoking, drinking, marijuana, and physical activity, and various covariates such as depression, stress, age affect, and behavioral cognitions over time [54, 57–64].

Although TVEM predicts the regression coefficients and allows the coefficients to be nonlinear functions of time, it has four limitations: (1) TVEM might not be able to capture the unknown, latent variables that are also related to the output [65]. In other words, as TVEM is extended from a generalized linear model, it cannot determine more complex underlying within-time associations [66] and is limited to contemporaneous relations in a single model. Similar to MLM, one can run multiple models to examine lagged associations, but that is not part of the core model. Tools applied from control systems engineering can fill this gap by incorporating the delayed effect of tailoring variables in the model.

(2) TVEM requires a meaningful zero point. This works fine in intervention-based approaches or when age or some developmental transition provide the zero point, but it is more challenging with purely observational work outside of an intervention context. (3) TVEM does not include random effects and constrains all people to the same functional form. Dynamical models used in our work are not constrained by the equivalence across individuals. (4) The impact of missing data is unexplored using this technique [54]. The problem of missing data is handled effectively in our studies.

MixTVEM is a finite mixture version of TVEM that allows the population to have heterogeneous pattern of change [65]. Still, this model does not take into account

the "memory effect". Another extended version of TVEM is differential time-varying effect model (DTVEM) that is capable of identifying time lags and estimating these lags within a state-space framework [67]. To investigate, identify, and fit group-based vector autoregressive models of unknown lag structures, DTVEM combines some of smoothing and estimation tools for fitting generalized additive mixed models and state-space estimation routines. Although these capabilities make DTVEM more practical in comparison to TVEM, it still has two limitations. First, it requires the lag level to be predefined. Dynamical system modeling approach proposed in the later chapters of this work identifies the length of lagged effect automatically through solving the optimization problem. Second, similar to TVEM, DTVEM does not consider the person-specific differences in exploring time-varying associations, which is addressed in the current study.

To explore the dynamic characteristics of intensive longitudinal datasets that are in the form of time series, one approach is to analyze them in the context of stochastic differential equation models. These models are capable of extracting the key dynamics of dataset as well as providing a platform to relate them to different covariates [68,69]. Dynamic factor analysis models are another type of models that can describe the structure and time-lagged relationships of unobserved psychological concepts [70]. The limitation of standard dynamic factor analysis models is that they can only be used for stationary time series. In other words, all modeling parameters have to be constant for the entire study period. However, nonstationary data are prevalent in practical studies [71]. Additionally, these models require large amount of data that might not always be available. The required volume of data depends on a variety of factors such as the type of data and application, intended accuracy, size of the network, etc. Similarly, techniques like reinforcement learning methods require large datasets. This problem and their incapability in handling noisy data make these algorithms inappropriate for this kind of analysis [72].

1.2.4 Dynamical Modeling for Behavioral Data

In summary, although different models have been applied by researchers to study the behavior and substance consumption patterns of the individuals or groups of users due to different inputs over time, they all suffer from some limitations. In the approaches proposed in this dissertation, we address the limitations mentioned above by taking into account the following criteria: First, the algorithms provided can leverage intensive high frequency longitudinal data gathered from sensors and activity monitors, providing the opportunity to investigate a range of moments immediately leading up to and following an event.

Previous studies using intensive longitudinal data mostly relied on self-reports that might be too infrequent to capture and/or predict the moments of vulnerability, opportunity, and receptivity. Since mHealth tools and activity monitors provided the means to collect high frequency data, i.e., as frequent as every minute, existing analytic tools are not well-suited. Second, this study is based on the dynamic behavior changes of individuals. More precisely, we seek to identify the person-specific models describing the relation between different variables over time. Additionally, we consider the "memory effect" in the system modeling. In other words, dynamical modeling is done according to the concept that the output at a specific moment is not only related to the input at the present moment, but it also is connected to the past moments of both the input and the output.

Additionally, the factor of how far to look back in time is not an a priori constraint for most of the developed algorithms. This parameter is identified by the algorithm and may be different for each individual. Third, to the best of our knowledge, no study has practiced a systematic way of handling the missing data in the datasets. Existing literature only relies on planned missing data designs by planning for reducing the number of data points in time series as missingness, by blocking irregularly spaced data [73]. This work provides a novel tool to handle the fragmented data; i.e., intervals of proper measurements accompanied by intervals of missing data.

Next section provides a background on logistic regression model and the state of the art in this context. In chapter 6, we discuss a generalization of logistic regression, the problem formulation and results obtained.

1.3 A Brief Introduction to Logistic Regression

Discriminative modeling is one of the common statistical classification tools and is mainly used for supervised learning. Examples of these methods are logistic regression, k-nearest neighbors, SVMs, etc. Another main category of models in machine learning is generative models such as Naive Bayes, Bayesian Networks, Hidden Markov models, Auto-regressive models, etc., that can be applied to the same problem.

Comparing discriminative models to generative models from different perspectives, i.e., performance, missing data, and accuracy reveals that (1) generative models require fewer sample data to train the model since they are more biased and consider stronger assumptions like assumption of conditional independence. (2) Since discriminative models require all features to be observed, it cannot work well with the missing data i.e., unseen

data. In contrast, generative models can handle the missing data by marginalizing over the unseen variables. (3) In the case of violating the conditional independence assumption, the generative models are less accurate than the discriminative ones.

The advantages of discriminative methods and its application for our work, derived us to consider them for the analysis in this chapter. Although the developed model here is based on the concepts of logistic regression as a discriminative model, it is developed in a way to also address the limitations of such models. Developed model can provide the simplest possible model that fits the data. Additionally, it can handle the problem of missing data and data fragmentation by considering different chunks of data containing continuous intervals of observed data. Moreover, it can model the small amounts of data as well as large data sets.

Next, a background on logistic regression model, maximum likelihood estimation, and their assumptions and formulations is provided.

Considering the multiple logistic model of the form

$$E(y_i|x_{1i}, x_{2i}, \ldots, x_{ki}) = p(y_i|x_{1i}, x_{2i}, \ldots, x_{ki}) = \sigma(a + b_1 x_{1i} + \cdots + b_k x_{ki}), \tag{1.1}$$

since the logit model is nonlinear in the parameters, this model cannot be estimated using ordinary least squares. Instead, it relies on other methods to estimate its parameters. One approach that can be used is estimation by nonlinear least squares (NLS); but this technique is inefficient. That is, there are other estimation techniques with smaller variance. Nonlinear least squares estimates the parameters $a, b_1, \ldots, b_k$ by minimizing the sum of the squared residuals (similar to ordinary least squares)

$$\sum_{i=1}^{N} [y_i - \sigma(a + b_1 x_{1i} + \cdots + b_k x_{ki})]^2. \tag{1.2}$$

Although nonlinear least squares estimation is a consistent approach that produces estimates that are normally distributed in large samples, other methods like maximum likelihood estimation (MLE) are more efficient than NLS. The principles of MLE were first developed by Fisher in 1920s stating that the optimal probability distribution is the one that makes the observed data most likely. In other words, MLE estimates the unknown parameters choosing them such that the likelihood of model producing the sample observed is maximized [74, 75].

This probability is measured by means of the likelihood function, the joint probability distribution of the data. As maximum likelihood estimates are normally distributed

in large samples, statistical inference for coefficients in nonlinear models like Logistic regression can be made using the same tools that are used for linear regression models such as t-statistics and confidence intervals. Still, many inference methods in statistics such as chi-square test and modeling random effects are developed based on MLE.

MLE is a standard approach for approximating the parameters and inferring the statistic and it has four main optimal properties in estimation [76]: sufficiency (enough information on parameter of interest), consistency (asymptotic recovery of the true parameters), efficiency (estimating parameters with lowest variance asymptotically), and parameterization invariance (beyond the used parameterization, same MLE solution).

Study has shown that for analyzing clinical research data, methods such as artificial neural networks, support vector machines, decision trees, etc., are not superior to logistic regression [77]. One main difference between such methods and logistic regression is the approaches each take regarding the data. While logistic regression focuses on assumptions and theory, the methods mentioned above emphasized on models that automatically learn from the data.

1.3.1 Logistic Regression Model

In this section, a brief background on the basis and formulations of logistic regression model will be provided. Logistic regression expresses the relationship between a binary response variable/outcome or output and one or more independent variables called stimuli/predictors or inputs. The following assumptions have to be made in order to obtain the logistic regression model.

Assumption 1.1 This is assumed that we have a sample of m independent observations $(x^{(i)}, y^{(i)})$ where $i \in \{1, 2, \cdots, m\}$, and $X \in \mathbb{R}^{m \times n_x}$ and $Y \in \mathbb{R}^{m \times 1}$ include the input and output samples that can be represented as

$$X = \begin{bmatrix} x^{(1)} \\ x^{(2)} \\ \vdots \\ x^{(m)} \end{bmatrix}, Y = \begin{bmatrix} y^{(1)} \\ y^{(2)} \\ \vdots \\ y^{(m)} \end{bmatrix} \tag{1.3}$$

where n_x is the number of inputs/features, $x^{(i)} \in \mathbb{R}^{n_x}$, and $y^{(i)} \in \{0, 1\}$, denoting the value of the binary output variable.

Assumption 1.2 To find the probability model of Y given X, although we do not make a priory assumptions about the model, a primary assumption is that this model exists such that the conditional distribution of $y^{(i)}$ given $x^{(i)}$ is $p(y^{(i)}|x^{(i)})$.

Assumption 1.3 We assume that the binary random variable $y^{(i)}$ follows the Bernoulli distribution as

$$y^{(i)} \sim Bernoulli\left(1, p(y^{(i)} = 1|x^{(i)})\right) \tag{1.4}$$

where $p(y^{(i)} = 1|x^{(i)})$ is the conditional probability of $y^{(i)} = 1$ given the features $x^{(i)}$. Given that, the logistic regression model with the unknown parameters β for the i-th sample is of the form

$$p(y^{(i)} = 1|x^{(i)}) = \sigma(x^{(i)}\beta) = \sigma(z^{(i)}) = p_y^{(i)} \tag{1.5}$$

where $\beta \in \mathbb{R}^{n_x+1}$ are the model parameters to be identified and $\sigma(.)$ is the sigmoid or logistic function. It should be noted that $x^{(0)} = 1$ to account for the constant parameter. In that regard, $z^{(i)}$ is defined as

$$z^{(i)} = x^{(i)}\beta \tag{1.6}$$

The general case, considering all samples can be written as

$$p_Y = p(Y = 1|X) = \sigma(X\beta) = \frac{1}{1 + e^{-(X\beta)}} = \frac{e^{(X\beta)}}{1 + e^{(X\beta)}}. \tag{1.7}$$

The transformation of the probability function $p(Y = 1|X)$ is called the logit transformation, log odds of the probability, or the logit link function, and is given by

$$logit(p) = \log \frac{p_Y}{1 - p_Y} = X\beta \tag{1.8}$$

where p_Y is the conditional probability of positive outputs, $Y = 1$, given X.

Given the assumptions, the conditional distribution of $y^{(i)}$ given $x^{(i)}$, $p(y^{(i)}|x^{(i)})$, can be formulated as

$$p(y^{(i)}|x^{(i)}) = p_y^{(i)^{y^{(i)}}}(1 - p_y^{(i)})^{(1-y^{(i)})}, \text{where} \begin{cases} p(y^{(i)}|x^{(i)}) = p_y^{(i)} & \text{if } y^{(i)} = 1 \\ p(y^{(i)}|x^{(i)}) = 1 - p_y^{(i)} & \text{if } y^{(i)} = 0 \end{cases} \tag{1.9}$$

To find the maximum likelihood (ML) estimator of parameters $\beta \in \mathbb{R}^{n_x+1}$, the

likelihood function for the logistic regression model, $L(\beta)$, is defined as

$$L(\beta) = \prod_{i=1}^{m} p(y^{(i)}|x^{(i)}) = \prod_{i=1}^{m} p_y^{(i)^{y^{(i)}}} (1 - p_y^{(i)})^{(1-y^{(i)})}. \tag{1.10}$$

The likelihood function presents the necessity condition for an ML estimate existence where the parameters can be identified by maximizing the likelihood function. Since maximizing the likelihood function is equivalent to maximizing the log of that function, we work with the log-likelihood function which makes the mathematical operations easier. The log-likelihood function is defined as

$$\log L(\beta) = \log(\prod_{i=1}^{m} p(y^{(i)}|x^{(i)}) = \sum_{i=1}^{m} \log(p(y^{(i)}|x^{(i)}). \tag{1.11}$$

1.3.2 Maximum Likelihood Estimation of the Parameter β

Considering a set of m observations in order to estimate the true value β^0 of the vector $\beta \in \mathbb{R}^{n_x+1}$, where n_x is the number of features, the aim is to identify and analyze the maximum likelihood estimator $\hat{\beta}$ of the true parameter vector β^0. The likelihood function described above can be rewritten as

$$L(\beta) = p(Y|X) = \prod_{i=1}^{m} p(y^{(i)}|x^{(i)}) = \prod_{i=1}^{m} \frac{e^{y^{(i)}x^{(i)}\beta}}{1 + e^{x^{(i)}\beta}}. \tag{1.12}$$

Accordingly, the log-likelihood function will be of the form

$$\log L(\beta) = \sum_{i=1}^{m} y^{(i)} \log(p_y^{(i)}) + (1 - y^{(i)}) \log(1 - p_y^{(i)}) \tag{1.13}$$

or similarly, of the form

$$\log L(\beta) = Y^T X\beta - \sum_{i=1}^{m} \log(1 + e^{x^{(i)}\beta}), \tag{1.14}$$

where $X\beta$ represents the $x^{(i)T}\beta$ over all the samples i.

To determine the maximum of the log-likelihood function, its derivative can be calculated as

$$\nabla \log L(\beta) = X^T \left(Y - \sigma(X\beta)\right). \tag{1.15}$$

Therefore a necessity condition for $\hat{\beta}$ being the maximum likelihood estimator of

β^0 is $\nabla \log L(\beta) = 0$. Another condition should be satisfied to guarantee that the log-likelihood function is a maximum around $\hat{\beta}$ and not a minimum. To satisfy this condition, the second derivatives of the log-likelihood function should all be negative, that is $\nabla^2 \log L(\beta) < 0$ [76].

The second derivative of the log-likelihood function or the Hessian matrix of the log-likelihood function, $H_{\log L(\beta)}$, can be derived as

$$\nabla^2 \log L(\beta) = \frac{\partial^2}{\partial \beta_j \partial \beta_k} \log L(\beta) = -\sum_{i=1}^{m} x_j^{(i)} x_k^{(i)} \sigma'(x^{(i)}\beta) = -X^T W X \tag{1.16}$$

where W is a $m \times m$ diagonal matrix which the entries on its diameter are $\sigma'(x^{(i)}\beta)$.

Fact 1.1 The Hessian matrix of the log-likelihood function, $H_{\log L(\beta)}$, is negative semi-definite for any $\beta \in \mathbb{R}^{n_x+1}$.

Therefore, the log-likelihood function, $\log L(\beta)$, will be a concave function of the parameter β. Accordingly, any root of $\nabla \log L(\beta)$ is a global maximum of $\log L(\beta)$ and a maximum likelihood estimator of β^0.

Next section describes the two important properties that the maximum likelihood estimation satisfies which are consistency, and asymptotic normality. These properties are discussed in more detail in [78].

1.3.3 Existence, Strong Consistency, and Asymptotic Normality of the Maximum Likelihood Estimator

For the maximum likelihood estimators to exist and satisfy the consistency property, a couple of assumptions has to be made:

Assumption 1.4 The input variables/features are uniformly bounded. That is $\exists M_0 : |x_{in_x}| \leqq M_0, \forall i, \forall n_x$.

Assumption 1.5 Considering the λ_{1m} and $\lambda_{n_x m}$ as the smallest and largest eigenvalues of $\sum_{i=1}^{m} x^{(i)} x^{(i)} \sigma'(x^{(i)}\beta^0)$, there exists M_1 such that $\lambda_{n_x m}/\lambda_{1m} < M_1, \forall i$.

`Assumption 1.5` is implied by the regular condition that there exists a function $f(m)$ such that $\frac{1}{f(m)} \sum_{i=1}^{m} x^{(i)} x^{(i)} \sigma'(x^{(i)}\beta^0)$ converges to a positive definite matrix. From the dynamical systems viewpoint, these two assumptions are consequences of the system's stability. `Assumption 1.4` makes sure that the features are of finite values and `Assumption`

`1.5` is basically an observability condition that guarantees observing the system's dynamics through the oscillations. That is, not just observing the extreme 0 and 1 probabilities. Additionally, in the case that features are too small or too big, the system remains stable.

Given the above assumptions, we will have the following theorems on consistency and asymptotic normality of the maximum likelihood estimator:

Theorem 1.1 If `Assumption 1.4` and `Assumption 1.5` are satisfied, the maximum likelihood estimator $\hat{\beta}$ of β exists almost surely as m goes to $+\infty$, and $\hat{\beta}$ converges almost surely to the true value β^0 if and only if $lim_{m\to\infty}\lambda_{1m} = +\infty$.

Theorem 1.2 Assuming `Assumption 1.4` and `Assumption 1.5` are satisfied, and if $\hat{\beta}$ converges almost surely to β^0, therefore

$$\left(\sum_{i=1}^{m} x_j^{(i)} x_k^{(i)} \sigma'(x^{(i)}\hat{\beta})\right)^{1/2} (\hat{\beta} - \beta^0) \xrightarrow[m\to\infty]{d} \mathcal{N}(0, I), \tag{1.17}$$

and $\hat{\beta}$ is asymptotically normal, where $\xrightarrow[m\to\infty]{d}$ denotes the convergence in distribution and $\left(\sum_{i=1}^{m} x_j^{(i)} x_k^{(i)} \sigma'(x^{(i)}\hat{\beta})\right)^{1/2}$ is a symmetric positive matrix.

That concludes the consistency and asymptotic normality properties of the maximum likelihood estimators. Next section provides information on statistical analysis consisting confidence interval and confidence ellipsoid to investigate the significance of the identified coefficients.

1.3.4 Statistical Analysis

1.3.4.1 Confidence Interval

The confidence interval of coefficient β represents the upper and lower bands of the expected change in $logit(p)$ due to a unit change in the input variable. Following steps lead to a systematic way of computing the confidence interval:

- Identifying the sample statistics, i.e., the logistic regression coefficients, β.
- Selecting a confidence interval level that describes the uncertainty of the sampling method, for example, 95% confidence level.
- Finding the margin of the error based on the critical value and standard error; this should be noted that the critical value can be computed performing a $z - test$, as

the test statistic is approximated by a normal distribution, provided having a large enough sample.

- Specifying the confidence interval; the range of the confidence interval is defined by sample statistics ± margin of error.

Therefore, in general, the $(1-\alpha)100\%$ confidence interval for the coefficient β can be formulated as

$$\beta \pm Z_{\alpha/2} \times SE(\beta), \tag{1.18}$$

where Z is the z-distribution and $SE(\beta)$ represents the standard error for coefficient β. This method has been widely used by statistical computing packages to compute the confidence interval for logistic regression coefficients. This should be noted that computed errors used in (1.18) are accurate only if the logistic regression model is correctly specified. In other words, $y^{(i)}$ are independent random variables with Bernoulli distribution $p_y^{(i)}$ where $logit(p)$ is a linear combination of the terms.

1.3.4.2 Confidence Ellipsoids

Another method to investigate the significance of coefficients is confidence ellipsoid, as described in [79]. Assuming that the assumptions on asymptotic normality of the maximum likelihood estimators are satisfied and the sample m is sufficiently large, in order to obtain the confidence, the asymptotic result can be formulated as

$$m(\hat{\beta}-\beta)^T\Sigma^{-1}(\hat{\beta}-\beta) \xrightarrow[m\to\infty]{d} \chi^2_{q+1} \tag{1.19}$$

where χ^2_{q+1} is the chi-squared distribution on $q+1$ degrees of freedom with q being the number of input coefficients β. Defining $\hat{\Sigma}$ as the estimation of the covariance matrix, the covariance matrix can be estimated from the inverse of the sample information matrix as

$$\hat{\Sigma}/m = J^{-1}, \tag{1.20}$$

where the jf-th element of J can be computed as

$$J_{jf} = -\frac{\partial^2}{\partial\beta_j\partial\beta_f} l(\beta|x^{(1)},\ldots,x^{(m)})|_{\beta-\hat{\beta}}, j, f = 0,\ldots,q, \tag{1.21}$$

where $l(\beta|x^{(1)},\ldots,x^{(m)})$ is the natural log of the likelihood function or $\log L(\beta)$. As mentioned in the previous section, this can also be represented as

$$\nabla^2 l(\beta) = -X^T \hat{W} X, \tag{1.22}$$

where $\hat{W}$ is a $m \times m$ diagonal matrix. The approximate sampling distribution of $\hat{\beta}$ for large m is $\mathcal{N}(\beta, (X^T \hat{W} X)^{-1})$. With a sufficiently large m, the equation (1.19) can be reformulated as

$$(\hat{\beta} - \beta)^T J(\hat{\beta} - \beta) \dot{\sim} \chi^2_{q+1} \tag{1.23}$$

where $\dot{\sim}$ denotes the approximate distribution. Therefore, $1 - \alpha$ confidence ellipsoid for β can be defined as

$$p[(\hat{\beta} - \beta)^T J(\hat{\beta} - \beta) \leq \chi^2_{q+1,\alpha}] = 1 - \alpha. \tag{1.24}$$

where $\chi^2_{q+1,\alpha}$ denotes the upper α percentage point of the χ^2_{q+1} distribution.

The next section describes the problem facing in order to select the model and estimate the parameters and how to circumvent this problem and acquire the significance level of the coefficients.

1.3.5 Parameter Estimation and Evaluating the Significance Level

Using the same data to both select the model and estimate the coefficients is recognized to lead to a misleading good fit, but this is not an easy problem to notice and address. There has been a number of studies aiming to circumvent this problem, each with its own difficulties [80–82]. One approach to consider and evaluate the significance level of the coefficients is by splitting the data [83]. Usually, using data splitting approach, data divides into two halves and the first half uses to select the model and the second half uses to obtain the significance level and model validation. The inferences achieved using this method are conditional on the selected model obtained by the first data half [84].

Another way to use data splitting approach is the use the first half of the data for model selection as before, but the second data half for estimating the parameters of the selected model [85]. This is the approach that we use in this chapter. This approach circumvents the problem of overfitting since it uses a separate new data to estimate the coefficients. Estimating the parameters using this method, we employ the confidence interval and confidence ellipsoid methods discussed in the last section to investigate the significance of the parameters.

1.4 Specific Behavioral Medicine Problems

In different chapters of this dissertation, we investigate and estimate the dynamical models for a couple important health related problems in behavioral medicine. Physical activity is one of the areas of interest since it has many immediate and long-term health benefits and can be promoted from the early adulthood to decrease the chance of many future diseases. On the other hand, smoking is one of the main causes of death that can be managed and prevented through efficient programs.

Algorithms developed here are used to identify the models representing the physical activity and smoking behavior change to different inputs/stimuli [15, 86–89]. The results obtained from the analyses of participants responses in these studies provide insights on a variety of factors such as the intervention frequency, the timing, and content of intervention among others. Such information can be used to design and implement efficient just-in-time adaptive interventions in future to prevent adverse effects of such global issues.

1.4.1 Physical Inactivity

Studies have shown a strong relationship between physical inactivity, sedentary behavior, and a large range of diseases such as cardiovascular and metabolic diseases, type 2 diabetes, and some types of Cancer. 117 million American adults are diagnosed with preventable chronic diseases, a significant portion of which can directly be prevented or mitigated by regular physical activity. Additionally, physical fitness has shown to be associated with a reduction in cardiovascular disease mortality and all-cause mortality [90].

The World Health Organization and the United States Department of Health and Human Services recommended accumulating at least 150 minutes per week of moderate-intensity physical activity, 75 minutes per week of vigorous-intensity physical activity, or an equivalent combination of them [91]. However, national studies indicate that 80% of American adults do not meet guidelines for aerobic and muscle-strengthening activity and only 50% meet guidelines for general aerobic activity [90, 92]. Young adulthood is a critical developmental stage because risk factors that compromise cardiovascular health start to accumulate. Studies on the effects of physical activity on people with disabilities, chronic conditions, or disease survivors such as people with Parkinson's and Alzheimer's disease, cancer survivors, and mental illnesses have shown promises to improve some aspects of the disorders and impairments [90]. Therefore, interventions aim at increasing the physical activity during young adulthood can reduce long-term chronic disease risk.

Aerobic activities can be tracked with wearable devices to provide behavioral feedback on physical activity. That feedback can also integrate with other widely adopted mobile technologies, such as smartphones, to promote aerobic physical activity in the natural context of daily life.

A recent systematic review shows that digital messaging interventions for physical activity promotion are associated with small-to-medium sized increases in daily step counts (standardized mean difference = 0.38) [93]. These estimates are based on differences in aggregated physical activity levels between participants who receive digital messages and those who do not. They do not speak to the effects of individual messages on subsequent physical activity. This gap is important because physical activity is a dynamic process that varies over time within each person and understanding those dynamics can improve predictions about behavior change [94].

Accelerometer data from the NHANES dataset revealed normative differences in physical activity as a function of the time of day and day of week [95]. Based on this within-person variation, just-in-time interventions may be useful for providing support to regulate the dynamics of physical activity. To realize the potential for just-in-time interventions, it is important to understand whether (and how) the dynamics of physical activity are impacted by different contexts such as weather conditions i.e., temperature and precipitation. That information will inform decisions about generalizing models across contexts and the value of adapting models based on accumulating information.

Previous studies applying this approach have led to important insights. Both daily and momentary physical activity dynamics are regulated differently on weekends and weekdays [1]. As a consequence, it is best to model physical activity dynamics as a switched system; that is, as a pair of models that describe weekend and weekday dynamics separately. Additionally, since one size does not fit all, a generic model of physical activity dynamics can be overly conservative for estimating the effects of digital messages on physical activity. Person-specific models are better suited to describing the idiosyncratic effects of different messages on physical activity. It has to be investigated that how features of the momentary environment and contextual changes such as a pandemic can alter responses to digital messages. Understanding the context around a person can lead to more accurate predictions about their expected responses to different types of messages at that moment and therefore, an important concept to be investigated.

1.4.2 Smoking

Cigarette smoking is the leading preventable cause of death in the United States, responsible for about one in five deaths annually [96]. The costs of direct medical care for adult smokers, lost economic productivity caused by smoking-related disability and premature mortality, and secondhand smoking exposure exceed $300 billion per year in the United States [97, 98]. Comprehensive smoking control programs require a clear understanding of the dynamics of smoking triggers and behaviors; however, few studies have attempted to describe those systems.

Stress is long known to be an incentive for addictive substance use e.g. cigarette smoking [99–102]. A recent study on smoking motives among smokers in London reported stress relief as the highest rated motive for smoking [99]. It has been suggested that the main incentive behind smoking behavior in young people is to reduce the stress of difficult times [100]. In another study, Torres and colleagues reported that, in women, stress was a primary factor for initiating tobacco use and relapsing during abstinence [101].

Using electronic diaries for smoking recording and daily EMA for stress, Shiffman et al. have found an association between higher stress and higher smoking in lower educated and African American smokers [103]. Using self-reported data on stress and smoking, Pesko et al. described a consistent positive association between short-term stress and smoking [104]. It has also been reported that affect dysregulation, particularly, negative mood variation, is a potential factor for future smoking escalation. These Studies provided evidence on the effect of stress and negative affect on the chance of smoking.

Smoking is a dynamic behavior. In other words, smoking can occur due to a variety of causes over time. Analysis of behavioral dynamics of smoking requires new tools to capture this criterion, despite the existing analytic tools for behavioral studies that are not well-suited to using all intensive longitudinal information and providing conclusive results on the relation between components i.e., stress and smoking.

Employing tools and developed dynamical systems modeling techniques in this dissertation, we were capable of using high-frequency sensors and novel markers of both stress and smoking to describe system dynamics and then simulate how stress influences subsequent risk for smoking. Analyzing the stress-smoking relation at the moments preceding and following a smoking episode and using the personalized model parameters provides the opportunity to design effective smoking cessation interventions and treatments.

1.5 Contributions and Outline

Contributions of this work are presented in chapters 2-6.

Chapter 2 represents how tools from control systems engineering and machine learning techniques can be used to identify person-specific models of physical activity in response to digital messaging intervention. These tools are developed to incorporate the dynamics of both inputs and output i.e., three types of messages (Affective, Social-Cognitive, and Inspirational Quotes messages) and physical activity in the form of step counts. Physical activity was modeled as a switched system with separate models to reflect different amount and patterns of physical activity on weekdays and weekends. Features of the simulated impulse and cumulative step responses were extracted for each message type and statistical tests were performed. This work aims at closing the gap that has led to challenges for developing optimal content for digital messaging interventions using advanced developed tools.

Building on the results of our prior work and the algorithms developed for chapter 2, chapter 3 explores the effect of the COVID-19 pandemic on the dynamics of physical activity responses to digital messaging interventions. Literature has shown that the COVID-19 pandemic adversely impacted physical activity, but little is known about how contextual changes following the pandemic declaration impacted either the dynamics of people's physical activity or their responses to micro-interventions for promoting physical activity. To investigate the changes in dynamics of physical activity from prior to after the pandemic declaration, person-specific dynamical models of physical activity in response to different intervention messages (Move More, Sit Less, and Inspirational Quotes), were identified for pre-pandemic and post-pandemic stages, over the weekdays and weekends. In addition to extracting features from each simulated response, magnitude of each systems' dominant pole was used as a measure of responses speed.

Chapter 4 leverages concepts from dynamical systems and signal processing areas to develop tools that can identify dynamic models that consider the delayed input effects and binary outputs. Although the focus in this chapter is on binary outcomes, the proposed approach can be extended to other types of outcomes such as multi-valued or continuously valued data. The approach presented can leverage intensive high frequency real data that often has missing measurements and provides simple models that predict the response to inputs. The models obtained can be used not only to study how an individual responds to different inputs but also as a first step in the process of designing just-in-time adaptive interventions.

To apply the developed tools and algorithms in chapter 4, taking advantage of advances in wearable sensing technology and digital markers of stress and smoking, in chapter 5, person-specific models of stress and smoking system dynamics were identified by considering stress immediately before, during, and after smoking episodes. Sensor-detected stress probabilities indicate a vulnerability for smoking that may be used as a tailoring variable for just-in-time interventions to support quit attempts.

In chapter 6 a time-varying version of logistic regression method in combination with regularized l_1-norm, to induce sparsity, is developed to identify the models that best describe the dynamics of the data with continuous input and binary output. The algorithm developed can handle the missing data and data fragmentation, and considers sparsity in the modeling.

Finally, Chapter 7 concludes the dissertation, and publications are represented in Appendix A.

Chapter 2
Personalized Dynamical Modeling in an mHealth Intervention

Approximately half of adults in the US do not attain recommended levels of health-enhancing aerobic physical activity [92]. Given the widespread lack of physical activity in the US population, innovative methods with high potential reach are needed to improve public health. One inexpensive mode for delivering physical activity interventions at scale involves digital smartphone messaging. Determining which validated targets to engage with different messages is a persistent challenge for content development and intervention delivery.

Developing person-specific dynamical models of behavior by applying tools from control systems engineering and comparing the behavioral responses to different types of intervention content can inform both intervention and theory development by extending target validation research from group-level to person-level analyses. However, limited research has compared different proximal effects of different message types on physical activity behavior after message receipt.

This study compared the effects of different motivational message types on physical activity behavior following message receipt. Building on our prior work, we developed person-specific dynamical models of physical activity in a digital messaging intervention. Developed models employ intervention messages as the inputs and consider the present and recent past messages and recent physical activity behavior related to responses to different types of messages to predict the activity at the present time.

2.1 Physical Activity Dynamics Affecting by Motivational Message Framing

2.1.1 Digital Messaging Interventions

Digital messaging interventions have the potential to reach large portions of the young adult population because 97% of young adults currently own a smartphone [105]. Smartphones are highly accepted by participants in physical activity promotion research and intervention delivery via digital messages is a low-cost method for instigating behavior change [93,106]. In a meta-analysis, digital messaging interventions significantly increased device-measured steps per day (d=0.38) [93]. This effect exceeded the 90th percentile for physical activity interventions according to recent benchmarks for digital intervention effects on physical activity [107]. Despite the acceptability, feasibility, and effectiveness of using digital messaging interventions, little is known about the most effective types of messages for increasing physical activity.

A scoping review of physical activity messaging interventions proposed that messages should be framed positively and highlight beneficial short-term outcomes related to social and mental health, be tailored to the recipient, and use psychological theory and/or social marketing principles [108]. This framework does not specify which psychological theories should guide content development or which behavior change techniques should be incorporated. Many physical activity interventions are grounded in social-cognitive theories, such as the Theory of Planned Behavior and Health Action Process Approach [109].

Such theories posit that attitudes (i.e., positive outcome expectations), subjective norms and perceptions of behavioral control are precursors for intention formation, and that planning processes mediate the translation of intentions into physical activity behavior [110, 111]. Emerging work also suggests that linking physical activity with desirable affective experiences can activate affective processes that motivate physical activity [112, 113]. Consistent across these approaches is the idea that persuasive messaging can be used to frame the benefits of physical activity and influence decisions to be active.

2.1.2 Attitude Change Validated as a Target for Physical Activity Promotion

Attitudes represent evaluative beliefs about an activity's consequences and can be either instrumental (focusing on social or tangible costs or benefits) or affective (focused on affective experiences) [111]. Attitude change has been validated as a target for behavior change. Changing attitudes has a medium-sized effect on intention strength and a small effect on behavioral outcomes [114]. Comparisons of affective attitudes and instrumental attitudes toward physical activity have revealed that affective attitudes are more strongly associated with physical activity intentions than instrumental attitudes [115]. These findings suggest that affectively-framed message may be more effective than instrumentally-framed messages for strengthening physical activity intentions.

Three experimental studies have evaluated the effects of affective or instrumental benefit messages on physical activity behavior directly. These studies provided mixed results with two studies favoring affectively-framed messages and one study showing no difference between affectively- and instrumentally-framed messages [116–118]. These mixed results could reflect that the effects of different message types vary by person. Each of these studies focused on self-reported physical activity outcomes one to three weeks after message delivery. The proximal effects of affectively- and instrumentally-framed messages on physical activity in the minutes and hours after message delivery are not known and were the focus of the present study. To identify the dynamics between message receipt and response and understand potential person-specific responses to message types, a dynamical modeling approach is needed.

2.1.3 Addressing Treatment Heterogeneity with Person-Specific Dynamic Modeling of Physical Activity

Device-based measures of physical activity can provide minute-level data of movement throughout the day. Step counts represent a valid measure of total physical activity volume accumulated throughout the day that is associated with cardiometabolic risk reduction, easy to measure and widely accessible in consumer devices [119]. About 70% of variability in physical activity occurs within people over time so this study focused on proximal changes in a person's physical activity following message delivery [120–122].

Prior work from our group applied system identification methods to develop dynamic models that described physical activity over time and the proximal effects of digital

messages on that behavior [1, 15, 123]. Behavioral responses to digital messages varied as a function of message content from weekends to weekdays, and from person to person. In that study, message content was differentiated by the target behavior change (e.g., move more versus sit less). Messages in the Move More and Sit Less content libraries provided prompts or cues to form intentions regarding the desired behavior change and also systematically varied in whether they were framed in terms of affective outcomes of physical activity or a combination of instrumental outcomes of physical activity and social-cognitive strategies for behavior change like goal setting, planning, identification of barriers, and engaging social support. We supplemented messages targeting instrumental outcomes with social-cognitive principles based on prior evidence that affective attitudes are more strongly associated with physical activity intentions than instrumentally-framed messages. For simplicity, these two message types are described as Affective and Social-Cognitive hereafter. This study examined whether message framing impacts proximal changes in physical activity.

2.2 Methods

2.2.1 Participants

Insufficiently-active young adults were recruited using fliers posted on campus and community bulletin boards, university listservs, and Studyfinder, a web-based recruitment tool for Penn State researchers, from April 2019 to July 2020. Eligible participants were 18-29 years of age, ambulatory, free of functional activity limitations, free of visual impairment that would interfere with smartphone use, had verbal and written fluency in English and were capable of giving informed consent. Participants had to be smartphone users (iPhone iOS v10.0 or later or Android operating system v7 or later) willing to place the custom software, Random AIM, and Fitbit apps onto their phone.

Participants were excluded from the screening stage if they reported engaging in 90 minutes or more of moderate or greater intensity physical activity per week, were part of organized programs with mandated physical activity, needed assistive devices for mobility, had a prior diagnosis of cancer, cardiovascular disease, type I or type II diabetes, or metabolic syndrome, were pregnant or had a plan to become pregnant in the following 6 months, or had any contradictions to engaging in physical activity according to the Physical Activity Readiness Questionnaire.

2.2.2 Measurements

2.2.2.1 Demographic and Anthropometric Characteristics

Participants self-reported age, sex, race, and ethnicity, educational attainment, and employment status. Researcher measured weight (to the nearest 0.1 lb.) and height (to the nearest 0.5 inch) in duplicate using a digital scale and wall-mounted stadiometer, respectively, upon removal of the participant's shoes.

2.2.2.2 Physical Activity Screening

Participants were instructed to wear a wGT3X-BT activity monitor (Actigraph, Pensacola, FL) for a week during their waking hours for a minimum of 10 hours each day. The participants kept a paper record of the times that the device was placed on in the morning and removed at night, as well as other removals for bathing, swimming, or other reasons. The wGT3X-BT monitor was worn at the waist on the participant's dominant side at the midline of their thigh. The monitor used a 3-axis accelerometer to measure high-resolution activity with a defined 30 Hz sampling rate.

Activity data was collected in minute intervals. Wear time was validated using the proprietary Troiano 2007 algorithm in the ActiLife v.6.13.4 software [124]. Non-wear times, defined as greater than 90 minutes with zero activity counts, were excluded from the analysis. Valid days were defined as those with at least 600 minutes of wear time. At least 5 valid days of wear were required for analysis in order to be considered for qualification into the intervention study. The Freedson algorithm was used to classify minutes as light ($\leq$ 1952 counts/min), moderate (1952 - 5724 counts/min), and vigorous ($>$ 5724 counts/min) physical activity [125].

2.2.2.3 Ambulatory Physical Activity Monitoring

Participants wore a Fitbit Versa/Versa Lite smartwatch on their wrist for 6 months to track minute-level step counts and heart rate. These devices have demonstrated similar accuracy for step counting to research-grade Actigraph monitors and are suitable for use in adults with no limitations on mobility [126, 127]. Minute-level step count and heart rate data were used to classify minutes as valid wear time or device non-wear.

2.2.3 Procedures

Participants were enrolled in two stages with separate informed consent processes: screening and intervention. All procedures were approved by the Institutional Review Board at the Pennsylvania State University (Study#00009455).

2.2.3.1 Screening

A researcher conducted individual telephone interviews with participants and scheduled provisionally-eligible participants for a lab visit. In the lab visit, participants provided informed consent and completed questionnaires. The participant's height and weight were measured, and the participant was provided with an Actigraph wGT3X-BT activity monitor to wear at the waist during waking hours for one week (along with a paper wear time log to document device removals).

After 7 complete days in the field, participants returned the activity monitors to the lab and were compensated ($25). Participants who had at least 5 days of valid device wear (600 min/day) and accumulated less than an average of 21.4 min/day of moderate-to-vigorous physical activity (the equivalent of 150 min/week) were invited to participate in the second stage of the study.

2.2.3.2 Intervention

Eligible participants provided informed consent for the next stage of research and received a Fitbit Versa/Versa Lite smartwatch to wear on their nondominant wrist for the next 6 months. This device recorded minute-level step counts and heart rate (in five-minute moving averages). The researcher assisted the participants with installing the custom designed study mobile application, Random AIM app, and Fitbit mobile applications on their personal smartphone.

Participants identified an availability window of 10+ hours on weekdays and weekends when they were available to receive digital messages. They could adjust this availability window at any time during the study by contacting the researcher. Participants were provided with information about the US Physical Activity Guidelines for Adults to assign a goal, potential benefits from increasing physical activity, and the principle of progressive adaptation to reduce musculoskeletal injury risk. Participants were asked to contact study personnel if they were injured or ill or wanted their notifications off for a period of time as it may impact their activity levels.

For the next 6 months, the Random AIM app delivered between 0-6 messages/day as notifications via the operating system to each participant. The frequency (0-6 messages for the day), timing within the availability window, and content of daily messages were determined randomly every night by the backend server. The only restriction was that consecutive messages could not be delivered within 15 minutes of each other. Messages were drawn randomly from three content libraries: Affectively-framed (54 messages), Social-Cognitively framed (54 messages), and Inspirational Quotes (27 messages).

The Affective and Social-Cognitive libraries were both evenly split between messages focused on moving more and sitting less. Affectively-framed messages additionally presented information about emotional consequences of engaging in those behaviors. Social-Cognitively framed messages incorporated information about health consequences of engaging in those behaviors, and included a prompt for goal-setting, action planning, social support, or problem solving. The third message library, Inspirational Quotes, did not reference physical activity or changing movement patterns and did not prompt use of any self-regulatory strategies aimed at promoting movement. Half of the messages in each library were accompanied by an image corresponding to message content (i.e., physical activities, standing activities, natural landscapes).

Participants were asked to acknowledge receipt by clicking on the message when they read it (triggering a round-trip message to the backend server). Participants received a micro-incentive for each message acknowledgement ($0.25) and message notifications were removed if a message was not acknowledged within 30 minutes of delivery. Participants were compensated at 2-month intervals throughout the study to support engagement and protocol compliance.

Research staff contacted participants via telephone or e-mail anytime they observed three consecutive days without Fitbit heart rate data (suggesting device non-wear) or three days without acknowledging Random AIM messages. After 6-month intervention period, participants were scheduled the last lab visit to be guided through the processes for removing the Random AIM app from their smartphone and switching their Fitbit app to a personal email account. Participants answered end of study questionnaires and engaged in a brief interview on their experience with the app and the intervention.

2.3 Developing Dynamical Models

2.3.1 Data Analysis

Three data tables were merged using timestamps to model physical activity dynamics following messages: person-level availability window for messages, minute-level physical activity, and minute-level heart rate. Days prior to the start date or following the end date were removed. Any days corresponding to dates when participants reported injury or illness, and/or notifications being off were trimmed. Table 2.1 provides the information on start and end date of the study for each participant, number of days included in the analysis, number of missing days, distributions of days used for identifying the models and missing days over the weekdays and weekends, and their availability hours per day, individually. This should be noted that in the table, "wd" and "we" refer to weekday and weekend, respectively.

Physical activity and heart rate data were trimmed to include the period from two hours before the messaging availability window started to two hours after it ended to ensure sufficient activity data. This choice provided enough data for modeling the physical activity behavior changes after receiving a message either at the beginning or end of the availability window. Appropriate pre-processing step was taken for participants with changes in their provided availability time through the study.

Activity data was separated for weekdays and weekends and classified as missing if zero steps were recorded and heart rate data was not available for a minute. If the missing minutes were smaller than or equal to 3, step counts for those minutes were interpolated using linear interpolation. Minutes with missing heart rate and zero step counts were not included in the model, in addition to messages scheduled and sent from the server that were not received and displayed on a participant's device. The available and valid minute-level physical activity data were aggregated into sums for each 15-minute epoch. Days were treated as independent; therefore, message effects on physical activity were not modeled across days.

2.3.2 Linear Regression Model with Multiple Variables

Linear regression model with multiple variables has employed to identify the person-specific dynamical models of physical activity based on the effect of digital messaging micro-interventions. Implementation is done using the Python programming language [128]. Physical activity was modeled as a switched system with different models associated

Table 2.1: Some data statistics on days for each participant.

Participant	Start	End	days	missing	days_we	missing_we	days_wd	missing_wd	hours_we	hours_wd
aim101	4/16/19	10/12/19	180	0	51	0	129	0	14	14
aim102	4/16/19	10/12/19	173	7	49	2	124	5	11	11
aim103	4/16/19	10/12/19	173	7	49	2	124	5	10	10
aim105	4/16/19	10/12/19	177	3	50	1	127	2	12	13
aim108	4/27/19	10/23/19	180	0	52	0	128	0	10	10
aim109	4/27/19	10/23/19	180	0	52	0	128	0	12.5	14
aim110	4/29/19	10/23/19	178	0	50	0	128	0	13	15
aim111	4/29/19	10/23/19	178	0	50	0	128	0	10	12
aim112	4/27/19	10/23/19	180	0	52	0	128	0	11	12
aim113	5/11/19	11/6/19	180	0	52	0	128	0	10	10
aim114	5/11/19	11/6/19	164	16	48	4	116	12	12	12
aim115	5/30/19	11/25/19	166	14	49	3	117	11	10	10
aim116	5/29/19	11/24/19	180	0	52	0	128	0	10	12
aim117	5/30/19	11/25/19	180	0	52	0	128	0	10	10
aim118	6/7/19	12/3/19	180	0	52	0	128	0	10	10
aim119	6/12/19	12/8/19	180	0	52	0	128	0	10	10
aim120	6/19/19	12/15/19	180	0	52	0	128	0	10	10
aim121	6/19/19	12/15/19	168	12	50	2	118	10	10	10
aim122	6/19/19	12/15/19	180	0	52	0	128	0	10	10
aim123	6/20/19	12/16/19	166	14	46	6	120	8	10	10
aim124	6/21/19	12/17/19	180	0	52	0	128	0	10	10
aim125	6/21/19	12/17/19	180	0	52	0	128	0	10	10
aim126	6/25/19	12/21/19	180	0	51	0	129	0	10	10
aim127	6/22/19	12/18/19	180	0	52	0	128	0	10	10
aim128	7/9/19	12/27/19	172	0	48	0	124	0	10	10
aim130	7/6/19	1/1/20	174	6	50	2	124	4	10	10
aim131	7/6/19	1/1/20	180	0	52	0	128	0	10	10
aim132	7/17/19	1/12/20	180	0	52	0	128	0	10	10
aim133	7/11/19	1/6/20	165	15	46	6	119	9	10	10
aim134	7/12/19	1/7/20	180	0	52	0	128	0	10	10
aim135	7/17/19	1/12/20	168	12	50	2	118	10	10	10
aim136	7/23/19	1/18/20	161	19	46	5	115	14	10	10
aim137	7/23/19	1/18/20	180	0	51	0	129	0	10	10
aim138	7/26/19	1/21/20	166	14	49	3	117	11	10	10
aim139	7/30/19	1/25/20	159	21	45	6	114	15	10	10
aim140	7/30/19	1/25/20	180	0	51	0	129	0	10	10
aim141	8/6/19	2/1/20	161	19	45	6	116	13	10	10
aim142	8/9/19	2/4/20	178	2	52	0	126	2	10	10
aim143	8/13/19	2/8/20	164	16	46	5	118	11	10	10
aim144	8/15/19	2/10/20	162	18	48	4	114	14	10	10
aim145	8/22/19	2/17/20	173	7	50	2	123	5	10	10
aim146	8/22/19	2/17/20	180	0	52	0	128	0	10	10
aim147	8/22/19	2/17/20	165	15	48	4	117	11	10	10
aim149	8/31/19	2/26/20	155	25	44	8	111	17	10	10
aim150	9/17/19	3/14/20	176	4	50	1	126	3	10	10

with physical activity responses following receipt of each message type on weekdays and weekends [1, 15, 129]. The linear regression model with multiple variables and noise is of the form

$$\hat{y}(kd) = a_0 + \sum_{i=1}^{5} a_i y(kd - id) + \sum_{j=1}^{3} \sum_{i=0}^{5} b_{ij} u_j(kd - id) + \epsilon(kd) \tag{2.1}$$

where $\hat{y}(kd)$ is the system output at time kd which is the predicted step counts at time kd, $y(kd - id)$ is the actual step count recorded by the activity monitor or linearly interpolated if the missing minutes were less than or equal to 3, $u_j(kd - id)$ are the inputs for the three message types (Affective, Social-Cognitive, and Inspirational Quotes) at time $(kd - id)$, (0: message not sent and 1: message sent), d is the sampling time (15 min), $\epsilon(kd)$ is noise at time kd, and a_0, a_i, b_{ij} are the unknown coefficients of the model to be identified.

The trade-off between model complexity and size of the model error led to the model order of 5. This means that, to predict the output (step counts) at the present epoch, in addition to the present 15-min epoch of input data (whether a message of any type received at this time or not), the last five epochs or 75 minutes of both input (messages) and output (step counts) data were used. As mentioned before, each epoch is 15 minutes long. Identification of the system coefficients is done using the least square method by minimizing the square root of residuals as

$$\begin{aligned} &\min_{a_0, a_i, b_{ij}} \sum_k r_{kd}^2 \\ &\text{s. t.} \qquad r(kd) = y(kd) - \hat{y}(kd) \end{aligned} \tag{2.2}$$

where $r(kd)$ is the residual at time kd. The residual provides the difference between the recorded and predicted step counts at any time instant and the goal of the optimization problem is to make the predicted output as close as possible to the recorded one.

2.3.3 Response Dynamics

Models from weekdays and weekends were used to simulate responses to each message type. Impulse responses represent expected step count changes during each 15-minute epoch following receipt of each message type (compared to expected step counts if a message not been received). Cumulative step responses represent the total expected effect of each type of individual message. Error bounds were estimated for each response curve to indicate whether effects exceeded the threshold of noise in the model. Error bounds were computed taking the following steps:

1. Model coefficients are identified by solving the optimization problem 2.2.

2. The residual is computed using the formula $r(kd) = y(kd) - \hat{y}(kd)$.

3. The confidence interval is computed for the residual margin as

$$CI = \mu(r) \pm 2\sigma(r) \tag{2.3}$$

where $\mu(r)$ and $\sigma(r)$ are the estimated mean and standard deviation of residual, respectively.

4. The input response (zero state) and intrinsic response (zero input) are computed.

5. The error bound used to investigate the validity of responses to each message type is computed as the confidence interval for the input response as follows

$$CI_{input-response} = \frac{mean(y_{input}) * CI}{mean(y_{input}) + mean(y_{int})} \tag{2.4}$$

where y_{input} and y_{int} are the outputs of the system related to the input and intrinsic responses, respectively.

Seven features were extracted from the simulated impulse response and cumulative step response curves. Each feature was extracted separately for weekends and weekdays. These features include initial delay, peak magnitude, peak delay, steady state, rise time, settling time, and effective time, and are illustrated in Figure 2.1. This figure represents all these features on the impulse and cumulative step responses of a participant to one message type. This should be noted that in the figure, SS, RT, ST, EfT, InDel, PMag, and PDel refer to steady state, rise time, settling time, effective time, initial delay, peak magnitude, and peak delay, respectively.

As shown in the figure, initial delay, peak magnitude, and peak delay extracted from the simulated impulse response curve (left panel) are represent features of the latency to initiate a momentary message effect, i.e., the time that it takes for the message to start having a momentary effect, magnitude of peak momentary message effects that is the maximum momentary effect that the message has, and latency to peak momentary message effects that is how long it takes for the message to have its maximum momentary effect, respectively.

In the cumulative step response plot (right panel), the curved line is the upper error bound, and the thin straight black lines depict lines y = 10%, 90%, 95%, and 105% of the steady state. Steady state value is the ultimate amount of the cumulative step response, i.e., the summation of all step counts taken after receiving the message. Rise time is the time that it takes for the cumulative step response to advance from 10% to

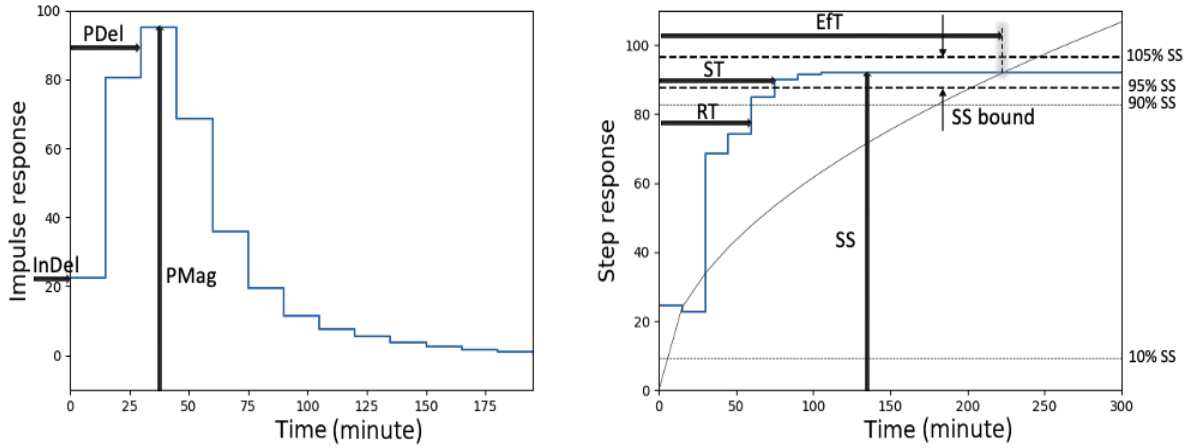

Figure 2.1: Features of the simulated impulse response (left panel) and cumulative step response (right panel) represented on the response of a participant to one type of messages shown in blue.

90% of the steady state, i.e., the time that takes for the massage to rise from low to high effect, as a ratio of the ultimate step counts. Settling time describes the time that the step response enters a boundary around the steady state with the upper- and lower bounds being 95% and 105% of the steady state which means the time that the response settles down around and close to the ultimate value. Effective time is the duration that the system response is above the noise level (outside the error bounds), i.e., the time that the effect of the message is measurable/differentiable from the noise.

2.3.4 Statistical Analysis

Descriptive statistics mean, standard deviation, and range were calculated for each model feature segmented out by message and day type. We conducted a series of two-way repeated measures ANOVAs with within-person factors for message and day type and each model feature as an outcome, to understand the main effects of message and day type and their potential interaction.

Two model features, effective time and peak delay did not meet the normality assumption, thus we conducted Friedman's Test for these two features looking at the main effects of message type on each model feature within datasets for weekdays and weekends. Effect sizes were calculated as η^2 for the two-way repeated measures ANOVA and Kendall's W for the Friedman's Test. For main effects that were found to be statistically significant, multiple pairwise comparisons were calculated to identify which groups significantly differed.

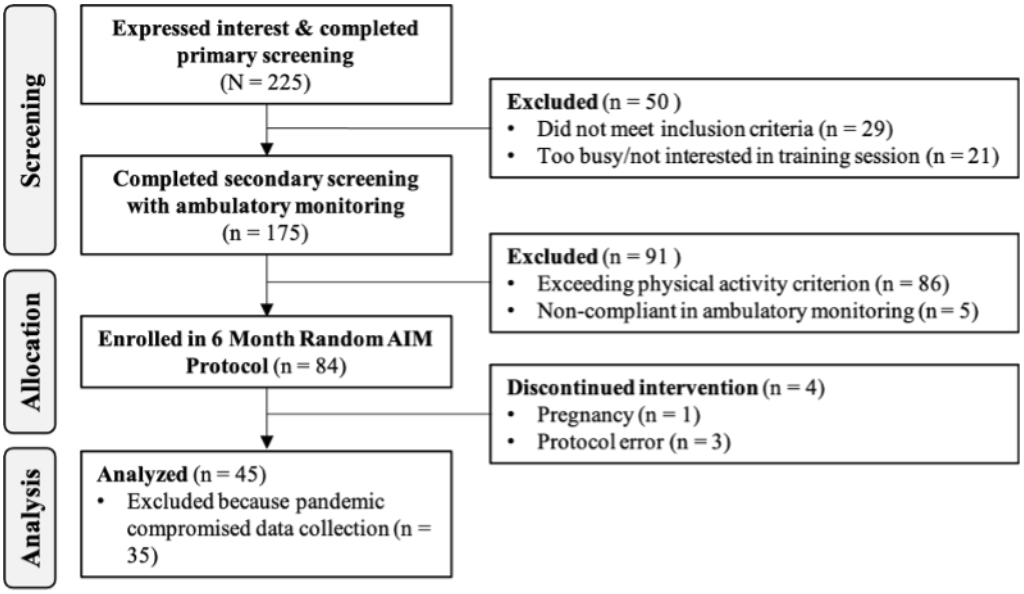

Figure 2.2: Participant flow in the Random AIM trial.

2.4 Results

Participant flow in the Random AIM trial is summarized in Figure 2.2. Approximately 45% of interested participants qualified and enrolled. The analytic sample (n = 45) was mostly women (n=30 [67%]) who identified as White (n=29 [64%]) and not Hispanic or Latino (n=43 [96%]). The sample included participants who identified as Asian (n=10 [22%]), African-American (n=4 [9%]) and two or more races (n=2 [4%]). The average age was 24.4 years (SD = 3.1, range = 18 – 29) and participants' highest level of education included no college education (15.9%), some college (22.7%), bachelor's degree (34.1%), and graduate or professional degrees (27.3%).

2.4.1 Message Delivery

For the 45 participants in the analytic sample, a total of 24,123 messages were scheduled on the server (M = 3.05 messages/person/day, SD = 0.16). Of the scheduled messages, 96.0% were received and displayed on the mobile device with the total of 23,149 messages (M = 2.92 messages/person/day, SD = 0.33), and 78.2% were acknowledged within 30 minutes of receipt (M = 2.38 messages/person/day, SD = 0.33). The mean latency of acknowledgements was 00:05:26 (SD = 00:20:46). Overall, 20,689 messages were paired with valid physical activity monitoring data for analysis and received messages were distributed as 40% Affective (8299 messages), 39% Social-Cognitive (8187 messages), and

20% Inspirational Quotes (4219 messages).

Most messages were delivered on weekdays (72%). The average Do Not Disturb window for participants spanned from 19:50 (95% CI = 16:30 - 23:10) to 09:20 (95% CI = 06:40 - 12:00) for weekdays and 20:30 (95% CI = 18:00 - 23:00) to 10:10 (95% CI = 08:00 - 12:20) for weekends. Acknowledged messages were distributed across the day so messages provided suitable coverage outside of waking hours outside the Do Not Disturb window (Figure 2.3, top row). Messages were distributed across all four seasons (Figure 2.3, bottom row). Due to the 6-month protocol duration, no participant was sampled in more than three seasons.

2.4.2 Dynamic Responses

Person-specific dynamical models of physical activity based on recent physical activity and three message types i.e., Affective, Social-Cognitive, and Inspirational Quotes, were identified over the weekdays and weekends. Simulated impulse response and cumulative step response curves were plotted for all the participants. Figures 2.4 and 2.5 illustrate these curves for two participants over the weekdays (top row) and weekdays (bottom row). As Shown in figure 2.4, this participant responded dominantly to Affective messages both on weekdays and weekends. On weekends, they also had a short positive response to Social-Cognitive messages but no effect was observed for other messages.

Second participant, illustrated in figure 2.4, responded positively only to Affective messages, with an increase of 222 steps, on weekdays. On weekends, they responded significantly to Social-Cognitive messages, an increase of 318 steps, and there was an interval of 90 minutes of positive response to affective messages. But no affect was observed for Inspirational Quotes messages either on weekdays or weekends.

Table 2.2 shows the means, standard deviations, and ranges for six model features extracted from person-specific dynamic models separated by day and message type. Initial delay was uniformly zero for this dataset, thus we focus on reporting results based on the other six features. Descriptively, the ranges present in this table show that there is significant heterogeneity in participants' behavioral responses to messages, especially on weekends when more extreme behavior change was observed for all message types.

Tables 2.3, 2.4, 2.5, 2.6, 2.7, and 2.8 represent seven features based on person-specific models individually over the weekdays and weekends in response to Affective, Social-Cognitive, and Inspirational Quotes messages (each in two sets; for participants 1-23 in the first table and participants 24-45 in the second table), respectively. Again, in each table, SS, RT, ST, EfT, InDel, PMag, and PDel refer to steady state, rise time, settling

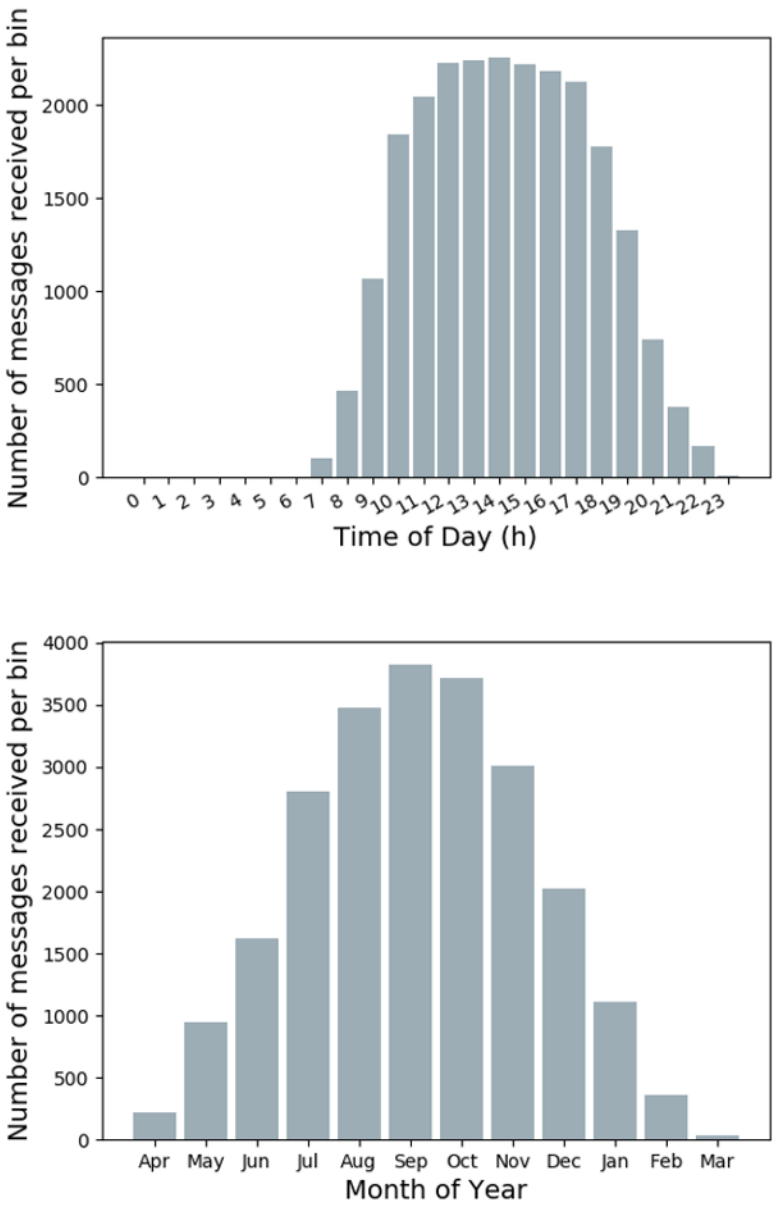

Figure 2.3: Message timing in the Random AIM trial. Frequency of daily timing outside of the do not disturb time window (top row) and across the calendar year (bottom row).

time, effective time, initial delay, peak magnitude, and peak delay, respectively.

2.4.3 Statistical Analysis

Table 2.9 presents the results from a series of two-way repeated measures ANOVAs with message and day type as within person factors and each model feature as the outcome

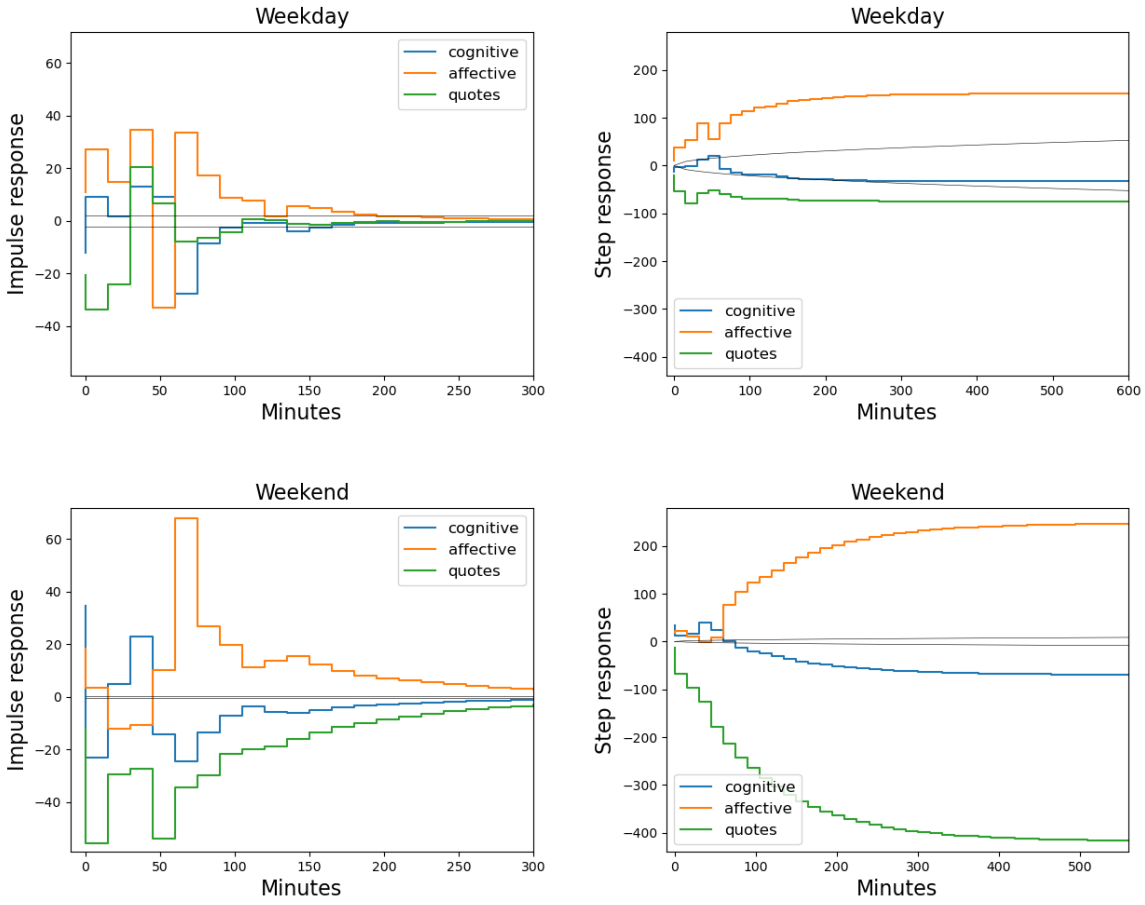

Figure 2.4: Simulated impulse (left panel) and cumulative step (right panel) responses following receipt of three types of messages on weekdays (top row) and weekends (bottom row).

of interest. The data were not normally distributed for effective time and peak delay; thus Friedman's Test was implemented to evaluate the relationship between message type and these two features, respectively. This table shows that there were no significant interactions between message type and day type for any of the model features.

Significant main effects were observed for day type with rise time, settling time, and peak magnitude meaning that the time it took for a message to go from low to high effect, the time that the effect settles close to steady state, and the magnitude of maximum momentary message effects were significantly associated with day type. Multiple pairwise comparisons revealed that each of these model features were significantly larger on weekends compared to weekdays.

Significant main effects for message type were observed with peak magnitude, meaning

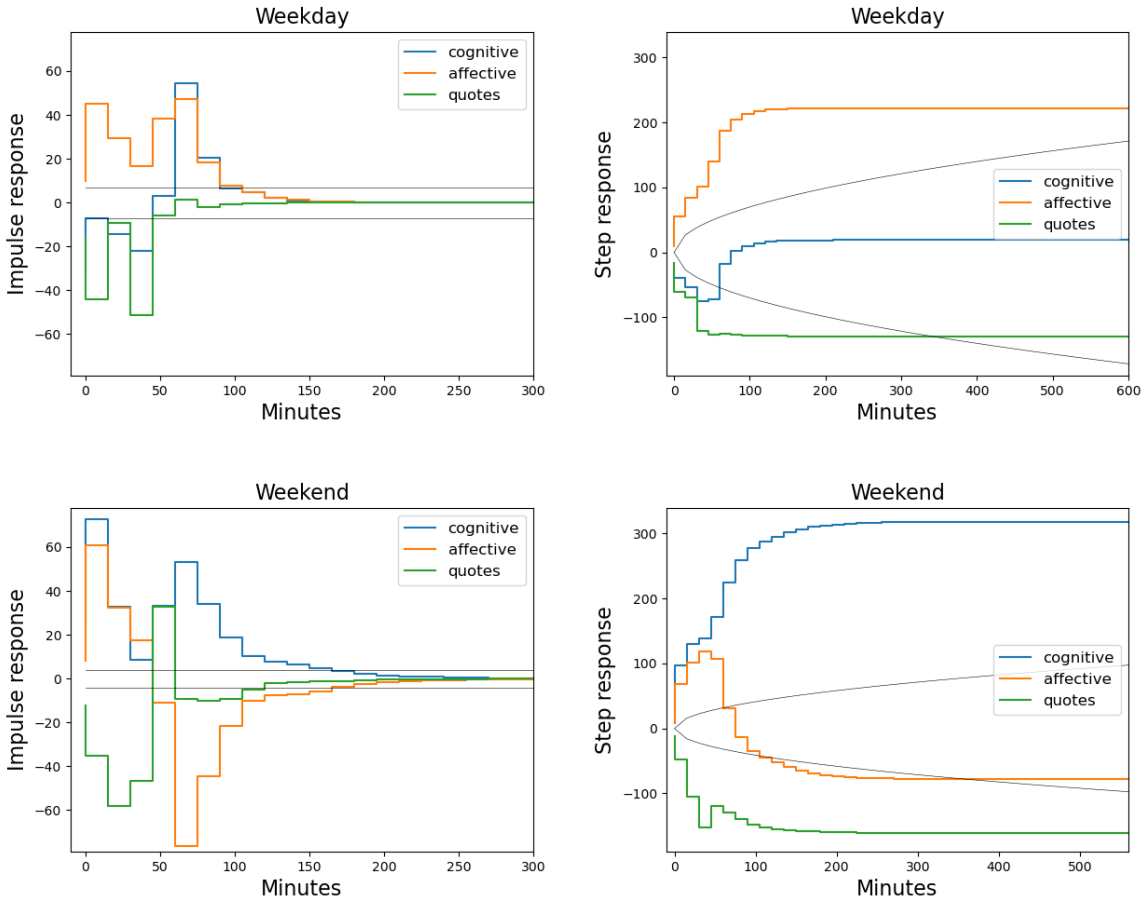

Figure 2.5: Simulated impulse (left panel) and cumulative step (right panel) responses following receipt of three types of messages on weekdays (top row) and weekends (bottom row).

that the magnitude of maximum momentary message effects differed significantly by message type. Multiple pairwise comparisons of these significant main effects revealed that affective messages and social cognitive messages had significantly larger peak magnitude than quotes.

Figure 2.6 shows the average steady state for each message type per participant separated by weekends and weekdays arranged by order of magnitude. This figure presents three key descriptive findings from this analysis: (1) the magnitude of the responses to each intervention message type was lower on weekdays than weekends, (2) average participant responses varied by intervention messages, with the minimal average response below zero and the maximal average response close to 800, and (3) average participant responses to intervention messages differed by person across message type.

Table 2.2: Descriptives of average model features by day and message type.

	Affective		Social-Cognitive		Inspirational Quotes	
	Mean (SD)	Range	Mean (SD)	Range	Mean (SD)	Range
Steady State						
Weekday	48.68 (87.68)	-152.95, 259.75	48.8 (129.3)	-101.86, 608.72	51.88 (117.69)	-169.52, 266.37
Weekend	90.77 (181.09)	-267.99, 796.6	49.62 (191.48)	-400.09, 516.8	12.28 (264.95)	-466.87, 753.93
Rise Time						
Weekday	76.33 (47.09)	0, 165	79 (49.38)	0, 240	71.67 (39.28)	0, 165
Weekend	89 (62.94)	0, 210	88.67 (62.16)	0, 270	96 (65.41)	0, 270
Settling T.						
Weekday	139.33 (47.93)	60, 240	151.33 (56.02)	60, 330	139 (46.72)	60, 270
Weekend	180.33 (60.63)	60, 345	182.67 (100.18)	75, 480	179 (71.89)	45, 375
Effective T.						
Weekday	134.67 (213.35)	15, 600	158.67 (222.01)	15, 600	221.33 (259.36)	15, 600
Weekend	231.67 (266.92)	15, 600	234 (262.71)	15, 600	252.67 (280.13)	15, 600
Peak Magn.						
Weekday	32.02 (14.84)	3.31, 67.58	37.65 (26.36)	10.11, 156.41	50.77 (25.49)	16.5, 120.92
Weekend	50.54 (24.7)	14.53, 121.9	55.34 (28.66)	10.63, 126.55	63.76 (39.01)	8.21, 196.92
Peak Delay						
Weekday	30 (21.92)	0, 60	26.33 (23.53)	0, 60	29.33 (22.38)	0, 60
Weekend	28.33 (24.19)	0, 60	23.67 (22.04)	0, 60	27.67 (23.05)	0, 60

Some participants differed by more than 250 steps per message between the different intervention message types. Thus, if a participant received the three messages of the optimal type, they would be expected to increase daily physical activity 750 steps more than if they received the same dose of their least optimal message type.

2.5 Discussion

We conducted a 6-month intervention in insufficiently active young adults to promote increases in step counts via digital messages. This secondary, exploratory analysis compared intervention responses to affectively-framed, social-cognitively framed and inspirational quotes messages to identify if one message type elicited a consistently greater intervention response after the delivery of one message.

Using system identification, we generated person-specific dynamical models of physical activity and found that ultimate step counts did not statistically significantly differ by message type, but the magnitude responses was greater on weekends compared to weekdays for all message types. We also observed significant participant heterogeneity such that some participants achieved their highest steady state from Affective messages, some from Social-Cognitive messages, and some from Inspirational Quotes. Thus, this exploratory analysis suggests that personalizing messages for participants in an intervention

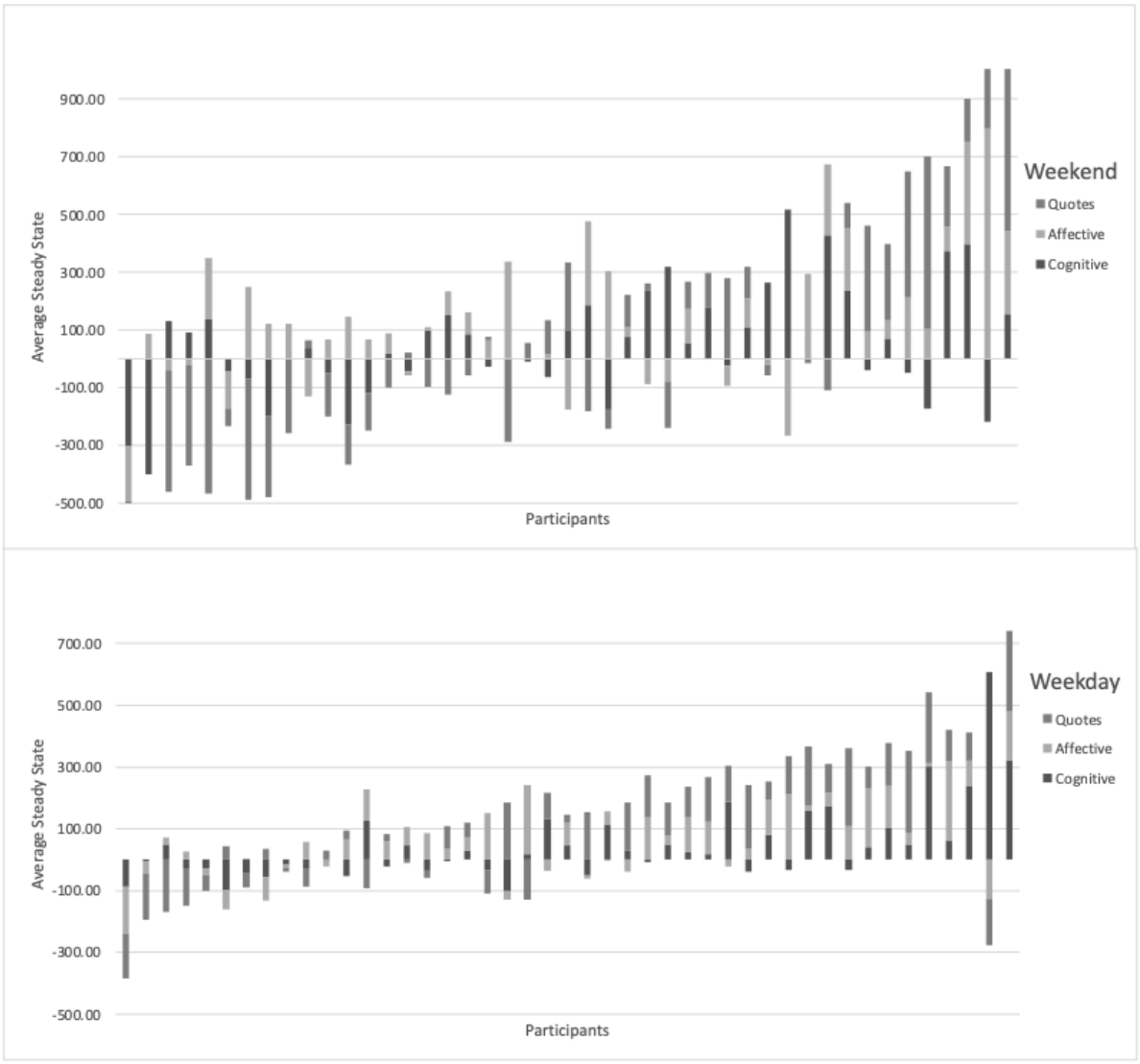

Figure 2.6: Participant-level differences in average steady state between affectively-framed and social-cognitively framed messages.

may be a worthy endeavor for generating greater step responses over time.

Prior research has yielded mixed results regarding whether affectively- or instrumentally-framed messages were more effective at promoting physical activity. Our results suggest that message effectiveness may be person-specific given the large ranges in steady state and the lack of statistically significant main effects by message type for steady state. The cognitive-affective system theory of personality may help provide further explanation for why we see varied responses to intervention messages [130]. This theory proposes that individuals have networks of cognitive and affective processing units that can be activated when an individual processes a situational feature, like an intervention message [130].

The specific nature of cognitive and affective processing units activated by messages account for individual differences in behavior change following a message [130]. Within each person, this system of units is consistent and results in predictable patterns of behavior across time [130]. Thus, applying this theory to our findings suggests that participants each have different systems of cognitive and affective processing units that result in idiosyncratic physical activity behavioral responses. Identifying the patterns of these behavioral responses over time can inform the selecting and timing of message content.

The favorable responses of some participants to the Inspirational Quotes were unexpected, given that these messages were purposefully not based in behavior change techniques or theories of behavior change and were intended to serve as a simple comparator. It may be that the Inspirational Quotes generated an affective response that led to a playful, exploratory behavior (broaden and build theory) or intentions to be active, however, we are unable to discern the mechanistic process from this analysis [131].

One observation that aligned well with past literature was that the ultimate step counts looked different on weekends and weekdays [1]. Message framing effects may be dependent upon the social context in which they are received. Given the reduced magnitude of step count responses to all message types on the weekdays, this difference could reflect an environmental constraint, such as work or school, that prevented action after the delivery of an intervention message. Personalization approaches that identify optimal times for message delivery may be especially valuable on weekdays.

This work echoes our prior work which showed differences in step count responses by day type and significant participant heterogeneity in response to message type; however, our prior work focused on Move More and Sit Less messages as opposed to affectively-framed and social cognitively-framed messages [15]. The median effect of digital interventions with adults is 943 steps/day [107], thus if a future intervention included multiple messages per day, knowledge of optimal participant response could become meaningful since about one-third of this sample showed a minimum of a 250 step difference between message types.

The heterogeneity between participants indicates that future interventions can benefit from methods that can both explore the effects of multiple message types on physical activity and exploit the most effective message types for an individual once identified. Given that messages have proximal effects on behavior in the minutes and hours after message delivery, the use of wearables for measuring physical activity behavior provides a rich source of information about behavioral dynamics. Harnessing this technology,

system identification and dynamical modeling can inform future work that uses model predictive control to continuously tune interventions based on participants' responses over time [132, 133].

This study used innovative person-specific dynamic modeling of intensive longitudinal data collected from a small sample of participants. Conventional statistical methods would dictate that this limits the inferences that can be drawn from these findings; however, in this method it is important to consider that each participant had six months of data and received a randomly-selected intervention message zero to six times per day, in the natural context of their daily life.

Other psychosocial and environmental factors could be influencing step counts that we are unable to account for in our models. However, the random aspect of our message delivery and type should mitigate the impact of potential confounding factors on our results. Conclusions may not generalize to other age groups given that messages were written for a young adult audience.

2.6 Conclusions

Inactive young adults may benefit from digital messaging interventions to promote increases in step counts. In this sample, there was not a consistent difference in step responses to affectively-framed and social-cognitively framed messages. Participants demonstrated heterogeneity in which message type elicited their highest average step response, with some showing more preference than others. Future work should consider incorporating multiple message types so that content can be continuously tuned to the individuals who respond more favorably to specific types of messages. Coefficients identified by the developed algorithm in this study can be used to design and implement just-in-time adaptive interventions by incorporating other tools from control systems engineering such as Model Predictive Control.

Table 2.3: Features of cumulative step and impulse responses to Affective messages; participants 1-23.

		Affective						
Participant	Day Type	SS	RT	ST	EfT	InDel	Pmag	PDel
AIM101	Weekday	57.42	45	135	60	0	32.57	60
	Weekend	120.69	135	195	600	0	28.56	15
AIM102	Weekday	-39.05	135	210	30	0	16.9	60
	Weekend	-20.19	15	300	135	0	48	0
AIM103	Weekday	44.33	60	90	15	0	36.82	45
	Weekend	75.46	15	195	600	0	37.96	0
AIM105	Weekday	150.31	165	225	600	0	34.57	30
	Weekend	247.78	210	345	45	0	68.02	60
AIM108	Weekday	-28.23	150	165	15	0	25.19	45
	Weekend	-190.71	150	195	15	0	71.4	45
AIM109	Weekday	-11.05	15	240	150	0	23.55	60
	Weekend	11.63	0	240	120	0	23.85	0
AIM110	Weekday	-127.97	45	75	15	0	41.34	15
	Weekend	120.35	0	165	600	0	104.57	0
AIM111	Weekday	-75.44	45	90	15	0	39.26	45
	Weekend	81.62	75	165	15	0	59.62	60
AIM112	Weekday	213.2	75	105	525	0	67.58	45
	Weekend	303.03	135	165	600	0	75.62	45
AIM113	Weekday	12.81	15	150	15	0	33.76	45
	Weekend	334.22	165	240	15	0	49.55	15
AIM114	Weekday	222.31	75	105	600	0	47.26	60
	Weekend	-78.16	105	225	75	0	76.44	60
AIM115	Weekday	80.75	120	150	15	0	32.49	60
	Weekend	-38.25	45	105	60	0	51.16	0
AIM116	Weekday	109.46	60	120	15	0	44.79	15
	Weekend	-267.99	60	105	15	0	67.78	45
AIM117	Weekday	39.82	120	150	15	0	16.3	60
	Weekend	86.94	165	180	15	0	53.61	60
AIM118	Weekday	29.29	45	165	15	0	17.57	30
	Weekend	-87.5	180	240	75	0	46.22	60
AIM119	Weekday	189.88	135	180	15	0	36.37	15
	Weekend	-129.45	105	135	600	0	37.07	30
AIM120	Weekday	87.09	150	225	15	0	16.77	60
	Weekend	117.96	90	195	15	0	55.78	60
AIM121	Weekday	36.05	15	75	30	0	18.36	0
	Weekend	-16.86	0	195	255	0	21.4	0
AIM122	Weekday	56.96	90	120	600	0	29.31	0
	Weekend	294.24	135	225	15	0	66.29	60
AIM123	Weekday	115.3	90	165	15	0	45.61	45
	Weekend	212.72	105	150	15	0	49.33	60
AIM124	Weekday	43.6	135	180	15	0	14.16	45
	Weekend	147.1	180	285	30	0	33.26	30
AIM125	Weekday	64.74	135	195	600	0	23.68	15
	Weekend	69.88	195	255	600	0	14.53	30
AIM126	Weekday	-37.45	90	135	15	0	18.69	45
	Weekend	215.63	195	255	600	0	56.28	0

Table 2.4: Features of cumulative step and impulse responses to Affective messages; participants 24-45.

		Affective						
Participant	Day Type	SS	RT	ST	EfT	InDel	Pmag	PDel
AIM127	Weekday	2.78	90	210	15	0	3.31	60
	Weekend	63.62	75	120	600	0	24.6	30
AIM128	Weekday	71.75	60	75	45	0	23	45
	Weekend	-175.92	105	135	600	0	64.12	30
AIM130	Weekday	106.03	105	165	15	0	41.23	45
	Weekend	95.71	105	135	15	0	36.44	15
AIM131	Weekday	-18.89	15	135	600	0	20.42	0
	Weekend	-0.5	0	210	75	0	16.83	0
AIM132	Weekday	25.91	150	225	30	0	21.71	15
	Weekend	66.7	180	255	600	0	19.66	0
AIM133	Weekday	-21.01	30	90	15	0	12.83	15
	Weekend	104.12	15	105	120	0	86.41	0
AIM134	Weekday	113.52	45	105	15	0	41.52	15
	Weekend	-3.61	0	180	15	0	21.65	60
AIM135	Weekday	-13.26	75	165	60	0	16.02	0
	Weekend	97.35	90	120	15	0	39.01	60
AIM136	Weekday	135.58	105	120	15	0	47.94	15
	Weekend	212.82	105	135	600	0	51.57	30
AIM137	Weekday	-38.31	150	165	15	0	23.85	60
	Weekend	245.7	30	60	15	0	108.03	30
AIM138	Weekday	35.17	15	75	165	0	24.4	0
	Weekend	-70.56	15	150	600	0	33.76	0
AIM139	Weekday	159.93	75	135	15	0	65.03	15
	Weekend	286.95	90	135	15	0	67.87	15
AIM140	Weekday	102.1	45	60	15	0	55.08	15
	Weekend	68.19	75	180	60	0	28.55	60
AIM141	Weekday	136.88	60	90	270	0	58.32	45
	Weekend	83.47	60	150	15	0	31.43	45
AIM142	Weekday	61.79	15	90	600	0	38.19	0
	Weekend	796.6	135	165	600	0	121.9	0
AIM143	Weekday	15.71	0	165	15	0	23.64	0
	Weekend	289.24	90	135	600	0	53.35	15
AIM144	Weekday	-60.5	60	75	195	0	24.51	30
	Weekend	14.66	0	210	600	0	36.21	0
AIM145	Weekday	21.71	0	120	30	0	25.3	30
	Weekend	32.64	15	105	60	0	51.6	15
AIM146	Weekday	-152.95	90	150	30	0	59.31	30
	Weekend	-21.14	135	270	60	0	27.23	0
AIM147	Weekday	35.66	30	105	15	0	34.88	0
	Weekend	354.4	105	135	15	0	79.37	60
AIM149	Weekday	259.75	90	120	450	0	44.96	0
	Weekend	63.95	45	120	15	0	46.07	30
AIM150	Weekday	-22.71	120	180	30	0	22.43	15
	Weekend	-129.83	75	150	15	0	32.2	45

Table 2.5: Features of cumulative step and impulse responses to Social-Cognitive messages; participants 1-23.

		Social-Cognitive						
Participant	Day Type	SS	RT	ST	EfT	InDel	Pmag	PDel
AIM101	Weekday	47.57	15	135	195	0	45.57	60
	Weekend	-4.19	0	420	195	0	60.08	0
AIM102	Weekday	30.61	120	180	15	0	31.67	0
	Weekend	91.48	15	180	600	0	56.1	30
AIM103	Weekday	172.95	150	210	585	0	29.85	15
	Weekend	85.59	105	195	15	0	34.27	30
AIM105	Weekday	-33.43	240	285	15	0	27.67	60
	Weekend	-69.87	225	390	75	0	34.62	0
AIM108	Weekday	-101.86	75	120	600	0	31.46	30
	Weekend	-302.29	135	165	15	0	67.65	45
AIM109	Weekday	-16.69	30	120	15	0	10.33	30
	Weekend	97.09	120	210	60	0	58.52	45
AIM110	Weekday	608.72	90	120	600	0	156.41	0
	Weekend	-195.41	30	90	600	0	87.53	15
AIM111	Weekday	-57.3	75	150	15	0	22.83	30
	Weekend	151.49	90	135	30	0	49.44	30
AIM112	Weekday	-33.95	15	90	15	0	29.62	45
	Weekend	-175.37	120	165	600	0	55.73	0
AIM113	Weekday	300.3	75	105	15	0	55.38	30
	Weekend	3.5	165	480	90	0	55.89	0
AIM114	Weekday	19.02	60	165	75	0	54.45	60
	Weekend	318.24	105	165	600	0	72.72	0
AIM115	Weekday	240.25	105	135	30	0	62.23	0
	Weekend	129.37	30	135	600	0	82.88	15
AIM116	Weekday	-34.22	75	165	15	0	23.46	60
	Weekend	516.8	105	120	600	0	108.58	60
AIM117	Weekday	115.64	30	90	330	0	43.83	15
	Weekend	372.46	90	165	15	0	100.85	45
AIM118	Weekday	49.14	165	210	45	0	12.86	0
	Weekend	236.2	165	195	600	0	50.16	0
AIM119	Weekday	40.07	150	225	15	0	24.6	45
	Weekend	37.93	30	150	150	0	50.06	15
AIM120	Weekday	-34.73	45	120	600	0	13.68	15
	Weekend	55.48	135	180	15	0	28.64	0
AIM121	Weekday	48.68	90	105	15	0	23.97	0
	Weekend	-40.79	15	105	600	0	22.43	0
AIM122	Weekday	-27.03	90	135	600	0	13.02	0
	Weekend	0.52	135	480	60	0	42.41	45
AIM123	Weekday	22.71	90	195	30	0	26.27	0
	Weekend	-47.28	90	165	15	0	17.84	30
AIM124	Weekday	28.06	90	195	15	0	10.11	60
	Weekend	-227.7	180	270	15	0	37.52	45
AIM125	Weekday	-53.62	165	330	600	0	30.51	60
	Weekend	18.37	270	330	15	0	10.63	60
AIM126	Weekday	132.42	105	135	420	0	32.87	0
	Weekend	236.2	120	180	600	0	55.34	0

Table 2.6: Features of cumulative step and impulse responses to Social-Cognitive messages; participants 24-45.

		Social-Cognitive						
Participant	Day Type	SS	RT	ST	EfT	InDel	Pmag	PDel
AIM127	Weekday	-42.56	90	120	360	0	17.57	0
	Weekend	-27.84	105	120	30	0	21.39	45
AIM128	Weekday	47.55	75	105	15	0	32.29	15
	Weekend	98.33	45	135	600	0	62.5	30
AIM130	Weekday	16.48	105	225	45	0	35.99	60
	Weekend	-38.74	30	210	15	0	60.07	60
AIM131	Weekday	-2.34	60	210	105	0	12.39	45
	Weekend	-8.34	0	165	420	0	12.22	30
AIM132	Weekday	-28.47	165	210	30	0	21.1	15
	Weekend	-117.8	225	360	45	0	64.03	0
AIM133	Weekday	187.71	60	90	15	0	63.59	45
	Weekend	-171.1	75	135	15	0	74.73	60
AIM134	Weekday	81.17	60	60	30	0	47.2	0
	Weekend	178.66	45	75	285	0	67.83	0
AIM135	Weekday	-49.39	60	135	15	0	27.51	45
	Weekend	110.99	45	75	15	0	34.31	30
AIM136	Weekday	103.02	120	150	15	0	39.91	0
	Weekend	136.2	120	165	15	0	50.1	0
AIM137	Weekday	-5.69	0	195	15	0	28.3	45
	Weekend	426.45	105	150	30	0	112.41	60
AIM138	Weekday	-3.84	15	180	15	0	33.59	15
	Weekend	-23.39	0	105	600	0	23.21	0
AIM139	Weekday	320.16	90	120	15	0	122.07	15
	Weekend	156.42	30	90	15	0	75.23	15
AIM140	Weekday	124.57	45	105	15	0	39.26	60
	Weekend	-47.64	45	120	330	0	18.44	0
AIM141	Weekday	-8.3	75	195	75	0	44.76	60
	Weekend	-400.09	105	135	600	0	69.95	0
AIM142	Weekday	-22.88	30	150	15	0	28.18	15
	Weekend	-217.92	105	165	15	0	51.1	30
AIM143	Weekday	160.3	45	60	210	0	50	30
	Weekend	185.85	45	105	15	0	77.82	15
AIM144	Weekday	-98.93	105	135	495	0	19.78	60
	Weekend	-63.18	90	165	600	0	21.17	15
AIM145	Weekday	49	60	90	600	0	33.37	0
	Weekend	75.69	90	165	30	0	26.82	45
AIM146	Weekday	-86.69	90	165	15	0	45.07	0
	Weekend	265.56	45	105	600	0	126.55	0
AIM147	Weekday	-39.79	30	75	15	0	55.31	15
	Weekend	398.41	75	105	15	0	117.06	15
AIM149	Weekday	59.93	15	150	15	0	49.35	30
	Weekend	69.8	60	180	60	0	49.2	60
AIM150	Weekday	-28.48	15	165	150	0	34.8	0
	Weekend	-41.39	30	120	15	0	34.09	45

Table 2.7: Features of cumulative step and impulse responses to Inspirational Quotes messages; participants 1-23.

		Inspirational Quotes						
Participant	Day Type	SS	RT	ST	EfT	InDel	Pmag	PDel
AIM101	Weekday	-9.25	0	150	75	0	71.06	0
	Weekend	-252.85	120	180	600	0	56.46	0
AIM102	Weekday	154.53	30	150	600	0	78.46	0
	Weekend	-350.9	150	195	600	0	61.65	0
AIM103	Weekday	91.98	45	135	165	0	85.93	0
	Weekend	-56.33	0	270	15	0	66.44	0
AIM105	Weekday	-75.05	30	165	600	0	33.74	0
	Weekend	-418.01	225	315	600	0	55.74	0
AIM108	Weekday	183.93	90	105	600	0	78.49	0
	Weekend	-211.06	105	165	15	0	46.86	0
AIM109	Weekday	-10.1	30	180	15	0	18.18	30
	Weekend	-95.43	105	210	60	0	44.71	60
AIM110	Weekday	-149.24	105	135	15	0	44	30
	Weekend	-282.77	135	225	30	0	62.26	60
AIM111	Weekday	35.69	75	150	15	0	70.81	45
	Weekend	-124.36	45	105	30	0	57.07	30
AIM112	Weekday	123.19	60	105	15	0	51.41	45
	Weekend	-65.89	45	135	30	0	51.32	30
AIM113	Weekday	228.13	105	120	15	0	64.75	60
	Weekend	-289.26	165	240	600	0	69.48	45
AIM114	Weekday	-128.83	45	60	345	0	51.39	30
	Weekend	-160.95	30	135	600	0	58.26	15
AIM115	Weekday	92.39	90	150	15	0	46.01	30
	Weekend	-423.15	75	120	600	0	99.63	60
AIM116	Weekday	252.04	90	120	600	0	46.29	15
	Weekend	0.35	75	255	45	0	103.36	30
AIM117	Weekday	-0.82	60	270	45	0	26.2	0
	Weekend	208.99	90	135	15	0	63.48	15
AIM118	Weekday	106.36	135	195	600	0	25.04	30
	Weekend	26.4	0	195	45	0	63.49	45
AIM119	Weekday	71.38	120	225	45	0	37.98	30
	Weekend	25.89	150	195	15	0	41.53	15
AIM120	Weekday	-22.76	135	210	45	0	23.39	30
	Weekend	93.7	120	180	15	0	23.65	15
AIM121	Weekday	266.37	105	135	600	0	66.12	60
	Weekend	22.23	15	120	420	0	29.46	30
AIM122	Weekday	-58.8	60	120	600	0	25.89	45
	Weekend	-14.49	270	315	15	0	32.91	60
AIM123	Weekday	99.32	60	120	30	0	64.44	45
	Weekend	436.79	75	165	15	0	148.36	60
AIM124	Weekday	47.16	120	165	15	0	36.61	45
	Weekend	-138.32	195	285	15	0	35.44	60
AIM125	Weekday	28.69	15	255	600	0	26.11	45
	Weekend	-101.24	180	285	30	0	23.03	60
AIM126	Weekday	83.12	75	180	30	0	47.86	60
	Weekend	87.23	165	330	30	0	38.07	0

Table 2.8: Features of cumulative step and impulse responses to Inspirational Quotes messages; participants 24-45.

		Inspirational Quotes						
Participant	Day Type	SS	RT	ST	EfT	InDel	Pmag	PDel
AIM127	Weekday	-46.59	15	135	435	0	27.2	0
	Weekend	12.36	15	135	60	0	8.21	45
AIM128	Weekday	27.13	75	90	15	0	37.05	30
	Weekend	237.07	120	165	600	0	58.64	0
AIM130	Weekday	146.11	45	75	315	0	46.36	0
	Weekend	366.16	105	150	600	0	95.98	15
AIM131	Weekday	29.51	60	165	600	0	21.59	45
	Weekend	56.1	0	90	600	0	50.67	0
AIM132	Weekday	-120.8	165	210	600	0	16.5	45
	Weekend	-131.56	225	375	75	0	59.9	45
AIM133	Weekday	117.64	30	75	45	0	55.37	0
	Weekend	597.8	75	105	600	0	159.43	0
AIM134	Weekday	59.04	120	135	15	0	33.5	60
	Weekend	120.19	60	105	15	0	31.62	15
AIM135	Weekday	154.05	75	135	600	0	34.61	60
	Weekend	111.34	15	90	60	0	72.19	0
AIM136	Weekday	138.29	15	90	120	0	79.48	0
	Weekend	-466.87	120	150	600	0	151.85	45
AIM137	Weekday	-152.07	105	150	600	0	45.32	60
	Weekend	-108.37	15	45	15	0	72.48	30
AIM138	Weekday	73.67	120	135	15	0	55.06	60
	Weekend	278.12	105	150	600	0	89.14	15
AIM139	Weekday	261.79	60	120	15	0	112.04	30
	Weekend	753.93	90	135	600	0	196.92	15
AIM140	Weekday	-92.12	90	105	15	0	29.57	60
	Weekend	-152.29	75	120	600	0	38.81	30
AIM141	Weekday	135.93	30	75	15	0	85.65	30
	Weekend	2.11	30	210	15	0	12.78	15
AIM142	Weekday	20.33	15	165	105	0	76.46	0
	Weekend	597.38	135	180	600	0	99.63	15
AIM143	Weekday	190.21	45	120	15	0	120.92	30
	Weekend	-180.86	75	150	30	0	57.44	0
AIM144	Weekday	43.74	30	120	45	0	19.16	0
	Weekend	118.2	105	165	600	0	35.72	60
AIM145	Weekday	-169.52	75	75	600	0	55.62	15
	Weekend	112.48	15	120	600	0	67.78	0
AIM146	Weekday	-146.62	90	135	15	0	70.64	30
	Weekend	-35.89	180	225	15	0	41.58	45
AIM147	Weekday	206.52	60	75	45	0	89.3	60
	Weekend	147.01	75	135	15	0	53.28	60
AIM149	Weekday	100.37	105	120	15	0	29.63	30
	Weekend	263.63	75	135	15	0	60.94	45
AIM150	Weekday	-51.24	120	150	30	0	23.59	0
	Weekend	-61.9	75	165	15	0	21.33	60

Table 2.9: Repeated Measures ANOVA results for message and day type main effects and interactions.

Feature	Effect	F/Chi-squared test	P-value	Eta2/Kendall's W
Steady State				
	Message	1.074	0.346	0.008
	Day	0.003	0.957	0.00001
	Interaction	1.376	0.258	0.009
Rise Time				
	Message	0.021	0.98	0.0001
	Day	5.484	0.024	0.02
	Interaction	0.815	0.446	0.003
Settling Time				
	Message	0.802	0.5	0.003
	Day	18.868	<0.001	0.075
	Interaction	0.307	0.707	0.001
Effective Time				
	Message on wd	3.53	0.171	0.039
	Message on we	0.504	0.777	0.006
Peak Magnitude				
	Message	10.987	<0.001	0.057
	Day	34.429	<0.001	0.084
	Interaction	0.423	0.63	0.002
Peak Delay				
	Message on wd	0.824	0.662	0.009
	Message on we	0.658	0.72	0.007

Chapter 3
Dynamical Models of Physical Activity Changes due to Pandemic

In chapter 2, we developed algorithms to investigate the physical activity behavior change in response to different message types i.e., Affective, Social-Cognitive, and Inspirational Quotes as the system's input. As discussed before, physical activity is a dynamic process and can be affected by many internal and external factors. In this chapter, we apply the developed algorithms to access the effect of contextual changes, i.e., the COVID-19 pandemic declaration, on the participants' responses to a digital messaging intervention. To do so, person-specific switched systems have identified for pre- and post-pandemic declaration stages for all the participants, and response speed and system features were extracted and analyzed from impulse and cumulative step responses.

Dynamical system modeling provides a solid framework for developing person-specific models and interpreting the dynamic physical activity behavior of the participants. Other techniques like reinforcement learning algorithms cannot be applied to the amount of data used in this study. Additionally, these methods are not capable of handling the noisy data [72]. System identification methods applied in this work make a balance between using sensor collected data to explore the dynamic physical activity behavior of the participants and the efficiency in the amount of data required for analysis. Additionally, these tools are well-suited to handle noisy datasets.

3.1 Physical Activity Behavior

Physical activity reduces risk for chronic disease and promotes well-being [134, 135]. The correlates and determinants of physical activity span many levels of influence and include biological, psychological, social, environmental, and policy-related factors [136–138]. The

COVID-19 pandemic declaration abruptly changed many individuals' environments via stay-at-home orders and remote work arrangements. These contextual changes adversely impacted physical activity but little is known about how these changes specifically impacted the dynamics of people's physical activity or responses to micro-interventions for promoting physical activity [139]. The stability of these models needs to be understood to inform decisions about whether it is necessary to adapt model-based decision rules in the face of dramatic contextual changes. In that regard, here we focus on comparing how responses to digital messaging micro-interventions to promote physical activity changed from before to after the COVID-19 pandemic declaration.

3.2 Dynamical System Modeling

Dynamical systems modeling can be used to predict future behavior based on current and recent behaviors. In these models, systems refer to processes that connect past and present values of an input/stimulus (different types of messages) to an output/outcome (physical activity behavior/step count). System identification tools from the field of control systems engineering can be applied to characterize how physical activity changes following digital message delivery [1, 15]. For example, these models can regress physical activity during a fixed epoch (15 min) on physical activity during prior epochs and a series of binary variables indicating whether a person received a digital message during each of those epochs. These models can be expanded to include multiple series of binary variables, each representing a different type of intervention content, or to describe the dynamics of weekend and weekday activity separately [1]. Coefficients from these models are difficult to interpret by themselves but can be used to simulate expected responses to different digital messages under varying conditions.

Responses to momentary intervention content can be simulated using coefficients corresponding to each message type at different lags and plotted to reveal the timing and magnitude of instantaneous and cumulative behavioral responses to momentary interventions in impulse response curves and cumulative step response curves, respectively. These curves illustrate expected instantaneous behavior changes during specific epochs (e.g., 15 min following message delivery, 60 min following message delivery) and cumulative behavior changes over time. They can be compared visually or quantitatively by extracting features of the responses for statistical analysis [132]. For example, features such as initial delay, peak magnitude, and peak delay can be extracted from impulse response curves to describe how quickly and with what magnitude a momentary intervention has

its largest instantaneous effects on behavior [15]. Likewise, features such as the steady state, rise time, settling time, and effective time can be extracted from cumulative step response curves to describe the ultimate effect of a single momentary intervention, how quickly that effect initiates, and how much time is required both to achieve the maximal effect and to have an effect above the noise level [15].

Our previous work represented that understanding the context around a person can lead to more accurate predictions about their expected responses to different types of messages at that moment [15]. More precisely, we have shown that the momentary weather indices moderate the size of expected effects of digital messages on future behavior. This finding is important in the context of the COVID-19 pandemic. System dynamics – the processes that reflect how people regulate their behavior – can be altered by contextual changes. At one level, the need for switched models to capture differences in physical activity dynamics on weekends and weekdays and linear-parameter varying models to capture temperature-graded behavioral responses illustrate how context impacts behavior [1, 15]. The COVID-19 pandemic provides another example of an abrupt change in context that can affect both physical activity and the systems that organize physical activity responses to interventions.

3.3 Effects of the COVID-19 Pandemic on Physical Activity

Beginning in March of 2020 in the US, the COVID-19 pandemic became a significant life event with a variety of psychological, social, environmental, and policy implications. Workplaces, schools, childcare centers, universities, and non-essential businesses were shut down or moved to virtual environments and people were ordered to stay at home. Many daily behaviors and routines were affected such as physical activity, sleep, alcohol use and substance use [140–142]. Research evaluating post-pandemic declaration physical activity changes have shown an approximately 20% decrease in step counts in the US [139]. Furthermore, survey research with participants enrolled in behavioral interventions indicated that 68.4% felt that COVID-19 impacted their ability to adhere to behavioral recommendations [143].

Developmental systems theory proposes that severe changes in a person's habitual environment can result in functional system disorganization and prompt reorganization processes to reconcile the change [144]. The reorganized system will reflect altered

behavioral dynamics in the new context. Responses to system disorganization are proposed to be person-specific given the variety of factors (at multiple levels) that influence physical activity. To date, evaluations of physical activity changes following the COVID-19 pandemic have primarily focused on behavior aggregated over time across groups of people [139, 145]. Less is known about how the dynamics of behavior changed over time despite evidence that physical activity involves substantial variance within the person over time [94, 121]. Person-specific dynamical models can reveal if the pandemic impacted physical activity dynamics or behavioral changes in response to intervention messages in different ways.

This manuscript uses data from the unique subset of participants who were enrolled prior to and following the pandemic declaration. The analyses here capitalize on the temporally-dense data collected from wearable devices and the unique contextual change caused by the pandemic declaration to evaluate impacts of that declaration on physical activity and person-specific dynamics.

3.4 Study Design

3.4.1 Participants

Leading up to and following the pandemic declaration, we were actively collecting data from the participants enrolled in Random AIM physical activity promotion study. The recruitment and exclusion criteria is similar to the one described in chapter 2. Demographic and anthropometric measurements, and physical activity screening and monitoring process are also explained in detail there.

The United States of America declared the COVID-19 pandemic on March 13, 2020. All participants included in this analysis were enrolled between November 2, 2019 and January 24, 2020 to ensure that each had at least 6 weeks of data for each of the pre- and post-pandemic models. A total of 54 completed screening during that period and 32 were excluded due to excessive physical activity (n = 28), failing to meet wear time requirements (n = 2), or insufficient data either before or after the pandemic declaration (defined as $\leq$ 3 messages from a library with accompanying physical activity data; n = 2). The study lasted 6 months for all the participants but the precise number of days for pre-pandemic and post-pandemic stages was different for each individual due to variability in enrollment dates.

The analytic sample, n=22, compromised of 55% women and 82% students with

mean age of 22.23 years (SD = 1.667, range = 20 – 27). The sample consisted of White (n = 9 [41%]), African-American (n = 8 [36%]), and Asian (n = 5 [23%]) participants; the majority of them were not Hispanic or Latino (n = 21 [95%]). Participants had an average BMI of 27.1 (SD = 7.1, range = 20.3 – 46.6) with 27% having obesity (BMI $\geq$ 30), 27% having overweight (BMI = 25 – 29.9), and 45% having a normal weight (BMI =18.5 – 24.9). Table 3.1 shows the sample characteristics in detail. It should be noted that SD and GED refer to standard deviation and General Educational Development credential, respectively.

Table 3.1: Participants Characteristics

Characteristic	**N (%)**
Age (years; Mean [SD])	22.2 (1.7)
Sex	
Female	12 (55)
Male	10 (45)
Educational Attainment	
Completed high school or a received GED	3 (14%)
Some college/Associate's degree	7 (32%)
Completed college	9 (41%)
Graduate or professional degree	3 (14%)
Employment Status	
Employed full-time	1 (5%)
Employed part-time	2 (9%)
Student	18 (82%)
Unemployed and not looking for work	1 (5%)
Race	
Asian	5 (23)
Black/African-American	8 (36)
White	9 (41)
Ethnicity	
Hispanic or Latino	1 (5)
Not Hispanic or Latino	21 (95)
BMI (kg/m2; Mean [SD])	27.1 (7.1)
BMI Classification	
Normal weight (18.5 – 24.9)	10 (45)
Overweight (25 – 29.9)	6 (27)
Obesity ($\geq$ 30)	6 (27)

3.4.2 Data Collection

For 6 months, eligible participants wore a Fitbit Versa/Versa Lite smartwatch to track minute-level step counts and heart rate, and received between 0-6 messages/day via the custom-designed, Random AIM app. Messages were drawn randomly from three content libraries: (1) "Move More" motivational messages (108 messages), (2) "Sit Less" motivational messages (108 messages), and (3) "Inspirational Quotes" (with no relation to physical activity or sitting time; 54 messages).

Move More and Sit Less messages were based on social-cognitive theory, typically highlighting an affective or instrumental outcome of physical activity and prompting use of a self-regulation strategy (e.g., setting a goal, planning an activity). Half of the messages were accompanied with a relevant image (e.g., physical activity for Move More messages, standing activity for Sit Less messages, and natural landscapes for Inspirational Quotes). After 6 months, a Zoom meeting was scheduled to guide the participants through the processes for removing the Random AIM app from their smartphone and switching their Fitbit app to a personal email account.

3.5 Data Analysis

Fitbit and message data were downloaded for the study period. Days prior to the start date or following the end date were removed. Next, any days corresponding to dates when participants reported injury or illness, notifications being off, etc., were trimmed. Data were then separated for the pre-pandemic and post-pandemic stages. Dates were labeled as weekdays and weekends. For all days, Fitbit data were trimmed to exclude data recorded more than two hours before the availability window opened or more than two hours after the availability window closed. This choice provided enough data for modeling the physical activity behavior changes after receiving a message either at the beginning or end of the availability window.

Appropriate pre-processing step was taken for participants with changes in their provided availability time through the study. Minute-level heart rate and step counts data were used to classify minutes as valid or missing. If heart rate was recorded, the corresponding step count for that minute was valid. If heart rate was not recorded but steps were greater than 0, the step count for that minute was valid. If heart rate was not recorded and zero steps were recorded, the step count for that minute was classified as missing. If the missing minutes were smaller or equal to 3, step counts for those minutes

were interpolated using linear interpolation method. Finally, minute-level step data were aggregated up to 15-min summaries (total step counts for the 15 min epoch).

3.6 Dynamical System Modeling and Statistics

3.6.1 System Identification

System identification using linear regression model with multiple variables was performed to identify the person-specific physical activity dynamical models. Building on prior work, physical activity was modeled as a switched system with different models associated with physical activity responses following receipt of each message type on weekdays and weekends [1,15,129], for before and after the pandemic declaration. The model order was considered 5 for all the participants since it provided a good trade-off between the model complexity and size of the model error. As mentioned in detail in chapter 2, identification of the system coefficients is done using the least square method.

Based on the identified person-specific models, simulated impulse and cumulative step responses were computed for each message type using the six (corresponding to model order, that is 5, plus the present epoch) coefficients for each message type and coefficients related to past five epochs step counts. Impulse responses represent the expected step count changes during each 15-minute epoch following receipt of each message type (compared to what would be expected if the message was not received). Cumulative step responses represent the total expected effect of each type of individual message (compared to what would be expected if the message was not received). Error bounds were computed for each response curve to differentiate patterned behavior change from mere noise in the data and modeling error.

3.6.2 Intervention Response Speed

Intervention response speed can be estimated for the system as well as for individual messages. To describe the response speed, another concept in dynamical systems modeling, the location of poles of the system, is useful. Poles' location provides qualitative insights into the response characteristics of the linear system. Among the poles of a system, the pole closest to the unit circle or farthest from the origin, is called the "dominant pole" and plays a key role in determining the speed of the response.

Accordingly, when comparing two systems, the one with larger dominant pole has a slower response. For example, considering one participant and the pandemic declaration

as the change point, if the dominant pole of the system describing the post-pandemic declaration data has a larger value in comparison to the dominant pole value of the system describing the pre-pandemic declaration data, that means the post-pandemic system has become slower and it takes longer for the participant to respond to a typical message. To analyze this effect, we compared the magnitude of the dominant poles for pre-pandemic and post-pandemic stage systems to assess the change in speed of responses to messaging intervention due to the pandemic declaration.

To further investigate the concept of poles and impulse response of a system, a brief description of the overall response of a linear system is necessary (see [146] for a detailed description of linear systems). The response of a linear system is the sum of the intrinsic response (zero input response), $y_{int}(kd)$, and input response (zero state response with inputs being the messages here), $y_{input}(kd)$, plus an additional noise. The linear system of order 5 with 3 inputs can be formulated as

$$\hat{y}(kd) = a_0 + y_{int}(kd) + \sum_{i=1}^{3} y_{input_j}(kd) + \epsilon(kd) \tag{3.1}$$

where $\sum_{i=1}^{3}(.)$ provides the summation over the responses to the three inputs (three type of messages that are Move More, Sit Less, Inspirational Quotes messages) and $\epsilon(kd)$ is the noise at time kd. Considering a system of order 5, the poles $p_1, p_2, \cdots, p_5$ are the solutions of the equation

$$z^5 - a_1 z^4 - a_2 z^3 - a_3 z^2 - a_4 z^1 - a_5 = 0. \tag{3.2}$$

Given the poles of the system, the intrinsic response and the input response are of the form

$$\begin{aligned} y_{int}(kd) &= c_{int,1}p_1^k + c_{int,2}p_2^k + c_{int,3}p_3^k + c_{int,4}p_4^k + c_{int,5}p_5^k \\ y_{input_j}(kd) &= (h_j * u_j)(kd) \\ h_j(k) &= c_{input_j,1}p_1^k + c_{input_j,2}p_2^k + c_{input_j,3}p_3^k + c_{input_j,4}p_4^k + c_{input_j,5}p_5^k \end{aligned} \tag{3.3}$$

where $p_1, p_2, \cdots, p_5$ are the poles of the system, c_{input_j}'s are constants related to responses to input j, c_{int}'s are constants related to the intrinsic response, and k is the time instant. The operation $(. * .)$ is called convolution and the input response, y_{input_j}, is the result of convolving h_j, the impulse response of the system related to input j, and the input u_j at time kd. In the context of messaging intervention, y_{int} is the response if no message intervention is provided and y_{input_j} is the response directly related to the effect of receiving

the intervention message j.

Poles, p's, are complex numbers, and their location provides qualitative insights into the response characteristics of the linear system. It should be noted that all poles of the system should lie on or inside the unit circle in order to have a stable system, a system that does not diverge due to internal or external changes. The distance of poles from the origin of the unit circle is an indicator of the speed of the response. Poles close to the unit circle (poles with larger values) represent responses that are slow and last longer; poles close to the origin (poles with smaller values) represent responses that are fast and decay quickly.

3.6.3 Statistical Analysis

Descriptive statistics were used to characterize the participant sample and identify mean and standard deviations for step counts and model features. Normality of the distributions for pre- and post-pandemic declaration values for step count, intervention response speed, and message specific response features was assessed. Based on the findings of the normality check, we ran paired t-tests or Wilcoxon signed-rank exact tests to test the statistical significance of the change in means after the pandemic declaration. Cohen's d (standardized mean difference) and r were calculated to provide an estimate of effect size for parametric tests and non-parametric tests, respectively. Pearson or Spearman rank correlations between model features segmented by message type and day type were calculated to understand the consistency of rank orderings between pre- and post-pandemic averages for person-specific dynamic model features.

3.7 Results

3.7.1 Message Delivery

In total, 10,805 messages were received and displayed on mobile devices (M = 491.1 messages/person, SD = 81.7) of which 5860 (54%) messages (M = 266.4 messages/person, SD = 101) were received in the pre-pandemic stage and 4945 (46%) messages (M = 224.8 messages/person, SD = 70.8) were received after pandemic declaration. Received messages were distributed between the "Move More" (pre-pandemic: n=2327 [40%]; post-pandemic declaration: n=1994 [40%]), "Sit Less" (pre-pandemic: n=2313 [39%]; post-pandemic declaration: n=1945 [39%]), and "Inspirational Quotes" (pre-pandemic: n=1220 [21%]; post-pandemic declaration: n=1006 [20%]) content libraries. Messages

were randomly distributed across each participant's availability window. A total of 8994 (75%) messages met criteria for system identification through evidence of step count and heart rate data collection at the time of the message receipt.

3.7.2 Changes in Physical Activity

In total, 2,422,306 minutes of physical activity were used to identify the models, of which 1,373,960 minutes preceded the pandemic declaration and 1,048,346 minutes followed the pandemic declaration. On weekdays, a total minute of 986,045 and 758,426 were used in modeling for pre- and post-pandemic stages while for weekends a total minute of 387,915 and 289,920 were considered for each period. The recorded minutes of activity, missing minutes defined as no heart rate data and zero steps, interpolated minutes and the total minutes used for modeling are illustrated in Table 3.2 and Table 3.3 for each individual, before and after pandemic declaration, over the weekdays and weekends, respectively. It should be noted that the minutes used for modeling is calculated as the total recorded activity minutes subtracting the missing minutes and adding the interpolated ones.

On weekdays, participants took an average (M $\pm$ SD) of 6170.36 ± 2008.4 steps/day before the pandemic declaration and 3278.1 ± 1733.4 steps/day after the pandemic declaration. This difference represented a large and statistically-significant decrease, $t(21) = 6.55$, $p < .001$, Cohen's d = -1.40. On weekends, participants took an average of 4199.7 ± 1650.5 steps/day before the pandemic declaration and 3645.7 ± 2185.1 steps/day after the pandemic declaration. This difference was not statistically significant, $t(21) = 1.23$, $p = .23$, Cohen's d = -0.26.

Table 3.4 and table 3.5 summarize participant-level data on average daily steps and number of days before and after the pandemic declaration over the weekdays and weekends, respectively. As shown in the last column of each table, the percentage of change, the amount of daily step counts changes, were different among the participants. Some even showed an increase in their daily step counts after the pandemic declaration and some kept it quite the same. But on average, the daily step counts decreased significantly on weekdays, by 44%, and 10% over the weekends.

3.7.3 Response Dynamics

Four dynamical models were identified for each participant; for pre- and post-pandemic stages each over the weekdays and weekends. Simulated impulse and cumulative step responses were plotted based on the person-specific models. Dynamics of physical activity

Table 3.2: Minutes of activity analyzed, missing data, interpolated, and minutes used in modeling for each individual before and after pandemic declaration over the weekdays.

	Weekdays - Pre-Pandemic				Weekdays - Post-Pandemic			
Participant	Total	Missing	Interpolated	Modeling	Total	Missing	Interpolated	Modeling
AIM161	75600	3872	275	72003	27720	1331	125	26514
AIM163	78960	6111	525	73374	29400	1696	154	27858
AIM164	77280	15815	393	61858	30240	4842	102	25500
AIM165	77280	16648	642	61274	30240	5583	178	24835
AIM166	73920	3785	652	70787	29400	1841	341	27900
AIM167	70560	13933	800	57427	37800	13668	286	24418
AIM170	68040	11766	182	56456	36960	6530	146	30576
AIM171	67200	1528	702	66374	39480	698	255	39037
AIM172	66360	8069	280	58571	42000	5757	255	36498
AIM173	66360	29434	647	37573	42000	22648	220	19572
AIM174	57120	3823	401	53698	46200	5322	460	41338
AIM175	39480	2599	111	36992	46200	2832	199	43567
AIM176	58800	45633	4270	17437	48720	40421	2645	10944
AIM177	55440	2979	367	52828	52080	4780	310	47610
AIM179	36120	7062	52	29110	44520	11681	67	32906
AIM180	34440	1911	157	32686	73080	5657	469	67892
AIM181	35280	3427	219	32072	45360	26656	161	18865
AIM182	31920	4017	133	28036	48720	6596	222	42346
AIM183	28560	17284	42	11318	50400	39778	52	10674
AIM184	31920	10640	128	21408	75600	50452	161	25309
AIM185	30240	4075	243	26408	77280	13129	496	64647
AIM186	30240	2053	168	28355	77280	8155	495	69620
Summation	1191120	216464	11389	986045	1030680	280053	7799	758426

represented different patterns of change among the participants before and after the pandemic declaration. This variability reflected in participants' preference for responding to specific message type (for example, changing the preference/dominant response from Move More to Sit Less messages) as well as the volume of change in different directions, also affected by day type.

In the following, pre- to post-pandemic physical activity dynamics are illustrated for some participants with different patterns of activity in the form of cumulative step response. In all figures, left and right panels represent the response in pre- and post-pandemic stages, respectively. The x-axis represents time since message delivery in minute scale, and the y-axis represents the predicted cumulative step count changes as a function of time following message delivery and in response to different message types. The narrow black lines in each plot represent the error bounds for the cumulative step response. Figure 3.1 represents an increase in the number of step counts after receiving a message from 148 to 235 after the pandemic declaration. Besides, the participant tended

Table 3.3: Minutes of activity analyzed, missing data, interpolated, and minutes used in modeling for each individual before and after pandemic declaration over the weekends.

	Weekends - Pre-Pandemic				Weekends - Post-Pandemic			
Participant	Total	Missing	Interpolated	Modeling	Total	Missing	Interpolated	Modeling
AIM161	31920	1504	101	30517	10080	292	44	9832
AIM163	31920	3654	211	28477	10920	742	62	10240
AIM164	31920	6914	140	25146	11760	2445	27	9342
AIM165	31080	6068	233	25245	12600	2523	61	10138
AIM166	29400	1009	276	28667	12600	699	108	12009
AIM167	28560	10567	317	18310	14215	4093	119	10241
AIM170	28560	4586	64	24038	14243	2992	51	11302
AIM171	26880	792	297	26385	15120	212	97	15005
AIM172	26880	6014	118	20984	15960	1973	92	14079
AIM173	26880	13018	220	14082	15960	10645	51	5366
AIM174	23520	1136	123	22507	17640	871	61	16830
AIM175	16800	1023	56	15833	17640	925	75	16790
AIM176	25200	19621	2143	7722	18480	15901	798	3377
AIM177	23520	2699	146	20967	20160	1691	144	18613
AIM179	15120	6305	17	8832	16800	6387	19	10432
AIM180	15120	758	55	14417	28560	1740	191	27011
AIM181	13440	928	105	12617	18480	10024	71	8527
AIM182	13440	2442	31	11029	18480	1934	86	16632
AIM183	11760	7068	21	4713	20160	16190	17	3987
AIM184	13440	6906	33	6567	30240	17649	88	12679
AIM185	13440	4477	72	9035	30240	6820	229	23649
AIM186	13440	1686	71	11825	30240	6549	148	23839
Summation	492240	109175	4850	387915	400578	113297	2639	289920

to respond to Move More messages after the pandemic declaration rather than Sit Less ones. Figure 3.2 is an example of a decrease in response to intervention messages. This participant responded positively to all three message types before pandemic with Sit Less being the preferred message, while they responded positively only to Move More messages which that also dropped into the error bound after 90 minutes.

Figure 3.3 represents the changes in the physical activity from before (left panel) to after (right panel) pandemic declaration over the weekdays (top row) and weekends (bottom row). As shown, the participant responded to Move More messages with an increase of 286 steps before pandemic while this value decreased to 115 after the pandemic declaration on weekdays. On weekends, the number of steps increased by 98 in response to Move More motivational messages and a small step increase in response to Inspirational Quotes shortly after receiving the messages before the pandemic while no significant increase in step counts observed after the pandemic declaration.

Seven features including initial delay, peak magnitude, peak delay, steady state, rise

Table 3.4: Average daily step counts changes and number of days from before to after pandemic declaration over the weekdays for all the participants.

	Weekdays				
	Pre-Pandemic		Post-Pandemic		Percentage of
Participant	Days	Daily Steps	Days	Daily Steps	Change
AIM161	90	6414	33	2695	-58%
AIM163	94	6633	35	4350	-34%
AIM164	92	5649	36	3233	-43%
AIM165	92	4917	36	3025	-38%
AIM166	93	3832	30	4615	20%
AIM167	84	8333	41	2071	-75%
AIM170	81	4609	47	1292	-72%
AIM171	80	8715	47	6064	-30%
AIM172	79	7343	50	8227	12%
AIM173	79	1108	50	830	-25%
AIM174	74	5152	55	2612	-49%
AIM175	46	5915	55	3089	-48%
AIM176	70	5942	55	3730	-37%
AIM177	66	3738	62	3867	3%
AIM179	38	5422	53	4058	-25%
AIM180	41	6776	87	1675	-75%
AIM181	42	7711	40	1681	-78%
AIM182	38	8932	58	3871	-57%
AIM183	31	5385	39	1851	-66%
AIM184	38	5885	90	1396	-76%
AIM185	36	7032	91	2817	-60%
AIM186	36	10305	92	5068	-51%
Sample Mean	64.55	6170.36	53.73	3278.05	-44%

time, settling time, and effective time were extracted from the simulated impulse response and cumulative step response curves. Each feature was extracted separately for weekends and weekdays before and after the pandemic declaration. Initial delay was uniformly zero for this dataset, thus we focus on reporting results based on the other six features.

Tables 3.6, 3.7, and 3.8 summarize descriptive statistics for overall response speed of the system and features of the simulated impulse and cumulative step responses based on the person-specific models before and after the pandemic declaration for weekdays and weekends. As shown, the range of participant values for each response feature is very wide. For example, the average steady state value for Move More messages is 54.23 for pre-pandemic and -87.16 for post-pandemic stages over the weekdays while it ranges from -359.64 to 428.56 and -902.87 to 235.93 for the pre- and post-pandemic stages,

Table 3.5: Average daily step counts changes and number of days from before to after pandemic declaration over the weekends for all the participants.

	Weekends				
	Pre-Pandemic		Post-Pandemic		Percentage of
Participant	Days	Daily Steps	Days	Daily Steps	Change
AIM161	38	4856	12	2508	-48%
AIM163	38	7565	13	5026	-34%
AIM164	38	4714	14	4123	-13%
AIM165	37	3039	15	5350	76%
AIM166	35	4123	13	5691	38%
AIM167	34	3469	17	1983	-43%
AIM170	34	3935	18	1451	-63%
AIM171	32	7169	18	6792	-5%
AIM172	32	3862	19	9768	153%
AIM173	32	974	19	584	-40%
AIM174	30	2967	21	2784	-6%
AIM175	20	2269	21	1608	-29%
AIM176	29	5084	19	3770	-26%
AIM177	28	2707	24	3759	39%
AIM179	16	3902	20	4760	22%
AIM180	18	3977	34	1900	-52%
AIM181	16	5720	16	2287	-60%
AIM182	16	5932	22	5986	1%
AIM183	14	2640	15	1930	-27%
AIM184	16	4087	36	1298	-68%
AIM185	16	2799	35	3020	8%
AIM186	16	6604	35	3828	-42%
Sample Mean	26.59	4199.73	20.73	3645.73	-10%

respectively.

Although over the weekdays, the average steady state value in response to Move More and Inspirational Quotes messages decreased significantly after the pandemic declaration, the amount of decrease in response to Sit Less messages was much lower, changing from 39.24 to 29.27. While average participant responded positively to all three types of messages pre-pandemic and only Sit Less messages post-pandemic over the weekdays, on weekends, they responded positively significantly to Move More messages and the response to Inspirational Quotes message, although positive, was close to zero for both stages.

Tables 3.9, 3.10, and 3.11 show the features for all the participants individually over the weekdays for pre- and post-pandemic stages in response to the three different types

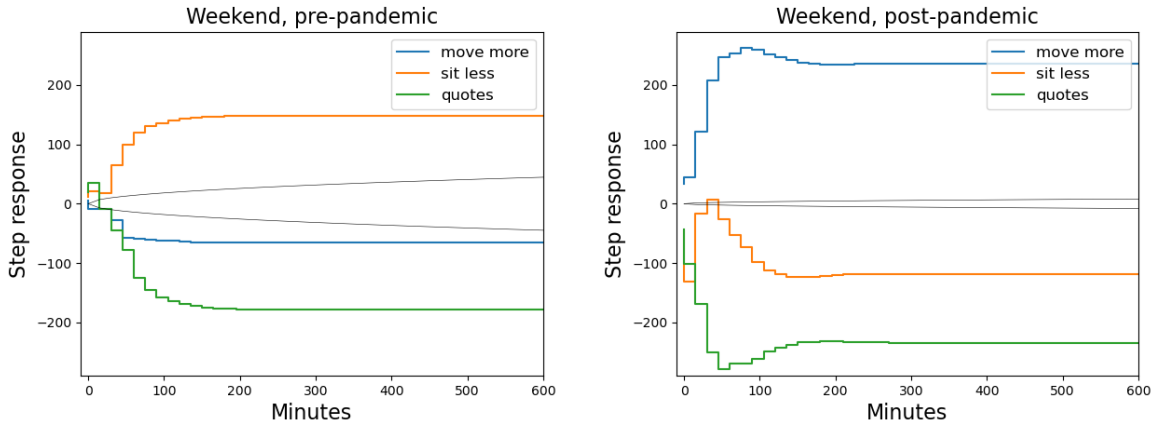

Figure 3.1: Simulated cumulative step response following receipt of three type of messages on weekends representing an increase in the physical activity following the pandemic declaration.

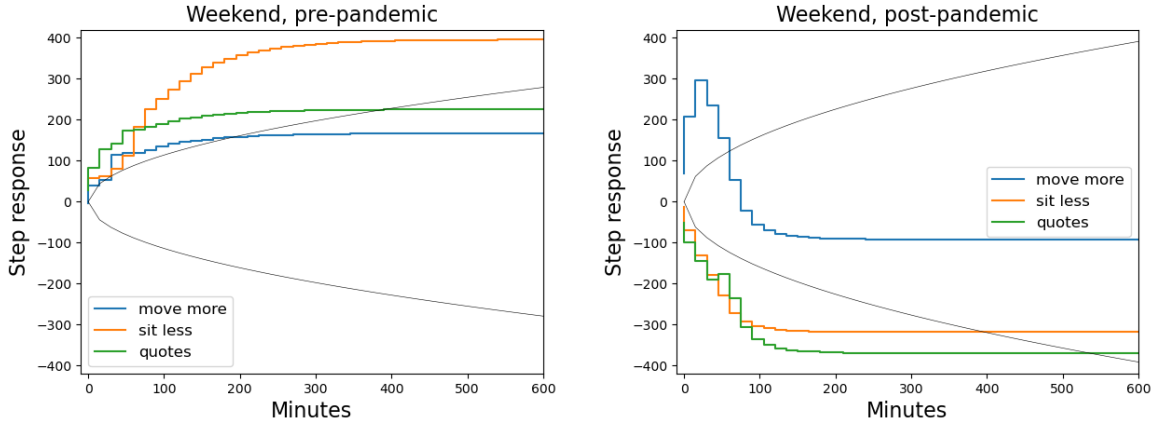

Figure 3.2: Simulated cumulative step response following receipt of three type of messages on weekends representing a decrease in the physical activity following the pandemic declaration.

of messages, respectively and Tables 3.12, 3.13, and 3.14 show such features over the weekends. For each participant, the top and bottom rows represent the features related to pre-pandemic and post-pandemic stages, respectively. All times are measured in minute scale. This should be noted that in each table, SS, RT, ST, EfT, InDel, PMag, and PDel refer to steady state, rise time, settling time, effective time, initial delay, peak magnitude, and peak delay, respectively.

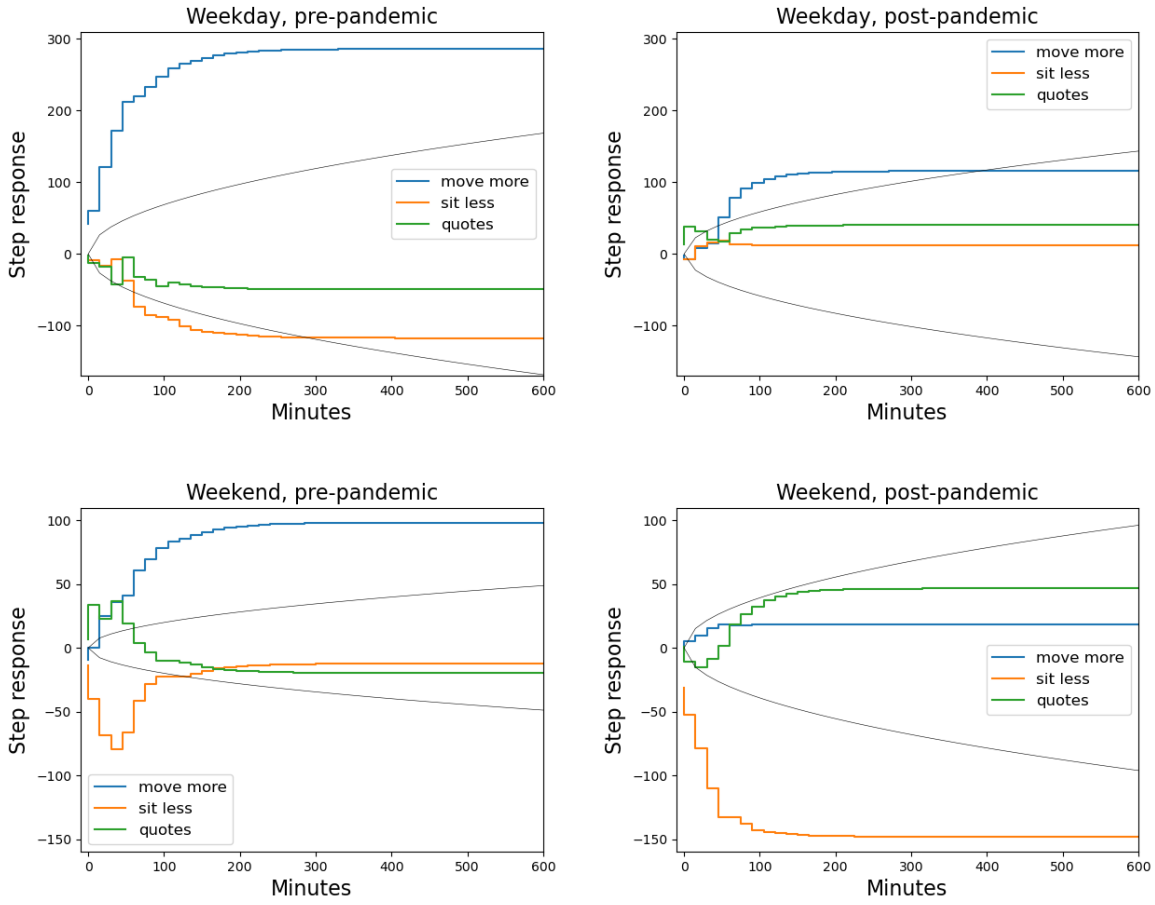

Figure 3.3: Simulated cumulative step response following receipt of three type of messages on weekdays (top row) and weekends (bottom row), representing a change in physical activity following the pandemic declaration affected by day type.

3.7.4 Absolute Changes in the Intervention Response Speed

The magnitude of the dominant poles represents the speed of the response. Poles were estimated separately for weekdays and weekends using data from before and after the pandemic declaration. Figure 3.4 represents examples of changes in the speed of response before and after pandemic declaration for two participants on weekdays (left panel) and weekends (right panel), respectively. As shown, for the participant on the left, the dominant poles got farther from the origin representing a decrease in the response speed while the participant on the right has their dominant pole closer to the origin after the pandemic showing a decrease in response speed.

On weekdays, the average dominant pole magnitude was 0.70 (SD = 0.10) before the pandemic declaration and 0.68 (SD = 0.08) after the pandemic declaration. On

Table 3.6: Average values of impulse and step response features and response speed for all person-specific models for pre-pandemic and post-pandemic stages over the weekdays.

Response Features &	Pre-Pandemic		Post-Pandemic	
Message Type	Mean (SD)	Range	Mean (SD)	Range
Response Speed	0.7 (0.1)	0.47, 0.86	0.68 (0.08)	0.54, 0.85
Peak Magnitude				
Move More	69.18 (51.14)	16.03, 195.05	43.97 (35.55)	7.97, 180.93
Sit Less	58.78 (32.93)	15.11, 130.27	39.6 (26.75)	15.53, 118.59
Inspirational Quotes	81 (81.64)	15.27, 413.79	49.8 (43.8)	9.29, 198.59
Peak Delay				
Move More	25.23 (22.39)	0, 60	26.59 (23.11)	0, 60
Sit Less	33.41 (23.11)	0, 60	25.23 (22.86)	0, 60
Inspirational Quotes	28.64 (21.17)	0, 60	31.36 (23.56)	0, 60
Steady State				
Move More	96.75 (263.86)	-472.77, 784.59	61.56 (262.98)	-240.24, 1106.29
Sit Less	-40.37 (203.49)	-583.64, 264.1	-19.02 (176.96)	-550.75, 279.76
Inspirational Quotes	-2.38 (326.65)	-470.83, 1072.26	0.95 (148.38)	-326.14, 354.66
Rise Time				
Move More	82.5 (64.6)	0, 270	103.64 (54.56)	0, 225
Sit Less	87.95 (56.75)	0, 225	85.91 (61.09)	0, 225
Inspirational Quotes	94.09 (52.41)	15, 225	64.09 (55.78)	0, 195
Settling Time				
Move More	159.55 (66.21)	60, 360	160.91 (54.81)	75, 330
Sit Less	163.64 (63.46)	75, 360	150 (60.53)	75, 315
Inspirational Quotes	162.27 (61.7)	60, 315	169.77 (71.92)	60, 315
Effective Time				
Move More	197.73 (249.31)	15, 600	239.32 (280.49)	15, 600
Sit Less	137.73 (218.73)	15, 600	262.5 (269.12)	15, 600
Inspirational Quotes	235.91 (264.31)	15, 600	111.14 (200.16)	15, 600

weekends, the average dominant pole magnitude was 0.73 (SD = 0.10) before the pandemic declaration and 0.70 (SD = 0.06) after the pandemic declaration. As seen in Tables 3.6, 3.7, and 3.8, dominant poles did not change significantly from before to after the pandemic declaration on either weekdays or weekends ($p > .05$). We concluded that, on average, the overall speed of the response describing physical activity dynamics did not change. Table 3.15 illustrates the absolute value of the dominant poles for all the identified models and the difference between the absolute value of the dominant poles from before to after the pandemic declaration.

Table 3.7: Average values of impulse and step response features and response speed for all person-specific models for pre-pandemic and post-pandemic stages over the weekends.

Response Features &	Pre-Pandemic		Post-Pandemic	
Message Type	Mean (SD)	Range	Mean (SD)	Range
Response Speed	0.73 (0.1)	0.54, 0.88	0.7 (0.06)	0.61, 0.88
Peak Magnitude				
Move More	60.53 (35.8)	19.78, 145.28	61 (45.68)	6.32, 209.86
Sit Less	62.51 (47.17)	22.14, 217.46	70 (52.79)	13.47, 238.5
Inspirational Quotes	97.85 (115.44)	26.66, 532.27	74.54 (55.55)	13.7, 216.33
Peak Delay				
Move More	23.86 (21.54)	0, 60	15 (16.69)	0, 60
Sit Less	27.27 (20.51)	0, 60	23.86 (22.04)	0, 60
Inspirational Quotes	23.86 (24.78)	0, 60	29.32 (21.45)	0, 60
Steady State				
Move More	54.23 (195.05)	-359.64, 428.56	-87.16 (225.44)	-902.87, 235.93
Sit Less	39.24 (246.55)	-325.55, 773.19	29.27 (253.44)	-614.32, 522.56
Inspirational Quotes	131.58 (400.83)	-200.49, 1458.44	-3.47 (218.04)	-455.16, 399.5
Rise Time				
Move More	115.91 (73.51)	0, 285	75 (48.55)	0, 150
Sit Less	102.95 (68.39)	0, 210	85.91 (66.63)	0, 270
Inspirational Quotes	90.68 (60.26)	0, 210	90 (51.75)	0, 225
Settling Time				
Move More	205.23 (73.1)	105, 420	158.86 (65.08)	90, 405
Sit Less	190.23 (76.54)	60, 330	158.86 (67.82)	90, 375
Inspirational Quotes	176.59 (63.46)	90	184.09 (59.31)	105, 300
Effective Time				
Move More	240 (268.17)	15, 600	246.82 (271.97)	15, 600
Sit Less	297.95 (284.31)	15, 600	301.36 (279.66)	15, 600
Inspirational Quotes	256.36 (265.8)	15, 600	296.59 (280.39)	15, 600

3.7.5 Absolute Changes in System Dynamics by Message Type

On weekdays, steady state, settling time, effective time and peak delay did not significantly change after the pandemic declaration for any message type ($p > .05$). As seen in Table 3.6, Wilcoxon signed-rank tests indicated that the median peak magnitude decreased significantly for both (a) Move More messages from before ($Mdn = 54.7$) to after the pandemic declaration ($Mdn = 35.8$), and (b) Sit Less messages from before ($Mdn = 51.5$) to after the pandemic declaration ($Mdn = 30.1$). The mean rise time for Inspirational Quotes also decreased significantly after the pandemic declaration.

On weekends, peak magnitude, peak delay, and effective time did not significantly change after the pandemic declaration for any message type. As seen in Table 3.7,

Table 3.8: Statistical tests on the features over the weekdays and weekends.

Response Features & Message Type	Weekdays			Weekends		
	Test Statistic	p	Effect Size	Test Statistic	p	Effect Size
Response Speed	t(21) = -0.84	0.408	d = -0.18	z = 0.86	0.389	r = .18
Peak Magnitude						
Move More	z = -2.09	0.036	r = -.45	z = 0.18	0.858	r = .04
Sit Less	z = -2.16	0.031	r = -.46	z = -0.11	0.91	r = -.02
Inspirational Quotes	z = -1.32	0.189	r = -.28	z = 0.60	0.548	r = .13
Peak Delay						
Move More	t(21) = 0.18	0.856	d = 0.04	z = 1.52	0.128	r = .32
Sit Less	t(21) = -1.05	0.307	d = -0.22	t(21) = -0.57	0.576	d = -0.12
Inspirational Quotes	t(21) = 0.39	0.699	d = 0.08	t(21) = 0.86	0.401	d = 0.18
Steady State						
Move More	z = -0.70	0.485	r = -.15	t(21) = -2.32	0.031	d = -0.49
Sit Less	t(21) = 0.48	0.635	d = 0.10	z = -0.08	0.935	r = -.02
Inspirational Quotes	z = 0.05	0.961	r = .01	z = 0.80	0.426	r = .17
Rise Time						
Move More	z = 0.96	0.337	r = .20	t(21) = -2.37	0.028	d = -0.50
Sit Less	z = -0.49	0.623	r = -.10	z = 1.09	0.276	r = .23
Inspirational Quotes	t(21) = -2.61	0.016	d = 0.56	t(21) = -0.04	0.966	d = -0.49
Settling Time						
Move More	z = 0.28	0.778	r = .06	z = 2.31	0.021	r = .49
Sit Less	z = -1.47	0.142	r = -.31	z = 1.32	0.186	r = .28
Inspirational Quotes	t(21) = 0.48	0.637	d = 0.10	t(21) = 0.35	0.729	d = 0.08
Effective Time						
Move More	t(21) = 0.48	0.634	d = 0.10	t(21) = 0.10	0.921	d = 0.02
Sit Less	z = 1.40	0.161	r = .30	t(21) = 0.05	0.961	d = 0.01
Inspirational Quotes	z = -1.45	0.147	r = -.31	t(21) = 0.48	0.635	d = 0.10

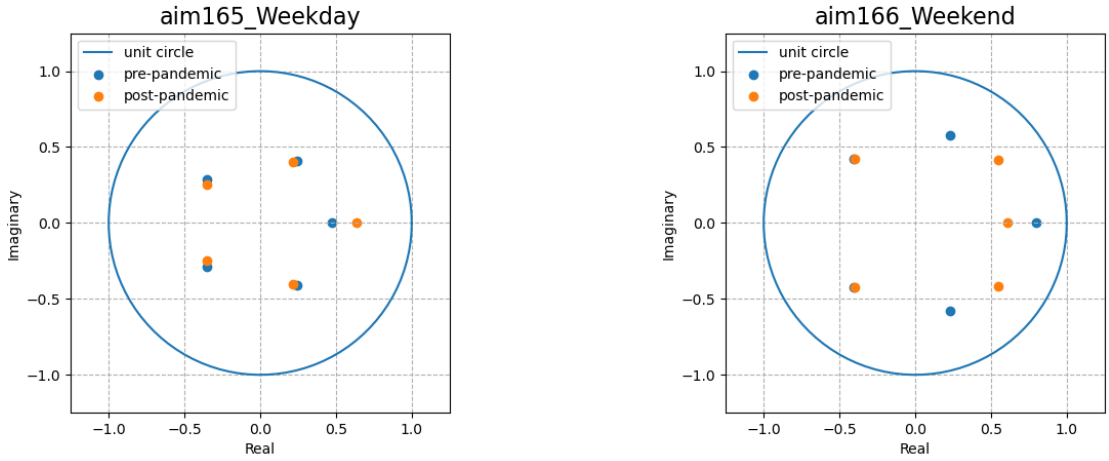

Figure 3.4: Poles location for two participants before and after the pandemic declaration.

the mean steady state and rise time for Move More messages decreased following the pandemic declaration, such that both the overall step response decreased and the time it took to move from 10% to 90% of that overall step response decreased after the pandemic declaration. Settling time increased significantly for Move More messages, indicating that more time was required for responses to reach their ultimate level following the pandemic declaration. Steady state, rise time, and setting time did not change significantly for Sit Less or Inspirational Quotes messages.

3.7.6 Relative (Rank-Order) Changes in System Dynamics by Message Type

Table 3.16 presents correlations between corresponding features of each message type before and after the pandemic declaration. Overall response speed pre-pandemic was not significantly correlated with post-pandemic declaration response speed on weekdays or weekends. Specific model features before and after the pandemic declaration were, with a few exceptions, weakly correlated and not statistically significant. On weekdays, rise time for pre- and post-pandemic declaration responses to Sit Less and Inspirational Quote messages exhibited statistically significant positive correlations, as did settling time for pre- and post-pandemic declaration responses to Sit Less messages. None of the other weekday response features were significantly correlated nor were any weekend response features significantly correlated.

3.8 Discussion

We investigated the impact of the pandemic declaration on physical activity and person-specific response dynamics to a digital messaging intervention. Step counts significantly decreased on the weekdays after pandemic declaration but not on weekends. We hypothesized that overall system intervention response speed would slow after the pandemic declaration and that message specific response features would change; however, on average, overall system response speed did not significantly change and, with few exceptions, most model response features did not change either.

Finally, we hypothesized that the rank ordering of model features would remain consistent after pandemic declaration and they would be significantly positively correlated; however, for the most part, correlations were weak showing that model features were not consistent within participants after the pandemic declaration. Together, these results

support the notion that significant changes in context can impact some aspects of physical activity behavior and participant response dynamics within a digital messaging intervention.

A key contribution of these findings is that the pandemic declaration impacted physical activity more on weekdays than on weekends. Prior work evaluating the impacts of the COVID-19 pandemic on physical activity in the United States have reported significant decreases in physical activity following the pandemic declaration [139,147,148]. Compared to analyses that specifically evaluated step counts, the change we observed was greater (1000 step/day decrease across 239,543 people [139]; 2232 steps/day decrease in 268 adults [148]). This could be due to age differences; our sample focused specifically on young adults whereas those studies sampled any US Argus app users ([139]) and US adults 18-74 years old ([148]).

A longitudinal study in England that looked at the effects of age showed that younger people 14-34 years old experienced the most change in activity after lockdown and remained the least active throughout compared to persons 35-44, 45-54, 55-64, and 65 years or older [149]. However, our work contrasts with an analysis of US college students physical activity based on pre-pandemic activity level [150]. Active students were the only group that experienced decreases, while inactive and moderately- active students experienced increases or no change based on activity intensity. Our entire sample was composed of insufficiently-active individuals. Another key difference is that we used device-based measures that could capture behavior before and after the pandemic declaration, whereas Barkley et al. used self-report measures that asked students to recall their activity before and after the pandemic declaration, which may have been susceptible to recall bias [150].

To our knowledge, this is the first evaluation that shows different physical activity changes on weekdays and weekends after the pandemic declaration. Physical activity is a dynamic behavior that can vary by time of day or from day to day across groups, and demonstrate significant variability within individuals [95, 121]. Given prior work showing different physical activity patterns on weekends and weekdays, it stands to reason that the impacts of the pandemic on physical activity would differ by day type. Lockdown/stay-at-home orders directly impacted engagement with work and school, which occupy a significant amount of time, typically only on the weekdays. The weekends inherently involve less exogenous control; thus, people may have experienced a less significant change in their routine on the weekends or they were able to adapt better to experienced changes due to having more discretionary time.

After evaluating absolute and relative changes in response dynamics by message type, we concluded that change occurred in intervention response post-pandemic declaration and the type and magnitude of the change differed within and between people. Relative changes in model features show that intervention responses were more stable on weekdays than weekends. This finding could be due to instability in the model due to having less weekend data or it could reflect larger reorganizations of behavior given the greater discretionary time that people have on the weekends compared to the weekdays.

Developmental systems theory proposes that when humans experience transformational change, they can reject or suppress the change and maintain existing organization, they can change aspects of themselves to accommodate the change, or they can change their relationship with their environment to accommodate the change [144]. This array of options for how change can be accommodated may provide framework for responses across varying contexts. It could be that pandemic-induced contextual changes affected cognitive, affective, or motivational processes resulting in a change in behavioral response to message content. However, we are unable to test this mechanistic speculation because this study design focused on measuring what excites the system and elicits a response rather than what changes inside the person.

This work extends a prior work represented in chapter 2 and publication from our group on dose-finding by showing that person-specific models vary as the context of behavior evolves [15]. We have previously found that generic models are conservative in representing the physical activity of individuals and there is a need for person-specific models [1, 15]. The person-specific models in this analysis showed considerable variability in extracted model features before and after the pandemic declaration, adding support that person-specific approaches are needed for dynamic behaviors. Additionally, differences in individuals' responses over the weekends and weekdays reinforce the need for switched systems based on the day of week [1]. These findings are consistent with prior findings that a structure describing group-level variations cannot describe the variations in the individual level and thus person-specific approaches may yield efficient treatment decisions for individuals [151].

Failure to deploy person-specific decision rules could lead to less effective interventions and potential treatment fatigue by users [152]. Furthermore, this analysis adds support for the development of continuous tuning interventions since it provides evidence that abrupt changes in context impact health behavior and intervention response within and between people. Continuous tuning interventions "use data about the individual to progressively refine and "tune" the intervention content, delivery feature(s) or timing to

the idiosyncrasies of the individual" [94]. We hope that we will not experience another pandemic, but other normal life events could dramatically impact behavioral systems (e.g., pregnancy, parenting a child, adopting a pet, moving, starting school or a new career). Physical activity interventions may need to be person-specific and continuously tuned in order to have the greatest effect across people. Future work is needed to empirically test the efficacy and effectiveness of person-specific adaptive interventions for physical activity promotion.

3.8.1 Limitations and Challenges

The small sample size reduced our ability to detect statistical significance, thus explaining the differences observed in significant p-values and meaningful effects. Findings were based on insufficiently-active young adults and may not generalize to more active young adults or to midlife and older adult populations. Physical activity behavior was measured with a wrist-worn Fitbit device, which may not be as accurate as a research-grade activity monitor worn at the waist or thigh. We investigated the effect of the pandemic as an external factor on physical activity behavior and intervention response; however, given that this was a natural experiment, other unmeasured factors may have influenced these changes, such as physical or mental health.

Young adults may have experienced temporary changes in living arrangements during campus closures or after loss of employment. From a statistical standpoint, assumptions were checked before running each test, however, there were some potential concerns with linearity for the correlation analyses. All of our dynamical models assumed similar memory (all order 5) and model parameters were constants and not allowed to vary as a function of other conditions at the time of message receipt, such as location or weather.

Notwithstanding these assumptions, dynamical system modeling provided a solid framework for developing person-specific models and interpreting the dynamic physical activity behavior of the participants. System identification methods applied here make a balance between using sensor collected data to explore the dynamic physical activity behavior of the participants and the efficiency in the amount of data required for analysis and are well-suited to handle noisy datasets.

3.9 Conclusions

This study revealed that the abrupt change(s) in daily life following the COVID-19 pandemic declaration significantly impacted both physical activity levels and the dynamics of physical activity, including how people responded to digital messaging interventions. Researchers evaluating behavioral interventions may want to consider the implications of the COVID-19 pandemic when assessing the efficacy or effectiveness of their intervention as this event may have impacted participant responses to other interventions as well. The implications of this work demonstrate the importance of developing person-specific, continuously-tuned interventions that take into consideration external factors that can cause reorganization of behavioral systems. The next step is to extend the developed algorithms and apply them in designing a controller that periodically updates the decision rule based on incoming data.

Table 3.9: Features of cumulative step and impulse responses to Move More messages for person-specific models over the weekdays.

		Weekday - Move More						
Participant	Stage	SS	RT	ST	EfT	InDel	Pmag	PDel
AIM161	Pre-Pandemic	-40.39	90	150	330	0	16.63	0
	Post-Pandemic	16.82	0	135	150	0	18.46	0
AIM163	Pre-Pandemic	102.89	270	360	15	0	30.92	60
	Post-Pandemic	-240.24	195	255	600	0	41.89	0
AIM164	Pre-Pandemic	58.58	0	75	600	0	62.35	0
	Post-Pandemic	66.92	60	165	45	0	35.67	30
AIM165	Pre-Pandemic	124.33	45	75	15	0	35.42	30
	Post-Pandemic	69.4	105	135	600	0	24.33	60
AIM166	Pre-Pandemic	85.92	75	135	15	0	37.3	45
	Post-Pandemic	-100.18	15	135	600	0	80.02	0
AIM167	Pre-Pandemic	-42.61	15	285	75	0	54.52	0
	Post-Pandemic	-101.97	135	210	15	0	31.36	15
AIM170	Pre-Pandemic	-19.06	0	150	30	0	27.8	0
	Post-Pandemic	34.67	225	330	30	0	24.26	15
AIM171	Pre-Pandemic	-133.44	105	165	30	0	40.22	45
	Post-Pandemic	-55.62	105	150	15	0	28.52	60
AIM172	Pre-Pandemic	269.31	105	150	600	0	84.33	15
	Post-Pandemic	1106.29	120	165	600	0	180.93	15
AIM173	Pre-Pandemic	25.15	15	135	285	0	16.03	45
	Post-Pandemic	17.63	75	135	45	0	30.19	30
AIM174	Pre-Pandemic	285.98	120	165	600	0	61.91	15
	Post-Pandemic	115.46	90	150	15	0	36.28	45
AIM175	Pre-Pandemic	-159.56	60	105	600	0	43.32	15
	Post-Pandemic	159.3	120	210	15	0	34.55	60
AIM176	Pre-Pandemic	655.13	135	195	15	0	111.6	30
	Post-Pandemic	117.41	75	135	15	0	61.56	15
AIM177	Pre-Pandemic	106.72	105	135	600	0	37.12	0
	Post-Pandemic	213.24	90	120	45	0	68.51	60
AIM179	Pre-Pandemic	94.27	30	60	15	0	57.68	15
	Post-Pandemic	-201.58	90	135	600	0	44.07	15
AIM180	Pre-Pandemic	24.65	60	135	15	0	50.29	30
	Post-Pandemic	-10.76	135	150	15	0	7.97	45
AIM181	Pre-Pandemic	784.59	120	195	15	0	187.67	60
	Post-Pandemic	-52.79	15	75	600	0	35.98	0
AIM182	Pre-Pandemic	160.96	90	165	15	0	54.85	45
	Post-Pandemic	-141.34	120	135	15	0	37.68	30
AIM183	Pre-Pandemic	-176.17	15	180	405	0	195.05	0
	Post-Pandemic	45.38	135	150	600	0	44.4	60
AIM184	Pre-Pandemic	248.63	150	180	30	0	87.63	0
	Post-Pandemic	221.42	75	90	600	0	66.01	0
AIM185	Pre-Pandemic	-472.77	165	195	15	0	69.67	60
	Post-Pandemic	82.63	150	180	30	0	21.45	30
AIM186	Pre-Pandemic	145.47	45	120	30	0	159.73	45
	Post-Pandemic	-7.72	150	195	15	0	13.26	0

Table 3.10: Features of cumulative step and impulse responses to Sit Less messages for person-specific models over the weekdays.

		Weekday - Sit Less						
Participant	Stage	SS	RT	ST	EfT	InDel	Pmag	PDel
AIM161	Pre-Pandemic	101.19	45	75	600	0	51.47	15
	Post-Pandemic	15.96	0	105	135	0	15.53	0
AIM163	Pre-Pandemic	-138.15	225	360	15	0	27.24	60
	Post-Pandemic	-38.54	255	315	30	0	23.52	15
AIM164	Pre-Pandemic	-114.88	90	135	600	0	23.99	0
	Post-Pandemic	-143.32	75	105	600	0	31.65	30
AIM165	Pre-Pandemic	-31.75	75	105	15	0	32.12	45
	Post-Pandemic	-53.2	60	90	495	0	18.85	0
AIM166	Pre-Pandemic	6.44	0	210	15	0	32.1	15
	Post-Pandemic	259.77	120	165	15	0	62.91	60
AIM167	Pre-Pandemic	-259.52	135	210	15	0	62.93	15
	Post-Pandemic	-157.74	120	210	15	0	29.71	60
AIM170	Pre-Pandemic	125.93	90	135	510	0	44.34	45
	Post-Pandemic	-49.65	195	255	405	0	19.73	0
AIM171	Pre-Pandemic	49.42	15	120	240	0	36.43	45
	Post-Pandemic	210.79	30	120	45	0	118.59	45
AIM172	Pre-Pandemic	-116.47	150	180	45	0	51.45	60
	Post-Pandemic	-550.75	135	180	600	0	99.98	0
AIM173	Pre-Pandemic	-30.91	90	210	30	0	15.11	60
	Post-Pandemic	65.5	15	120	15	0	38.5	30
AIM174	Pre-Pandemic	-117.23	120	195	15	0	36.66	60
	Post-Pandemic	11.87	15	120	15	0	18.27	15
AIM175	Pre-Pandemic	163.81	90	210	30	0	75.28	60
	Post-Pandemic	59.53	105	180	15	0	24.39	45
AIM176	Pre-Pandemic	150.2	120	180	15	0	47.2	0
	Post-Pandemic	-15.42	75	210	60	0	38.02	0
AIM177	Pre-Pandemic	-40.47	15	75	120	0	22.79	0
	Post-Pandemic	44.32	75	90	15	0	27.26	30
AIM179	Pre-Pandemic	-92.47	90	90	45	0	63.61	30
	Post-Pandemic	111.14	30	90	600	0	49.97	0
AIM180	Pre-Pandemic	264.1	75	120	15	0	105.81	45
	Post-Pandemic	74.67	60	105	600	0	18.89	45
AIM181	Pre-Pandemic	-144.44	135	165	15	0	74.29	45
	Post-Pandemic	-142.09	105	135	600	0	30.51	30
AIM182	Pre-Pandemic	92.42	0	150	30	0	107.41	0
	Post-Pandemic	-210.92	75	135	15	0	53.61	45
AIM183	Pre-Pandemic	-583.64	135	180	600	0	130.27	45
	Post-Pandemic	-93.59	120	135	600	0	43.95	45
AIM184	Pre-Pandemic	237.07	150	195	30	0	70.27	0
	Post-Pandemic	279.76	105	210	15	0	61.83	60
AIM185	Pre-Pandemic	28.82	30	195	15	0	59.25	45
	Post-Pandemic	33.67	15	75	285	0	18.82	0
AIM186	Pre-Pandemic	-437.65	60	105	15	0	123.04	45
	Post-Pandemic	-130.18	105	150	600	0	26.61	0

Table 3.11: Features of cumulative step and impulse responses to Inspirational Quotes messages for person-specific models over the weekdays.

		Weekday - Inspirational Quotes						
Participant	Stage	SS	RT	ST	EfT	InDel	Pmag	PDel
AIM161	Pre-Pandemic	-3.15	90	180	15	0	15.27	45
	Post-Pandemic	17.83	60	165	75	0	21.24	60
AIM163	Pre-Pandemic	-345.07	225	315	600	0	48.98	30
	Post-Pandemic	223.02	180	315	60	0	69.37	45
AIM164	Pre-Pandemic	36.44	75	150	600	0	51.51	45
	Post-Pandemic	-1.97	0	240	30	0	33.3	0
AIM165	Pre-Pandemic	78.03	60	90	15	0	26.25	15
	Post-Pandemic	-1.84	0	255	75	0	37.62	45
AIM166	Pre-Pandemic	71.91	45	135	15	0	42.78	45
	Post-Pandemic	-151.39	45	120	600	0	72.29	30
AIM167	Pre-Pandemic	-325.89	150	195	600	0	72.9	15
	Post-Pandemic	-108.74	105	150	15	0	25.04	15
AIM170	Pre-Pandemic	18.24	105	240	75	0	55.18	60
	Post-Pandemic	-104.22	195	285	15	0	20.37	45
AIM171	Pre-Pandemic	-44.6	105	195	45	0	76.37	0
	Post-Pandemic	-76.38	45	105	90	0	91.52	30
AIM172	Pre-Pandemic	-92.56	105	210	30	0	76.84	0
	Post-Pandemic	-326.14	105	225	60	0	83.62	60
AIM173	Pre-Pandemic	-32.62	150	195	15	0	22.18	30
	Post-Pandemic	0.39	0	285	15	0	20.62	60
AIM174	Pre-Pandemic	-49.35	90	165	15	0	37.42	45
	Post-Pandemic	40.23	15	150	30	0	24.54	0
AIM175	Pre-Pandemic	-74.18	165	210	600	0	34.86	45
	Post-Pandemic	137.9	120	195	15	0	40.48	15
AIM176	Pre-Pandemic	-298.95	30	120	240	0	98.15	30
	Post-Pandemic	354.66	30	90	600	0	198.59	0
AIM177	Pre-Pandemic	44.29	105	210	60	0	33	60
	Post-Pandemic	-86.48	45	75	15	0	48.22	45
AIM179	Pre-Pandemic	-182.17	45	75	600	0	65.74	15
	Post-Pandemic	122.11	105	135	30	0	51.17	30
AIM180	Pre-Pandemic	-83.11	30	90	45	0	81.22	15
	Post-Pandemic	-7.89	0	135	30	0	9.29	0
AIM181	Pre-Pandemic	571.21	135	165	600	0	89.29	45
	Post-Pandemic	257.67	30	60	600	0	121.01	0
AIM182	Pre-Pandemic	190.2	15	105	300	0	135.99	0
	Post-Pandemic	-72.36	75	150	15	0	27.4	0
AIM183	Pre-Pandemic	1072.26	105	150	600	0	413.79	0
	Post-Pandemic	-44.2	75	120	15	0	15.8	60
AIM184	Pre-Pandemic	167.18	30	60	90	0	97.65	0
	Post-Pandemic	-34.24	15	195	15	0	41.07	45
AIM185	Pre-Pandemic	-299.57	135	210	15	0	64.11	30
	Post-Pandemic	-103.5	105	180	30	0	26.12	60
AIM186	Pre-Pandemic	-470.83	75	105	15	0	142.61	60
	Post-Pandemic	-13.51	60	105	15	0	17.02	45

Table 3.12: Features of cumulative step and impulse responses to Move More messages for person-specific models over the weekends.

		Weekend - Move More						
Participant	Stage	SS	RT	ST	EfT	InDel	Pmag	PDel
AIM161	Pre-Pandemic	132.69	60	105	330	0	83.31	0
	Post-Pandemic	51.85	90	165	30	0	34.11	15
AIM163	Pre-Pandemic	346.53	195	270	600	0	51.55	15
	Post-Pandemic	-234.33	45	135	600	0	74.93	30
AIM164	Pre-Pandemic	-65.78	75	120	30	0	29.69	45
	Post-Pandemic	235.93	60	135	600	0	86.42	30
AIM165	Pre-Pandemic	357.45	105	210	15	0	86.2	45
	Post-Pandemic	-38.52	150	180	15	0	40.84	15
AIM166	Pre-Pandemic	81.98	150	240	15	0	37.21	0
	Post-Pandemic	96.39	105	135	375	0	75.35	0
AIM167	Pre-Pandemic	-229.09	180	225	600	0	52.33	45
	Post-Pandemic	-37.71	150	210	15	0	9.26	0
AIM170	Pre-Pandemic	27.04	90	180	60	0	34	45
	Post-Pandemic	-119.62	90	120	600	0	22.06	0
AIM171	Pre-Pandemic	166.95	150	225	15	0	61.46	30
	Post-Pandemic	-91.63	75	180	75	0	140.65	0
AIM172	Pre-Pandemic	-28.2	225	285	15	0	33.23	60
	Post-Pandemic	-902.87	90	150	15	0	209.86	15
AIM173	Pre-Pandemic	-14.66	0	135	15	0	19.78	30
	Post-Pandemic	6.43	0	225	15	0	31.86	15
AIM174	Pre-Pandemic	98.35	120	195	15	0	24.99	15
	Post-Pandemic	18.75	60	90	15	0	6.32	30
AIM175	Pre-Pandemic	-102.81	120	150	600	0	27.45	45
	Post-Pandemic	61.29	15	105	60	0	45.42	0
AIM176	Pre-Pandemic	-359.64	150	240	600	0	82.26	30
	Post-Pandemic	-252.24	30	90	465	0	105.34	15
AIM177	Pre-Pandemic	-113.84	120	150	600	0	24.42	0
	Post-Pandemic	31.83	0	105	15	0	55.24	15
AIM179	Pre-Pandemic	139.58	60	180	90	0	145.28	60
	Post-Pandemic	-205.87	105	150	600	0	68.74	15
AIM180	Pre-Pandemic	86.36	60	135	30	0	64.46	30
	Post-Pandemic	110.8	90	165	15	0	49.88	45
AIM181	Pre-Pandemic	261.19	150	270	600	0	49.68	0
	Post-Pandemic	-142.34	150	165	600	0	62.97	30
AIM182	Pre-Pandemic	-211.38	180	225	360	0	50.95	0
	Post-Pandemic	-317	120	165	600	0	68.89	0
AIM183	Pre-Pandemic	110.96	285	420	60	0	96.21	0
	Post-Pandemic	-135.98	30	150	45	0	58.08	60
AIM184	Pre-Pandemic	81.75	0	165	15	0	110.43	0
	Post-Pandemic	44.92	75	120	45	0	26.06	0
AIM185	Pre-Pandemic	-1.03	0	270	15	0	35.28	0
	Post-Pandemic	-20.25	0	405	30	0	31.86	0
AIM186	Pre-Pandemic	428.56	75	120	600	0	131.53	30
	Post-Pandemic	-77.35	120	150	600	0	37.9	0

Table 3.13: Features of cumulative step and impulse responses to Sit Less messages for person-specific models over the weekends.

		Weekend - Sit Less						
Participant	Stage	SS	RT	ST	EfT	InDel	Pmag	PDel
AIM161	Pre-Pandemic	70.97	180	210	15	0	22.14	60
	Post-Pandemic	-17.83	30	105	15	0	13.47	15
AIM163	Pre-Pandemic	-105.36	150	225	600	0	28.39	0
	Post-Pandemic	183.18	135	150	600	0	79.39	0
AIM164	Pre-Pandemic	148.63	90	135	600	0	48.11	30
	Post-Pandemic	-117.87	15	135	600	0	113.93	15
AIM165	Pre-Pandemic	63.78	165	210	15	0	33.77	45
	Post-Pandemic	522.56	45	135	15	0	238.5	30
AIM166	Pre-Pandemic	164.91	150	195	15	0	65.27	15
	Post-Pandemic	-36.32	15	240	90	0	53.32	60
AIM167	Pre-Pandemic	9.58	0	330	150	0	27.75	0
	Post-Pandemic	-8.34	0	180	30	0	20.01	15
AIM170	Pre-Pandemic	-78.42	120	150	45	0	42.27	30
	Post-Pandemic	-55.86	120	135	30	0	22.52	0
AIM171	Pre-Pandemic	395.81	210	270	600	0	70.67	60
	Post-Pandemic	-318.01	75	105	405	0	62.87	15
AIM172	Pre-Pandemic	149.83	165	210	600	0	37.18	0
	Post-Pandemic	-614.32	90	120	600	0	130.36	0
AIM173	Pre-Pandemic	-67.25	75	105	15	0	27.24	45
	Post-Pandemic	214.67	60	135	600	0	80.5	45
AIM174	Pre-Pandemic	-12.23	0	285	135	0	28.71	15
	Post-Pandemic	-147.96	90	105	600	0	31.44	30
AIM175	Pre-Pandemic	55.24	60	120	600	0	23.99	30
	Post-Pandemic	13.22	240	285	15	0	19.66	60
AIM176	Pre-Pandemic	110.68	0	135	600	0	129.73	15
	Post-Pandemic	-251.34	30	90	465	0	112.58	0
AIM177	Pre-Pandemic	59.68	105	210	30	0	25.83	45
	Post-Pandemic	70.82	15	105	15	0	45.52	15
AIM179	Pre-Pandemic	252.3	105	120	600	0	69.92	0
	Post-Pandemic	483.97	105	150	600	0	135.16	0
AIM180	Pre-Pandemic	43.36	15	90	45	0	50.2	30
	Post-Pandemic	193.12	90	135	15	0	82.72	30
AIM181	Pre-Pandemic	-322.02	150	255	600	0	83.6	45
	Post-Pandemic	193.01	90	150	600	0	83.24	45
AIM182	Pre-Pandemic	-325.55	180	315	60	0	113.32	60
	Post-Pandemic	249.72	105	165	600	0	72.66	0
AIM183	Pre-Pandemic	-277.49	195	270	600	0	83.75	0
	Post-Pandemic	51.48	90	150	30	0	24.98	45
AIM184	Pre-Pandemic	773.19	75	105	15	0	217.46	30
	Post-Pandemic	157.83	90	120	600	0	48.01	45
AIM185	Pre-Pandemic	37.44	30	180	15	0	34.72	30
	Post-Pandemic	-164.24	270	375	15	0	30.99	60
AIM186	Pre-Pandemic	-283.84	45	60	600	0	111.2	15
	Post-Pandemic	42.39	90	225	90	0	38.15	0

Table 3.14: Features of cumulative step and impulse responses to Inspirational Quotes messages for person-specific models over the weekends.

		Weekend - Inspirational Quotes						
Participant	Stage	SS	RT	ST	EfT	InDel	Pmag	PDel
AIM161	Pre-Pandemic	111.8	30	165	225	0	77.8	0
	Post-Pandemic	118.23	90	120	600	0	41.79	0
AIM163	Pre-Pandemic	-59.59	0	135	45	0	70.62	15
	Post-Pandemic	76	45	195	600	0	50.13	30
AIM164	Pre-Pandemic	-178.85	75	150	30	0	46.42	60
	Post-Pandemic	-234.1	45	135	600	0	81.5	30
AIM165	Pre-Pandemic	-109.61	135	195	15	0	30.19	45
	Post-Pandemic	-303.87	90	135	600	0	69.92	30
AIM166	Pre-Pandemic	105.24	165	225	15	0	30.5	0
	Post-Pandemic	202.46	30	150	60	0	116.9	15
AIM167	Pre-Pandemic	370.33	60	105	600	0	152.43	15
	Post-Pandemic	-61.25	165	300	75	0	101.44	45
AIM170	Pre-Pandemic	-59.31	15	135	15	0	43.58	15
	Post-Pandemic	83.55	105	150	15	0	25.55	45
AIM171	Pre-Pandemic	225.71	150	195	390	0	55.6	0
	Post-Pandemic	-369.39	105	135	540	0	68.84	0
AIM172	Pre-Pandemic	-151.65	105	135	600	0	60.67	0
	Post-Pandemic	289.35	90	240	105	0	214.75	15
AIM173	Pre-Pandemic	-70.73	75	120	45	0	35.18	0
	Post-Pandemic	-2.25	0	240	15	0	17.71	30
AIM174	Pre-Pandemic	-19.78	120	255	75	0	27.35	0
	Post-Pandemic	46.56	75	180	15	0	16.67	60
AIM175	Pre-Pandemic	-14.29	0	165	60	0	70.07	30
	Post-Pandemic	121.02	120	195	15	0	28.27	45
AIM176	Pre-Pandemic	227.19	135	255	600	0	108.66	60
	Post-Pandemic	134.96	15	180	165	0	216.33	30
AIM177	Pre-Pandemic	-138.64	135	180	600	0	26.66	30
	Post-Pandemic	399.5	90	135	15	0	104.45	60
AIM179	Pre-Pandemic	1458.44	60	150	45	0	532.27	60
	Post-Pandemic	111.1	105	225	75	0	99.13	60
AIM180	Pre-Pandemic	144.89	90	120	15	0	78.31	30
	Post-Pandemic	1.6	90	285	15	0	26.85	60
AIM181	Pre-Pandemic	96.43	210	270	600	0	28.44	60
	Post-Pandemic	-54.4	135	150	15	0	13.7	0
AIM182	Pre-Pandemic	-158.94	195	285	15	0	36.51	45
	Post-Pandemic	-455.16	150	210	600	0	83.27	45
AIM183	Pre-Pandemic	-188.01	15	300	600	0	99.28	0
	Post-Pandemic	164.35	30	105	600	0	96.52	0
AIM184	Pre-Pandemic	715.79	75	90	435	0	295.74	0
	Post-Pandemic	-183.58	90	120	600	0	38.55	15
AIM185	Pre-Pandemic	788.78	90	165	15	0	172.58	60
	Post-Pandemic	-266.35	225	300	600	0	57.84	0
AIM186	Pre-Pandemic	-200.49	60	90	600	0	73.88	0
	Post-Pandemic	105.31	90	165	600	0	69.82	30

Table 3.15: Magnitude of the dominant poles (absolute value) for all the participants over the weekdays and weekends, and their differences.

	Weekday			Weekend		
Participant	Pre-Pandemic	Post-Pandemic	Difference	Pre-Pandemic	Post-Pandemic	Difference
AIM161	0.65	0.60	-0.05	0.78	0.71	-0.07
AIM163	0.86	0.83	-0.03	0.84	0.64	-0.20
AIM164	0.67	0.66	0.01	0.65	0.69	0.04
AIM165	0.47	0.64	0.16	0.75	0.66	-0.09
AIM166	0.61	0.70	0.09	0.80	0.69	-0.11
AIM167	0.79	0.74	-0.05	0.80	0.79	0.01
AIM170	0.68	0.85	0.17	0.66	0.63	-0.04
AIM171	0.71	0.54	-0.18	0.83	0.61	-0.21
AIM172	0.74	0.75	0.01	0.79	0.69	-0.10
AIM173	0.76	0.62	-0.14	0.58	0.74	0.16
AIM174	0.76	0.67	-0.09	0.76	0.67	-0.09
AIM175	0.74	0.77	0.03	0.72	0.77	0.06
AIM176	0.77	0.66	-0.11	0.79	0.67	-0.12
AIM177	0.70	0.58	-0.12	0.76	0.63	-0.14
AIM179	0.51	0.68	0.16	0.59	0.73	0.14
AIM180	0.57	0.60	0.02	0.62	0.69	0.07
AIM181	0.74	0.57	-0.17	0.82	0.72	-0.10
AIM182	0.71	0.64	-0.07	0.83	0.79	-0.04
AIM183	0.75	0.58	-0.18	0.88	0.67	-0.21
AIM184	0.77	0.76	-0.01	0.54	0.68	0.15
AIM185	0.78	0.73	-0.05	0.68	0.88	0.19
AIM186	0.56	0.69	0.13	0.58	0.71	0.13
Sample Mean	0.70	0.68	-0.02	0.73	0.70	-0.03

Table 3.16: Correlations between pre- and post-pandemic response speed and response features to different message types for weekdays and weekends.

Response Features &	Weekdays		Weekends	
Message Type	r	p	r	p
Response Speed	0.26	0.24	-0.15	0.5
Peak Magnitude				
Move More	0.08	0.73	-0.07	0.76
Sit Less	-0.05	0.81	0	0.99
Inspirational Quotes	-0.08	0.74	0.1	0.67
Peak Delay				
Move More	-0.18	0.43	-0.12	0.6
Sit Less	-0.27	0.22	0.13	0.57
Inspirational Quotes	-0.06	0.79	0.17	0.44
Steady State				
Move More	0.13	0.57	0.08	0.73
Sit Less	0.41	0.06	-0.16	0.48
Inspirational Quotes	-0.05	0.75	-0.13	0.58
Rise Time				
Move More	0.04	0.86	0.17	0.46
Sit Less	0.54	0.01	-0.12	0.6
Inspirational Quotes	0.5	0.02	0.13	0.57
Settling Time				
Move More	0.28	0.21	0.17	0.45
Sit Less	0.68	$<.001$	-0.14	0.53
Inspirational Quotes	0.4	0.06	-0.33	0.13
Effective Time				
Move More	-0.16	0.47	0.3	0.18
Sit Less	0.26	0.24	0.34	0.12
Inspirational Quotes	0.05	0.83	-0.03	0.91

Chapter 4
Fragmented Data Dynamical Output Modeling (DOME)

To address some other challenges described in chapter 1, concepts from the general area of control engineering and dynamical systems to develop a modeling procedure that takes "memory" and fragmentation into account. Control engineering has several approaches that can address the challenges of the intensive longitudinal data. Dynamical systems are a powerful tool for modeling interaction between longitudinal variables and have been used in areas as diverse as aerospace [153], biology and medicine [154–156], agriculture [157] and economics [158]. Dynamical systems has also been used as a modeling tool in the area of psychology to model development and social interactions [159, 160].

4.1 Dynamical System Modeling

The drawbacks of the system identification methods described in chapter 1 and the efficiency of the atomic norm minimization technique have motivated us to develop a novel identification algorithm that considers sparsity using the atomic norm concept, and this method would belong to non-parametric identification methods. Therefore, to identify desired dynamical models, concepts from control systems engineering and sparse signal reconstruction have used to develop tools for parsimonious modeling of interactions between intensive longitudinal data streams. In other words, by developing a new parsimonious model identification algorithm, we seek to identify models that provide a desired explanation of the data with as few parameters as possible.

The proposed approach has two main strengths: i) since, from a computational point of view, it uses linear programming tools, it can easily handle very large data sets and ii) since it leverages concepts from sparse signal processing, when applied to small data sets

like data from a specific individual, it can identify *low complexity personalized models* that do not lead to over-fitting. Here, we focus on binary outcomes but the approach proposed can be extended to other types of outcomes such as multi-level or continuously valued data.

These computational personalized models can be used for any longitudinal data, to simulate the response of the individual to a variety of stimuli. Moreover, by leveraging tools from control engineering, the models can be used to design efficient decision rules for just-in-time adaptive interventions. For example, they can be used to develop a model predictive controller to deliver specific intervention messages at the right moment [133]. This personalized model approach has demonstrated in our other work on digital messaging intervention to promote physical activity [1, 15].

The objective of this chapter is not only to describe tools developed for intensive longitudinal data analysis but also to elaborate on the foundations of the proposed approach. To this end, we start by describing the conceptual underpinning of the algorithm developed. This requires the review of some basic concepts related to linear time-invariant dynamical systems. The steps for developing the algorithm and the validation procedure are followed in detail. Then, a description of the publicly available MATLAB® package developed is provided. The package consists of the model implementation files and various datasets with an explanation for each. Additionally, information on how the data should be inputted to the algorithm, what the output is, and examples on how to obtain and visualize the results are provided.

Finally, we provide results of identifying models for different datasets using the developed algorithms and how to interpret the results obtained. This should be noted that, since the final result of this analysis is a dynamical system that relates inputs to output, the identified "computational model" of interaction can be used to simulate responses to different inputs.

4.2 Dynamical Modeling of Binary outputs

This section provides a precise description of the inputs and outputs, assumptions on the data to be used, and the mathematical concepts central to the proposed modeling approach.

4.2.1 Inputs and Outputs

For simplicity, here, it is assumed that the main objective is to model the relation between one longitudinal input/stimulus/cause/micro-intervention and one longitudinal output/outcome. No constraints are imposed on the possible values of the longitudinal input. However, it is assumed that the output is binary, i.e., it takes value one if the event of interest occurred and zero otherwise.

As an illustrative example, throughout this chapter, a hypothetical study on the relation between stress and smoking is considered. This running example assumes that we can measure/estimate stress and consider that as the input longitudinal variable. The output considered is a binary longitudinal variable that, for each time instant, is one if smoking occurs and zero otherwise.

4.2.2 Assumptions on Data

Assuming that measurements are made at intervals of length T minutes, which is common when intensive longitudinal measurements are collected automatically, the data can be represented as

$$input(kT) \qquad \text{and} \qquad output(kT) \tag{4.1}$$

where u and y are the input and output, respectively, k is an integer and kT represents the time at which the measurements were made.

No enforcement on the continuity of input and output measurements is applied. Data available is only assumed to be composed of what is referred to as data "chunks". More precisely, chunks are intervals where we have continuous measurements of the input. For chunk i starting at time k_iT and of size n_i, it is assumed that the values of

$$u(k_iT), u((k_i+1)T), \ldots, u((k_i+n_i-1)T) \tag{4.2}$$

are available. On the other hand, we do not assume that, in these chunks, output is continuously measured; i.e., we can have a significant number of gaps/missingness in its knowledge. To provide consistent coding in output representation, at a given time kT, we allow three possible values for the output data

$$output(kT) = \begin{cases} 1 & \text{if output is True at time } kT \\ 0 & \text{if output is False at time } kT \\ -1 & \text{if output is Unknown at time } kT \end{cases} \tag{4.3}$$

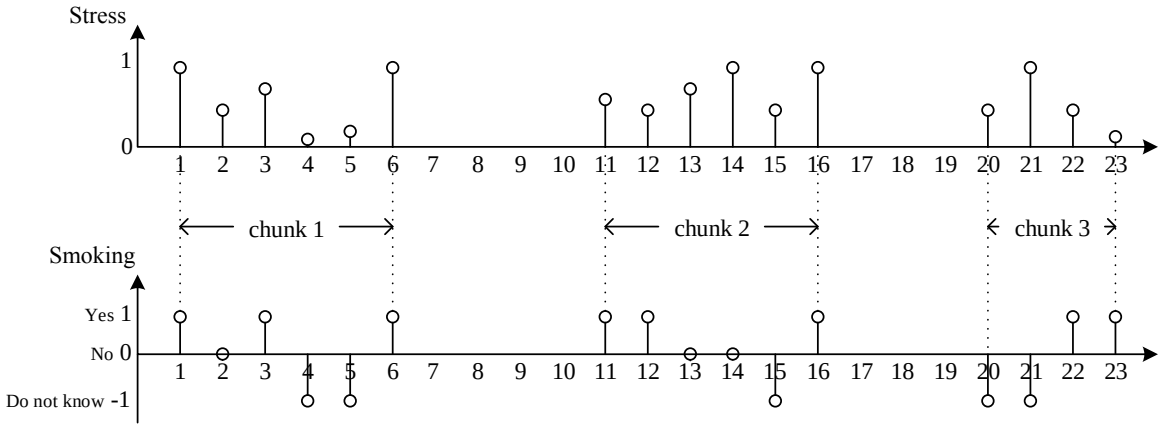

Figure 4.1: Example of stress and smoking data with 3 chunks and $T = 1$ min.

for all $k = k_i, k_i + 1, \ldots, k_i + n_i - 1$. Back to our running stress and smoking example, if we have the following data

$$y(T) = 1,\ y(2T) = -1,\ y(3T) = 0 \tag{4.4}$$

it means that smoking occurred at time T, we do not know if smoking occurred at time $2T$ or not, and smoking did not occur at time $3T$.

It should be noted that the starting point of a chunk is not necessarily a point where an input started; for example, we can have $u(k_iT) = 0$. It just means that data is available on the input continuously on a given interval or chunk, even if this information is that no input has occurred.

An example of such "data chunks" is provided in Figure 4.1. In this figure, there are three chunks with stress available for every sample time in them (assuming sampling time interval $T = 1$ min). As discussed before, this is not assumed that the output, in this case smoking event, is known for all time instants. Therefore, we see a code of -1 when no information on smoking is available. Note that no data is considered outside the chunks and inside each chunk, the length of the input and output time series is the same and the input and output variables are temporally aligned.

It should be noted that chunks of very small size do not provide much information in terms of modeling. Therefore, even if they are provided to the algorithm, they only increase computational time without improving results. Although it is hard to precisely define a priori what a small size chunk is, a good rule of thumb is to not use chunks whose size is smaller than the expected complexity or order of the model.

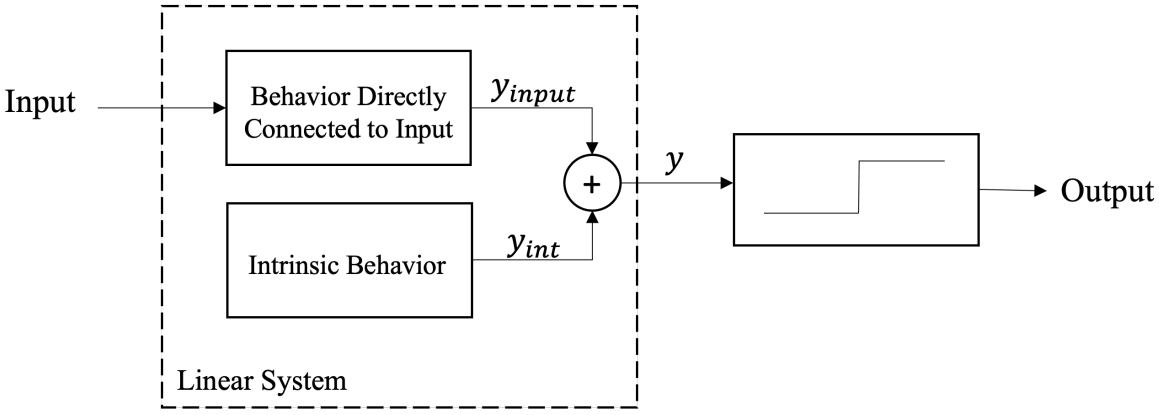

Figure 4.2: Dynamical system configuration.

In the next section, we discuss the mathematical model used to represent the dynamical relation between an input and an output. Also, some central concepts related to dynamical systems are introduced.

4.2.3 Dynamical Models

As mentioned earlier, the objective of the analysis tools provided in this chapter is to go beyond the "usual approach" to longitudinal data analysis where it is assumed that the input only has an immediate effect on the output. This "immediacy assumption" might hold if the sampling time T is very large. However, in the case of intensive longitudinal data, this assumption usually does not hold, i.e., the value of the output observed at present is not only influenced by the present value of the input but also by past values of it. For example, a stress event might result in an immediate increase on the probability of smoking as well as increasing the chance of smoking in the near future.

To model this "memory effect" in the interaction of longitudinal variables, we propose to use the concept of *dynamical systems*. More precisely, to be able to handle binary outputs, we propose to use an interconnection of a linear time invariant dynamical system (which has memory in it) in series with a non-linearity that provides the estimated value of the output. The proposed modeling technique is depicted in Figure 4.2.

In this model, when at a specific time, the output of the linear system, y, is at or above one, then the output at that time is one, representing that the event of interest occurs. If the output of the linear system is below one, then the output is zero and,

according to the model, the event does not occur. This can be formulated as

$$\begin{cases} output(kT) = 1 & \text{if } y(kT) \geq 1 \\ output(kT) = 0 & \text{if } y(kT) < 0 \end{cases}. \tag{4.5}$$

This choice of the threshold is arbitrary; but since we are dealing with linear systems, this choice does not change the identification problem or overall results. In other words, if a feasible solution to the linear system exists, applying any positive threshold in the sign non-linearity block does not impede the feasibility of the system's solution.

4.2.4 On Linear Systems

Before providing a complete description of the proposed approach, a background to the linear system whose input is the input u and the output is the intermediate variable y is needed. A more in-depth discussion can be found at [161]. The relation between u and the intermediate variable y can be modeled by an autoregressive (or difference) equation of the form

$$\begin{aligned} y(kT) =& a_1\, y[(k-1)T] + a_2\, y[(k-2)T] + \cdots + a_n\, y[(k-n)T] \\ &+ b_0\, u(kT) + b_1\, u[(k-1)T] + \cdots + b_n\, u[(k-n)T] \end{aligned} \tag{4.6}$$

where n is the order (measure of complexity) of the linear system. Therefore, identifying the model of the behavior is equivalent to estimating the coefficients a_i and b_i of the model above. However, the only data available is measurements of input and output. No information is collected on the "intermediate signal" y. To circumvent this issue, a new approach is needed.

From the definition of a linear system, the intermediate signal $y(kT)$ can be decomposed as

$$y(kT) = y_{int}(kT) + y_{input}(kT) \tag{4.7}$$

where $y_{int}(kT)$ is the intrinsic response of the linear system and $y_{input}(kT)$ is the input response. In control engineering jargon, $y_{int}(kT)$ is the zero-input response and $y_{input}(kT)$ is the zero-state response. These two parts of the response have very specific forms. Letting p_1, p_2, ..., p_n to be the so-called poles of the system, they can be computed as the solutions of the equation

$$z^n - a_1 z^{n-1} - \cdots - a_{n-1} z - a_n = 0. \tag{4.8}$$

Given the poles of a linear system, its intrinsic response is of the form

$$y_{int}(kT) = c_{int,1}\ p_1^k + c_{int,2}\ p_2^k + \cdots + c_{int,n}\ p_n^k \tag{4.9}$$

where the constants $c_{int,1}, c_{int,2}, \ldots, c_{int,n}$ depend of the state of the system, or in the running example, the person, before the input occurs. The form of the input response is slightly more complex. Letting $c_{input,1}, c_{input,2}, \ldots, c_{input,n}$ to be constants associated with the way the system responds to inputs, the so-called *impulse response* is defined as

$$h(k) = c_{input,1}\ p_1^k + c_{input,2}\ p_2^k + \cdots + c_{input,n}\ p_n^k. \tag{4.10}$$

We assume that the input was applied at time zero. But, the results below can be applied to any starting time. Then, the input response is

$$\begin{aligned} y_{input}(kT) =& h(0)\ u(kT) + h(1)\ u((k-1)T) \\ &+ h(2)\ u((k-2)T) + \cdots + h(k)\ u(0), \end{aligned} \tag{4.11}$$

which this operation is called convolution and is commonly represented as

$$y_{input}(kT) = (h * u)(kT). \tag{4.12}$$

As one can see, memory of the system appears in two ways: i) in the term y_{int} where the information about what happened before the input was applied is stored and ii) in the fact that the input response, y_{input}, depends not only on the present value of the input but also on its past values. For example, considering time $kT = 3T$, that is $k = 3$, the input response is of the form

$$\begin{aligned} y_{input}(3T) =& h(0)\ u(3T) + h(1)\ u(2T) \\ &+ h(2)\ u(T) + h(3)\ u(0). \end{aligned} \tag{4.13}$$

As such, the input response at time $3T$ does not only depend on the input at time $3T$, but also on all its past values at times $2T$, T and 0.

From the discussion above, it can be concluded that identifying the model of the system is equivalent to estimating the poles and the respective constants that are used to build the y_{input} and y_{int} responses. Moreover, the complexity of the model or the model order is equal to the number of poles used that is n.

Accordingly, in the formulation used in this chapter, we aim at identifying models

that use as few poles as possible in order to achieve the least complex explanation of the data and do not over-fit it. A final point about poles is that we assume all the poles have a magnitude of less than or equal to 1. This ensures that the system is stable and does not "diverge" if long chunks of data are provided; i.e., all internal signal are bounded.

4.3 Dynamical Output ModEling (DOME)

As mentioned, the data is provided in chunks of continuous input measurements. To be able to precisely describe the computational problem to be solved, we use the superscript i to denote the i-the chunk and its size by n_i. The total number of chunks is defined as N_{chunks} and it is assumed that each chunk starts at time 0. The starting time does not change the output of the approach presented. Therefore, the data available for chunk i is denoted as

$$input^i(0), input^i(T), \ldots, input^i((n_i - 1)T) \tag{4.14a}$$

$$output^i(0), output^i(T), \ldots, output^i((n_i - 1)T) \tag{4.14b}$$

It should be noted that, since what happened in the times between data chunks is not known, we have a different intrinsic response for each chunk. This issue is magnified as the interval between measurements increases (common in EMAs which do not record continuously) because the individual will be subjected to a large number of unmeasurable perturbations in between chunks. However, since we want to estimate a common model for all the data, the poles should be the same for all chunks and the impulse response, h, should also be the same.

To develop an implementable approach to address the modeling problem described, we start by gridding the unit circle, and work with only n_p poles. An example of the gridding circle is shown in Figure 4.3, here each small blue circle represents one candidate pole.

Moreover, we use a well-known approach from the literature on sparsity [32] to implicitly minimize the number of poles used. More precisely, given unit circle grid $p_1, p_2, \ldots p_{n_p}$, we solve the following optimization problem, which we refer to as Dynamical Output ModEling (DOME)

$$\min_{c^i_{int,p_j}, c_{input,p_j}} \quad \sum_{j=1}^{n_p} |c_{p_j}| \tag{4.15a}$$

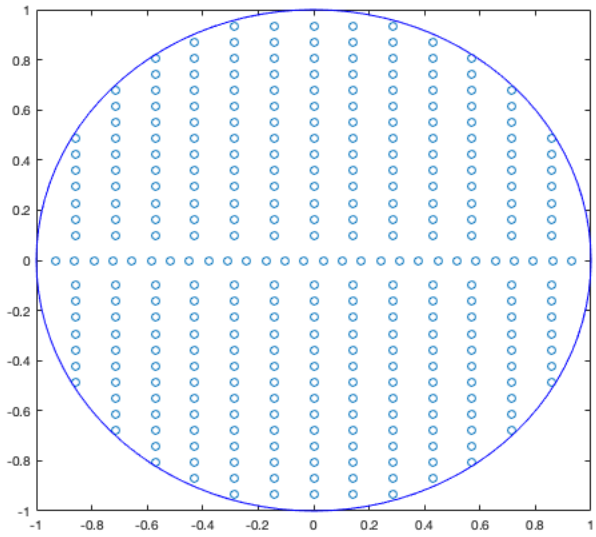

Figure 4.3: Gridding the unit circle.

$$\text{subject to } h(k) = \sum_{j=1}^{n_p} c_{input,p_j} \alpha_{p_j} p_j^k \tag{4.15b}$$

$$y^i_{input}(kT) = (h * u^i)(kT), i = 1, 2, \ldots, N_{\text{chunks}} \tag{4.15c}$$

$$y^i_{int}(kT) = \sum_{j=1}^{n_p} \alpha_{p_j} c^i_{int,p_j} p_j^k, i = 1, 2, \ldots, N_{\text{chunks}} \tag{4.15d}$$

$$y^i_{int}(kT) + y^i_{input}(kT) \geq 1 + \epsilon \text{ if } output^i(kT) = 1 \tag{4.15e}$$

$$y^i_{int}(kT) + y^i_{input}(kT) \leq 1 - \epsilon \text{ if } output^i(kT) = 0 \tag{4.15f}$$

$$c_{input,p_j} = c^*_{input,p^*_j}, \quad c^i_{int,p_j} = \left(c^i_{int,p^*_j}\right)^* \tag{4.15g}$$

$$|c_{input,p_j}| \leq c_{p_j}, \quad |c^i_{int,p_j}| \leq c_{p_j}. \tag{4.15h}$$

Before explaining each of the terms in the problem above, this should be noted that the quantities we are looking for here are i) the poles to be used, ii) the corresponding coefficients for the impulse response $h(k)$, and iii) the corresponding coefficients of the intrinsic responses for each chunk. Equation (4.15a) aims at determining the simplest explanation of the data provided; i.e., employing as few poles as possible. This is based on a common approach to sparsity used in signal processing/machine learning.

In (4.15b), the impulse response of the linear system is defined. Again, this is the same for all chunks since the linear system used is the same for all of them. This leads

to equation (4.15c) where the input response for each chunk is built. Note that they all use the same $h(k)$ but compute the input response according to the input data provided for each chunk. Equation (4.15d) provides the form of the intrinsic response for each chunk. Note that all of them use the same poles, p, but have different coefficients since the memory of the past events is different for each chunk.

Equations (4.15e) and (4.15f) make sure that the output of the nonlinearity matches the observed output data; i.e., it is made sure that for each time instant, the output of the linear system, y, is above one if the output is one and that is below one if the output is zero. This should be noted that if $output^i(kT)$ is unknown, in other words, if its value is equal to -1, no constraint will be applied on the value of $y^i(kT) = y^i_{int}(kT) + y^i_{input}(kT)$.

Moreover, $\epsilon > 0$ used in equations (4.15e) and (4.15f) is a small positive constant that allows for the use of non-strict inequalities which are more amenable for most optimization software packages. Finally, equation (4.15g) is a technical condition that ensures that the linear system identified has real output and z^* denotes the complex conjugate of complex number z.

Careful choice of the scaling factors α_p which are constants and the use of equations (4.15b) and (4.15d) provide a computationally efficient way to "encourage" the use of the least complex explanation of the data provided. The scaling factors are computed as

$$\alpha_p = \frac{1 - |p|^2}{1 - |p|^{2\overline{n}+2}} \tag{4.16}$$

where $\overline{n}$ is the average size of the data chunks (see [34] for details on this choice). This choice of scaling factors used in our approach have shown to have good numerical performance and, in the examples that we have run, do result in low complexity explanations of the data provided.

4.3.1 Validation

In order to validate the identified models, large datasets should be provided. This guarantees enough information to be divided between the modeling/train and test sets and identifying reliable models. Data can be divided using any common technique between the two sets. If decided to divide the data by a ratio, it should be in mind that since the number of samples in each chunk is not equal, the data distributed between the two sets might deviate from the considered ratio by a few samples, to have whole data chunk in either of the sets.

One of the common methods to validate a model is to minimize the error between

the predicted outputs and the observations or true outputs. We developed our validation technique based on this method, although there is a slight twist from the traditional methods here. As the first step, the optimization problem (4.15) should be solved for the modeling/train data to identify the models. The poles, identified coefficients for the impulse response, and accordingly, impulse response of the system can be retrieved from the models, and they would be the same for the system based on the test set. However, since there might be some initial conditions (related to intrinsic response) that have not been seen in the past, i.e., based on the train set, test set might have a different behavior according to its different intrinsic response.

The goal of validation here is to assess whether there is a good fit that considers this fact. Therefore, another optimization problem should be solved for the test set to identify the coefficients related to the intrinsic response based on this set. Identifying the coefficients of the intrinsic response for each chunk, the error will be minimized solving the following optimization problem

$$\min_{c^i_{int,p_j}} \quad \sum_{j=1}^{N} |\delta(kT)| \tag{4.17a}$$

$$\text{subject to } h(k) = \sum_{j=1}^{n_p} c_{input,p_j} \alpha_{p_j} p_j^k \tag{4.17b}$$

$$y^i_{input}(kT) = (h * u^i)(kT), i = 1, 2, \ldots, N_{\text{chunks}} \tag{4.17c}$$

$$y^i_{int}(kT) = \sum_{j=1}^{n_p} \alpha_{p_j} c^i_{int,p_j} p_j^k, i = 1, 2, \ldots, N_{\text{chunks}} \tag{4.17d}$$

$$y^i_{int}(kT) + y^i_{input}(kT) + \delta(kT) \geq 1 + \epsilon \text{ if } output^i(kT) = 1 \tag{4.17e}$$

$$y^i_{int}(kT) + y^i_{input}(kT) + \delta(kT) \leq 1 - \epsilon \text{ if } output^i(kT) = 0 \tag{4.17f}$$

$$c^i_{int,p_j} = \left(c^i_{int,p^*_j}\right)^* \tag{4.17g}$$

where c_{int,p_j}'s are the unknown coefficients to be identified, N is the total number of samples in the test set, and $\delta(kT)$ is the error at time kT. If sum of the errors is below a certain threshold (that can vary based on the dataset characteristics), the results are valid which represents that the predicted outputs closely follow the true observations.

4.4 DOME software Package

The DOME software package consists of four functions called `dome`, `dome_train_test`, `dome_response_plots`, and `chunk_creator`, and four datasets named `data_set_1`

through `data_set_4`. All functions are implemented in MATLAB® [162]. The `dome`, `dome_train_test` tools require the MATLAB® Control System toolbox (available for downloading on the Mathworks website) and the CVX toolbox [163]. The `dome` modeling tool has a single command whose syntax is

```
>> Lin_sys = dome(chunk,Ts,r,prec,epsilon);
```

where `Lin_sys` is the output, that is the identified linear system in sys format, and the structure of each of the inputs is as follows:

- `chunk` is a structured array whose size is the number of chunks and where each of the entries has two elements in its structure, `chunk(i).stim` and `chunk(i).out`. These are two arrays of the same size where `chunk(i).stim` contains the values of the input for the i-th chunk and `chunk(i).out` contains the corresponding outputs. Again, each entry of `chunk(i).out` takes the value 1 if the output is true, 0 if it is not true and -1 if output is not available.
- `Ts` is the sampling period of the data, which is equal for all chunks.
- `r` is the degree of discretization of the unit circle. The number of poles used is approximately proportional to r^2.
- `prec` is a bound used to decide when a quantity is assumed to be zero. In other words, if $|c| \leq$ `prec` then we assume that $c = 0$ and its value is negligible.
- `epsilon` is the small constant ϵ in the optimization problems.

`dome` modeling tool has only one output, `Lin_sys`, which is the identified system in sys format.

The `dome_train_test` tool requires a test and a train set, i.e., instead of input `chunk` in the `dome` function, it takes `chunk_train` and `chunk_test`, but the rest of the inputs remain the same. `dome_train_test` tool returns two outputs; `Lin_sys`, similar to the output of the `dome` function, and `error` that is sum of the absolute values of the differences between the true and estimated outcomes.

The function `chunk_creator` creates the structured array `chunk` from a regular dataset and defines the value of the sampling period, `Ts`. This value is set to 1 in the Dome package but if for other applications this value is different than 1, it has to be changed manually in the `chunk_creator` function. That is it takes a regular dataset and divides it into continuous intervals of data, to be used by `dome` and `dome_train_test`

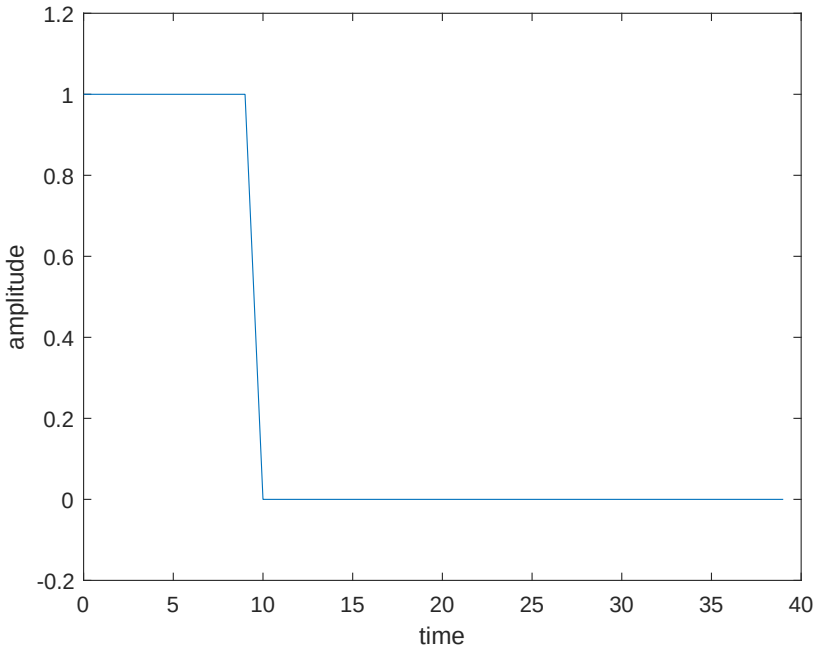

Figure 4.4: A pulse episode of length 10.

tools. Finally, the `dome_response_plots` m-file takes `Lin_sys`, outputted by either `dome` or `dome_train_test` tools, as the input and plots the impulse and pulse response curves.

4.5 Results

4.5.1 Interpretation and Robustness to Data Fragmentation

In this section, we provide some ways of analyzing the results obtaining from the `dome` modeling tool. Since we are studying the dynamic response to inputs, there are many characteristics that we can look at. For example, what is the delay in responding to inputs, how strong is the response, how long does it last, etc. In the following, we exemplify how one can precisely quantify some of these concepts.

The first step is to determine a "typical" input that is expected to be observed often. In the examples provided in this chapter, we selected a stress event of length 10 min, an arbitrary value to standardize the comparison among examples. This input event is shown in Figure 4.4 where the total length is the time horizon considered (in this plot, 40 sample periods) in order to observe what is the response after the input is applied.

This can be obtained by using the command

```
>> pulse_stim = [ones(1,10),zeros(1,40)].
```

This should be noted that, depending on the application, performance can be studied for more than one input. Since this is done by simulation, one can in principle study the response to most of the inputs that can occur.

To obtain the input response for the generated input, one can use the `lsim` command. More precisely, the following command can be used

```
>> ysim = lsim(Lin_sys,pulse_stim).
```

Since we deem the event to happen if the output of the linear system

$$y(kT) = y_{int}(kT) + y_{input}(kT) \tag{4.18}$$

is larger than 1, from a practical point of view, one can say that the input response y_{input} starts to have a significant impact when it is above 0.1. The time that it takes to reach this value is referred to as the delay in the response and denoted by t_d. This measures how long it takes for the input to start having an effect. On the other hand, we have the time at which the input response reaches 0.1 and stays below this value for the rest of the time. We refer to this as effective time and it is denoted by t_{eff}. This is the largest time for which the input has a measurable effect.

Finally, one can look at the time that the input has the biggest effect, in other words, when it has its peak response. We refer to this as peak time and denote it by t_{peak}. The peak value of the response is denoted by $y_{\text{input,peak}}$. These quantities are depicted in the diagram in Figure 4.5. It should be noted that these are not the only characteristics that one can look at. Depending on the specific data being analyzed, there might be other quantities of interest.

4.5.2 Simulated Data Analysis

To illustrate the results obtaining from the developed tool, we used a simulated dataset containing 1999 samples, distributed across 50 data chunks. The impulse and pulse responses of the true system versus the identified system are illustrated in figures 4.6(a) and 4.6(b), respectively. The response curves of the identified system can be plotted using the MATLAB® code implemented in `dome_response_plots` file provided in the DOME package by giving the `Lin_sys` as the input to it. As shown in figures 4.6(a) and 4.6(b), the identified system closely follows the true system curves.

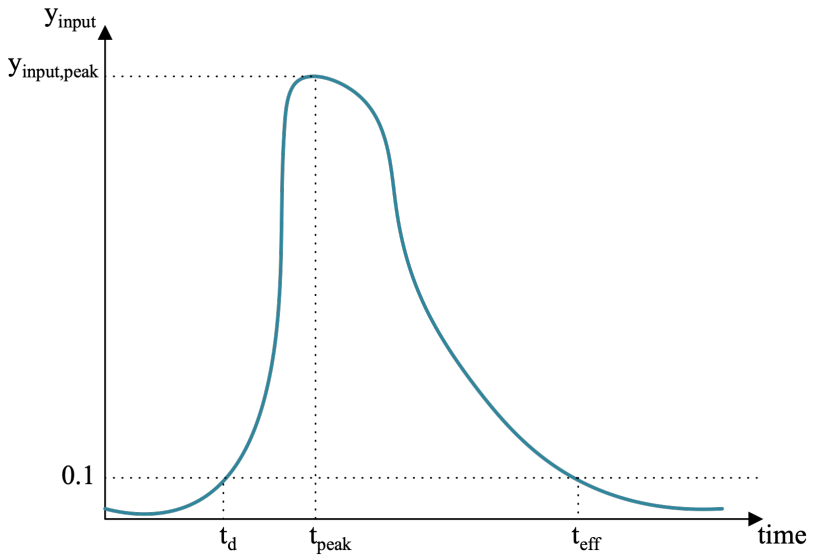

Figure 4.5: Performance measures.

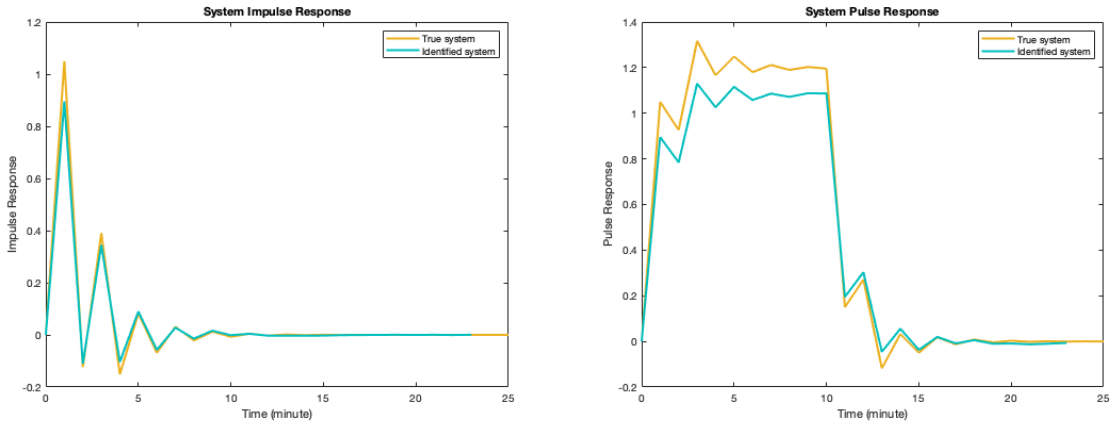

(a) Impulse response

(b) Pulse response

Figure 4.6: Impulse and pulse responses of a true and identified system for a dataset of 1999 samples.

The developed model is also capable of handling the random missing output data with high resilience. Figures 4.7 and 4.8 illustrate the pulse and impulse responses of the true and identified system with 5%, 10%, 20%, and 70% of missing output samples, respectively. As shown, the model is capable of taking care of large amounts of missingness since the identified systems' curves do not deviate much from the true systems'.

Having fewer data for modeling, the magnitude of the responses has changed a bit but most of the main characteristics of the system remained the same. More precisely,

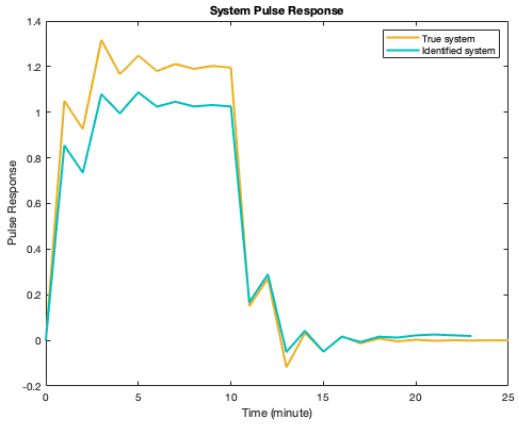

(a) Pulse response, 5% missing output data

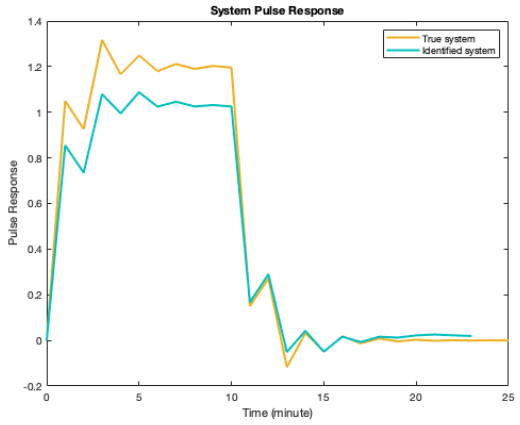

(b) Pulse response, 10% missing output data

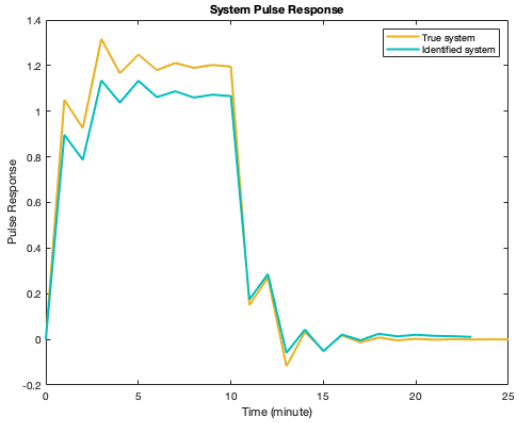

(c) Pulse response, 20% missing output data

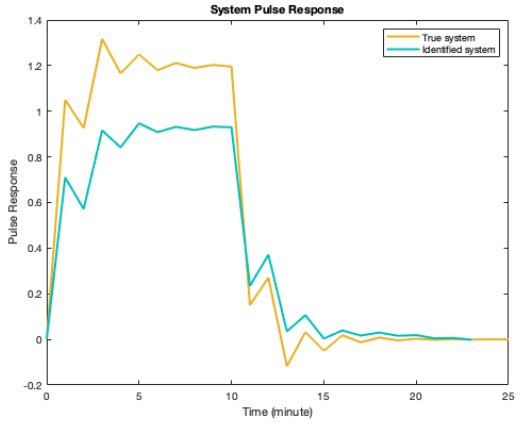

(d) Pulse response, 70% missing output data

Figure 4.7: Pulse responses of a true and identified system with 5%, 10%, 20% and 70% random missing output data.

this shows that the poles of the system have not changed much due to missingness. By increasing the percentage of missingness, the predicted responses start to have a lower magnitude in comparison to the true system responses. While losing some of the magnitude, the models have been able to capture the main dynamics of the behavior, even with large amount of missing data. `data_set_3` in the DOME package is the dataset with 1999 samples distributed across 50 data chunks with 20% randomly assigned missingness in the output.

As the final example, `data_set_4` provides the first three inputs needed for the `dome_train_test` tool that are `chunk_train`, `chunk_test`, and `Ts`. `dome_train_test` returns the `Lin_sys`, the identified system that can be used to plot the impulse and pulse

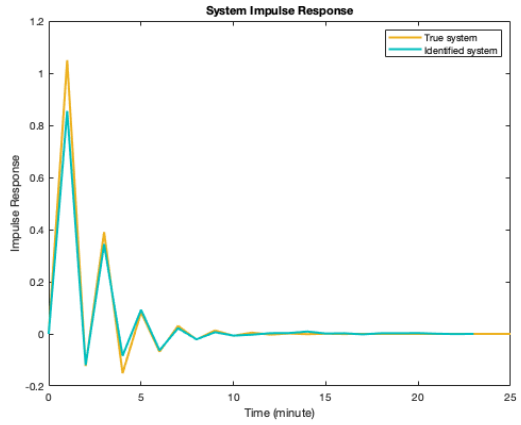

(a) Impulse response, 5% missing output data

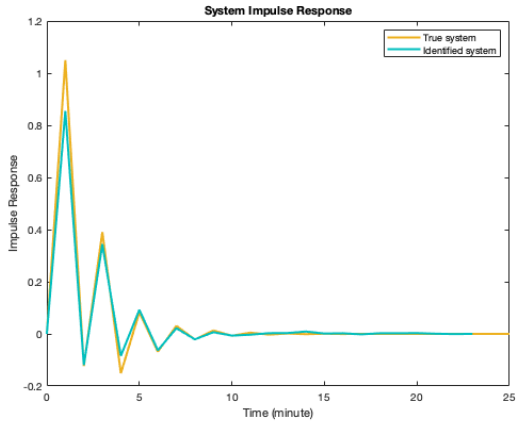

(b) Impulse response, 10% missing output data

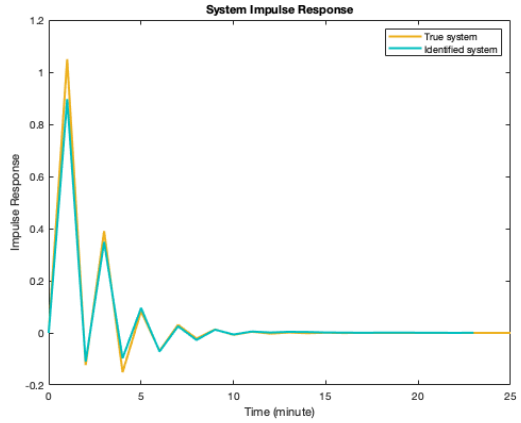

(c) Impulse response, 20% missing output data

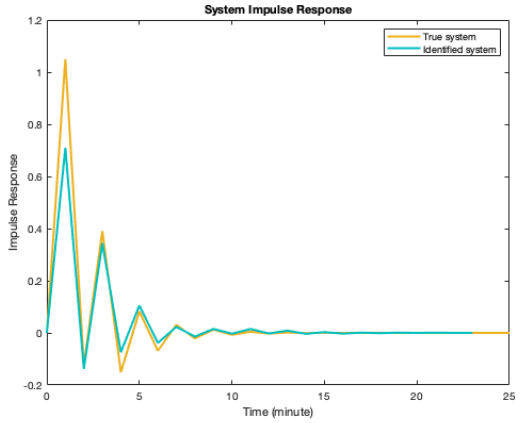

(d) Impulse response, 70% missing output data

Figure 4.8: Impulse responses of a true and identified system with 5%, 10%, 20% and 70% random missing output data.

responses of the system and the `error` value. `data_set_4` contains a train set of 1765 samples with 45 data chunks and a test set of 234 samples with 5 data chunks, while 20% random missing output data is present. Using this dataset, `error` that is sum of the absolute values of the errors between the true and predicted outputs of the system over the entire test set was computed as 1.91×10^{-16} which is zero from a numerical point of view and represents the high accuracy of the identified system.

This should be noted that all simulations described in this chapter are done on a MacBook Pro with a 2.3 GHz Dual-Core Intel Core i5 processor and a memory of 8 GB 2133 MHz LPDDR3. Using this system, solving the optimization problem for a large dataset of 1999 samples distributed across 50 data chunks takes only about 207

seconds. This should also be emphasized that the code uses "off the shelf" toolboxes and improving its speed is one of our next priorities.

4.6 Discussion

This chapter describes an approach to model the dynamic effects of a longitudinal input on a binary longitudinal output. Developed dynamical modeling technique allows for delayed effects and can handle fragmented input and output data. The provided tools take advantage of recent developments on the parsimonious systems identification domain i.e., efficient identification of sparse models using atomic norm minimization [32].

The developed approach has been implemented in MATLAB® programming platform. Effort is currently being put in porting this package to Python and R platforms. The provided MATLAB® package on GitHub includes the implemented algorithm, various datasets, and a description of each. The instructions on how to use the developed algorithm, a description of input and output to it, results of applying various datasets, and a discussion on how to interpret the results obtained are provided.

It should be mentioned, at this time, that the discussion on result interpretation is just one of many possibilities. The approach presented provides a computational model of the interaction between input and output which can be used to simulate the response to many different types of inputs. In other words, the interpretation provided here has aimed at studying the impact of a single event, but the model can be used to study many other cases such as the one where an input event occurs periodically.

Although different models have been developed and applied by researchers to study the behavior and substance consumption patterns of the individuals or groups of users in response to different inputs, described in chapter 1 in details, they are all confined by some limitations such as relying only of self-reports, being computationally expensive, not considering the memory effect, ability to handle missing data, etc. The proposed approach in this chapter has several contributions and effectively addresses those limitations.

First, the developed algorithm can handle very large datasets and therefore can leverage intensive high frequency longitudinal data gathered from sensors and activity monitors, allowing to investigate a range of moments immediately leading up to and following events. Previous studies using intensive longitudinal data mostly relied on self-reports that might be too infrequent to capture and/or predict the moments of vulnerability, opportunity, and receptivity. Additionally, since in our proposed approach the only optimization problems to be solved are linear programs, the computational

complexity of the developed tool, even for large datasets, is very low and DOME is capable of characterizing complex change patterns.

Second, the proposed approach allows for the use of very fragmented data. By using the fact that we estimate not only the response to the input but also the behavior associated with the current state of the "subject", it can handle data where the input is only available in "chunks;" i.e, available only in disconnected intervals of time. Moreover, the assumptions on the measurements of the output are much less restrictive. Such fragmented data is common when deploying sensors to extract digital biomarkers of health and behavior [20]. The proposed algorithm can handle any fragmentation of the output data, including (but not limited to) randomly occurring missing measurements. To the best of our knowledge, no study has practiced a systematic way of handling the missing data in either input or output data.

Third, our work is developed considering the dynamic behavior changes, i.e., relation between different tailoring variables "over time", considering the "memory effect". That is, dynamical modeling approach is developed according to the concept that the output at a specific moment is not only related to the input at the present moment, but it also is connected to the past moments of both the input and the output. To the best of our knowledge, techniques like JITAIs have not considered the "memory effect" of the tailoring variables.

Finally, since DOME aims at estimating the least complex model that is compatible with the data provided, it is also very well suited to handle small fragmented datasets. This is especially useful when using individual "small data" to estimate low complexity personalized behavior models which can later be used to develop person-specific just-in-time interventions. Additionally, the model order is not an a priori constraint in our model and can be different for each individual.

4.6.1 Limitations

The DOME tool described here, does not directly consider the fact that there might be external perturbations influencing the output. This can be addressed in multiple ways. If the perturbation is known, it can be incorporated in the model as another input, i.e., we can extend this framework to deal with multiple inputs. If the perturbation is not known, it can be modeled as noise and also be incorporated in the model. This matter does not change the basics of the approach described and we have planned to introduce these extensions in future versions of the DOME package.

Also, given the fact that the input response is modeled as a linear time-invariant

system in series with a fixed nonlinear term, it assumes that the effect of the input on the output is proportional to the magnitude of the input. Moreover, in its present form, it cannot address different inputs at different time scales. Extensions of the proposed approach to address these problems are the subject of the ongoing work.

4.7 Conclusion

In summary, we have shown that dynamical systems can be a powerful tool for modeling the interaction between longitudinal variables allowing for inputs effect that "stretches" over time. The approach presented can leverage "real data" that often has missing measurements and provides simple models that predict the response to inputs. The models obtained can be used not only to study how an individual responds to different inputs but also as a first step in the process of designing just-in-time adaptive interventions. More precisely, once an input response model is available, concepts from control engineering can be used to design effective robust interventions.

Chapter 5
Person-Specific Dynamic Models of Stress and Smoking

Cigarette smoking is the leading preventable cause of death in the United States, responsible for about one in five deaths annually [96]. The costs of direct medical care for adult smokers, lost economic productivity caused by smoking-related disability and premature mortality, and secondhand smoking exposure exceed $300 billion per year in the United States [97, 98]. Comprehensive smoking control programs require a clear understanding of the dynamics of smoking triggers and behaviors; however, few studies have attempted to describe those systems. Employing tools and developed dynamical systems modeling techniques in chapter 4, this study uses high-frequency sensors and novel markers of both stress and smoking to describe system dynamics and then simulate how stress influences subsequent risk for smoking.

5.1 Introduction

5.1.1 Stress, a Key Cause to Smoking

Stress and negative emotions have long been thought to be motives for smoking [99–102]. Stress represents the non-specific response of the body to a demand [164]. It manifests as distress and negative affect when the perceived demand exceeds the individual's coping potential [165]. Smokers identify stress as a reason for smoking [99–101]. One reason may be that they learn that nicotine self-administration can dispel negative affective states that are caused by withdrawal and produce acute psychological benefits such as improved mood and concentration [166–168].

Evidence based on a variety of methods supports the concept that stress-induced

negative affect is positively associated with smoking [169, 170]. For example, the acute stress of a terrorist attack in New York City increased smoking rates among residents [171]. On a faster time scale, Shiffman et al. found a positive association between repeated assessments of daily stress and smoking [103]. Affect dysregulation, particularly negative mood variation, has also emerged as a risk factor for future smoking escalation [172]. These findings point to stress responses as a target for behavioral interventions to reduce smoking and as a potential tailoring variable for interventions to reduce stress-related smoking.

The stress and smoking literature has three gaps that need to be addressed to inform intervention development efforts. First, most of the literature assessing links between stress or negative affect, on one hand, and smoking on the other, involves data collected during a quit attempt [173–177]. Assessments of stress taken after quitting smoking reflect both physiological arousal due to daily life experiences and distress due to nicotine withdrawal. Stress-smoking dynamics may be able to be characterized more consistently prior to a quit attempt, before prolonged nicotine withdrawal disrupts baseline stress – smoking dynamics. These dynamics can expose the duration of vulnerability between the onset of a stress response and smoking behavior. That information can be used to tailor decision rules (i.e., person-specific algorithms) for adaptive smoking cessation interventions in the future.

Second, available analyses have relied on periodic measurement of stress and smoking based on self-reports. However, these self-report assessments are made too infrequently to capture sufficient granularity in continuous stress dynamics leading to and following smoking events. Additionally, self-reports are vulnerable to bias from memory errors, psychiatric limitations and self-presentational concerns. The present study uses sensor-based markers of both stress and smoking to obtain more intensive data that can reveal the dynamics of stress and smoking.

Third, no attempts have been made to study the dynamics of stress in the moments immediately prior to and following smoking events. To date, stress has not been collected continuously and data have typically been limited to a single data point about stress prior to a smoking episode. The availability of sensors and digital markers of stress creates new possibilities for monitoring stress continuously so a time-series of stress measurements can be used to predict smoking events and to characterize changes in stress after smoking. In this study, intensive longitudinal digital assessments afforded sufficiently continuous, granular portrayal of stress dynamics to develop a model informed by stress immediately before, during, and after smoking episodes. This approach can provide the foundation

for predicting the temporal response of individuals to stress as a basis for developing evidence-based, just-in-time smoking cessation interventions.

5.1.2 mHealth Tools May Reveal Dynamics of Self-Medication Smoking Effect

Recent advances in wearable sensors and mHealth markers enable continuous monitoring and detection of stress states and smoking behavior. Useful measurements may include electrical activity of the heart, breathing dynamics, hand movements, and physical activity. Continuously-measured stress states (i.e., inferred from physiological arousal in the absence of physical activity) and smoking behavior sampled at high frequencies (e.g., minute-level) via wearable devices require different tools for their analysis than more sparsely-distributed periodic data from ecological momentary assessments to characterize system dynamics. Understanding these dynamics will provide a foundation for adaptive treatments on the individual level so interventions can be delivered at the moments of greatest need.

High-frequency data indicators of an output (e.g., minute-level smoking behavior) are not only dependent on the present moment of the candidate input (e.g., stress), but are also correlated with past values of that input. In other words, a stress episode can affect both the probability of smoking immediately, and increase the smoking likelihood in the minutes following the stress episode.

Therefore, data signifying present moments of smoking need to be connected to data from immediately prior values of stress to model the stress-smoking responses. As described in chapter 4, dynamical systems provide the necessary tools to model this so-called "memory effect": that is, the effect of past and present values of the input on the future output. In this context, the system is a process that connects past and present values of an input (stress) to an output (smoking).

5.1.3 Dynamical Systems

Smoking is a complex, dynamic behavior. It can be influenced by a variety of factors over time and is not necessarily the instantaneous result of stress (or other causes). Given the potential for a delay of unknown duration between stress and smoking, existing analytic tools for behavioral studies mentioned above are not well-suited to using all of the information in high-frequency intensive longitudinal data and providing a comprehensive description of the relation between system variables [132, 178].

In general, a system is a process that produces repeated outputs in response to repeated inputs. Identifying a model of the relations between variables (i.e., inputs and outputs) that unfold over time (hereafter, a system) is the starting point for developing algorithms to make informed decisions for controlling the system. Often the identified models need to be tuned for the specific system (e.g., for a specific home, vehicle, or aircraft) and this tuning is particularly important for systems describing human behavior which have a high level of uncertainty due to multiple causes.

We propose to leverage individual intensive longitudinal data to identify person-specific models that describe dynamic relations between stress and smoking for each individual. Models obtained by these techniques provide the parameters needed to potentially develop person-specific algorithms (i.e., decision rules) for adapting the delivery of a just-in-time intervention based on person-specific vulnerabilities. Such models could realize the potential for personalized behavior medicine to provide people with the right treatment only at the moment when they need it, based on the person-specific dynamics.

This approach allows for greater flexibility in designing just-in-time interventions because it can provide evidence-based, tailored – even person-specific – decision rules when stress-smoking systems differ between people (e.g., due to varying model complexity or input salience). In this work, we focus on stress as a potential tailoring variable for just-in-time interventions to prevent smoking behavior and model stress-smoking systems.

System identification methods – techniques to fit a dynamic model from longitudinal measurements of an input to an output – have been used to evaluate smoking cessation treatments [179]. These methods have been combined with model predictive controllers – controllers (decision rules) that rely on dynamic models of a process obtained by system identification to determine the "right" inputs to the process – to provide a foundation for designing adaptive intensive smoking interventions [180, 181]. Simulations by Lagoa et al. revealed that treatment outputs could be improved by delivering real-time interventions when and where needed [180]. Bekiroglu et al. also represented the relations between tobacco withdrawal-related processes over time using dynamical models [182].

Such works demonstrated the feasibility of applying system identification tools to model problems involving smoking. Moreover, they provided preliminary results on how the identified models can be used to develop just-in-time interventions. This study will provide the first application of system identification tools to model person-specific stress-smoking systems and will provide the basis for applying model predictive control tools to design an adaptive intensive, smoking intervention tailored on stress.

These prior smoking-related applications involved continuous output measures, leading to relatively straightforward modeling procedures. However, in our system, the input (stress) is represented by a continuous score and the output (smoking event) is represented by a binary value. Model identification of a connection of a linear system with a hard nonlinearity is known to be a complex problem because the resulting optimization problem is non-convex and, therefore, hard to solve numerically.

Developed tools for system identification described in chapter 4 in detail, provide computationally efficient convex relaxations aimed at obtaining the lowest complexity model compatible with the data available. Furthermore, to the best of our knowledge, system identification methods have never been applied to describe the person-specific dynamics of stress-smoking responses with a binary output.

5.1.4 The Present Work and Contributions

This study used wearable devices to collect intensive longitudinal data and applied algorithms to estimate the probability of stress (cStress) at every minute and detect smoking episodes (puffMarker) [183,184]. These two measures have been used to evaluate stress and smoking lapses in another study conducted by some collaborators of the current work [185].

Here, we applied the algorithms we developed in chapter 4 using system identification techniques from control systems engineering, to model person-specific dynamic relations between stress and smoking. In other words, using only data recorded from each individual, we modeled their individual behavior and, therefore, determined a different system/model for each participant.

Analyzing stress-smoking relations especially at the moments preceding and following a smoking episode and generating person-specific model parameters in the present study provides the basis for designing person-specific, tailored smoking cessation interventions and treatments from the parameters linking vulnerable moments (when stress is likely to lead to smoking) to intervention decisions in the future works.

5.2 Method

5.2.1 Design

This study is a secondary analysis of data from the Sense2Stop trial conducted through the MD2K Center of Excellence [19]. The Sense2Stop trial involved 15 days of data

collection: 3 days prior to a quit attempt, a quit day, and 11 post-quit days. This study used data from the 3 pre-quit days to develop dynamic models of stress and smoking.

5.2.2 Participants

Flyers posted in the community were used to recruit adult smokers interested in quitting smoking for the Sense2Stop trial. Prospective participants (n = 371) were screened for eligibility and 75 eligible participants enrolled. Participants were between 18 and 65 years, lived in the Chicago area, smoked more than one cigarette per day on average in the last year, were willing to abstain from non-cigarette tobacco products for the course of the study, willing to try to quit smoking for at least 48 hours (the parent trial focused on smoking cessation but the present study was limited to data from the pre-quit period), not taking any medications for smoking cessation currently or planned in the next 30 days, not pregnant or trying to get pregnant, and willing to provide an emergency contact, social security number, and address for study payment.

5.2.3 Procedures

Participants were provided with four devices and asked to wear them for up to 16 hours/day: two MotionSense wristbands, one Autosense chestband, and an Android smartphone [186, 187]. The Autosense chestband supports a wireless sensor suite that records continuous physiological measurements consisting of an electrocardiogram (ECG, 64 Hz), respiratory inductive plethysmograph (RIP, 21.3 Hz), and 3-axis accelerometer (10.7 Hz) [186]. Each MotionSense wristband contained a 3-axis accelerometer (16 Hz) and a 3-axis gyroscope (16 Hz) to record arm motion [184, 187].

The open-source mCerebrum software has been used to support continuous sensor data transfer from the chestband and wristbands to the smartphone [188]. Participants were compensated if they wore the devices above 70% of the requested wear time during the study period (i.e., 11.2 h/day); however, due to either battery issues or participants not wearing the devices correctly, the wear time was less than that for many participants. Full procedures for the Sense2Stop trial are available in [189].

5.2.4 Measures

Stress was operationalized as the minute-level probability of stress determined using the cStress algorithm [183]. cStress marker uses data from a 2-lead electrocardiograph and

a respiration inductive plethysmograph collected by chest-worn AutoSense sensors to estimate the probability of stress at each minute. Specific features used to construct minute-level stress probabilities from those sensors included the 80th percentile and mean of interbeat interval, and mean and median of the ratio between inspiration and expiration duration.

Stress probabilities were calculated every minute except when accelerometers in the chestband recorded physical activity (due to confounding factors from the physiological responses to activity) or when data were unavailable due to poor sensor attachments or other noise. This cStress model previously demonstrated a true positive rate of 88.6% and false positive rate of 4.65% on a test dataset from the lab. The cStress model achieved a median accuracy of 90% and 72% with self-reports from the lab and the field, respectively [183].

Smoking behavior was operationalized every minute as a binary score from the puffMarker algorithm [184]. This algorithm uses two sources of data: breathing dynamics collected from the respiration inductive plethysmograph in the chestband, and arm movements gathered from inertial sensors on each wrist. Puffs were identified from patterns of hand-to-mouth gestures and respiration cycles.

Features extracted consisted of inhalation and exhalation duration, respiration duration, minimum and maximum of the rate of change signal (first derivation of the respiration signal), and mean, median, standard deviation, and quartile deviation of magnitude of gyroscope, pitch, and roll. Excluding isolated puffs, smoking episodes were marked if a minimum of four smoking puffs was detected. The puffMarker algorithm achieved a true positive rate of 96.9% and a false positive rate of 1.1% on the training dataset [184].

5.2.5 Analyses

5.2.5.1 Data Quality Screening

Data were recorded from 75 participants, but participants were excluded if they were part of the pilot test (n = 5) or had excessive missing sensor data due to physical activity, improper attachment, non-wear, sensor failures, or insufficient data (i.e., less than five minutes of continuous data). After accounting for these problems (n = 25), the analytic dataset comprised 45 participants (60%). The flow of the participant recruitment and inclusion is shown in Figure 5.1.

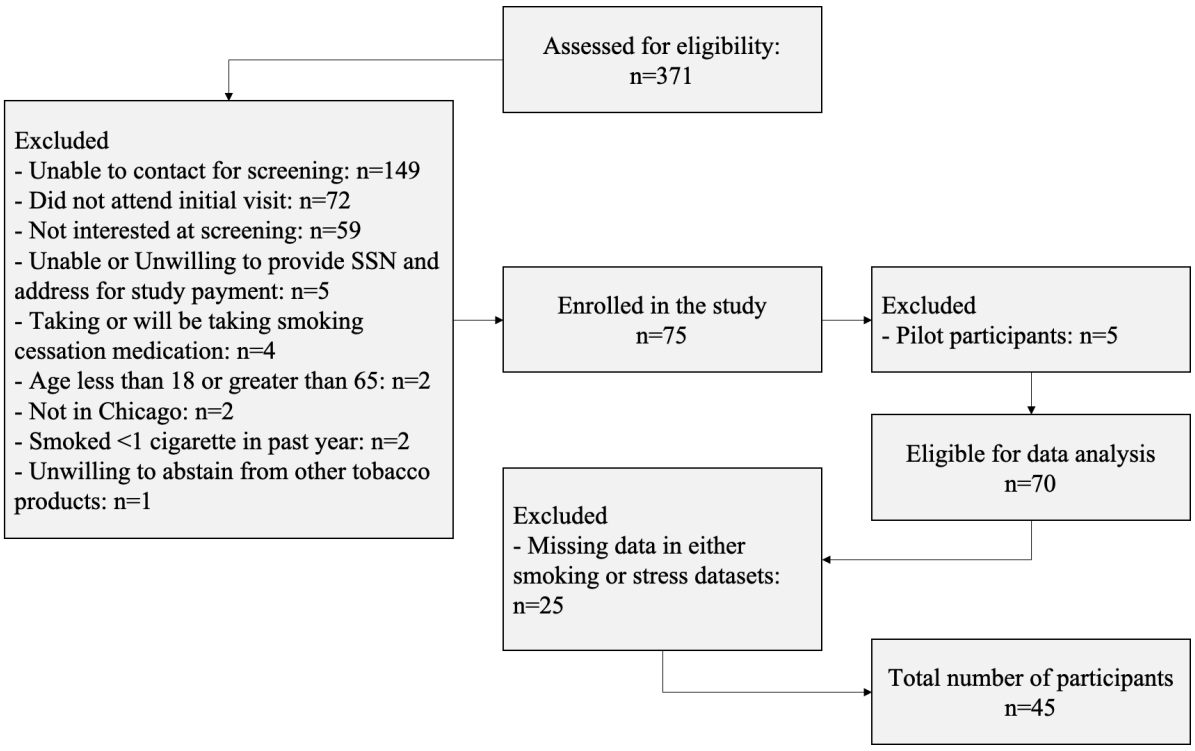

Figure 5.1: Participants flow in Sense2Stop trial and inclusion for this work analysis.

5.2.5.2 Modeling Strategy

The modeling strategy, algorithm development, and mathematical details of the system identification methods described in chapter 4 in details. For these analyses, stress probability is considered as the input and smoking is considered as the output. The modeling objective is to identify a system that represents the relation between these two longitudinal signals. Note that, in the proposed approach, we aim at modeling individual behavior and, therefore, a different system or model is identified for each participant.

Again, the system encompasses of two blocks including a linear system following by a "sign nonlinearity". The output of the linear system, y, is the summation of y_{input} and y_{int} that are the behavior of the system directly connected to stress and the estimate of smoking odds when the participant is not experiencing stress, respectively. The sign nonlinearity provides the binary output indicating whether, at a specific time, the participant is smoking or not. The response of identified system at a specific time t, $y(t)$,

has a nonlinear relation with smoking which is described as

$$\begin{cases} smoking(t) = 1 & \text{if } y(t) = 1 \\ smoking(t) = 0 & \text{if } y(t) = 0 \end{cases} \tag{5.1}$$

In equation (5.1), the use of a threshold equal to 1 is arbitrary; the choice of the threshold does not impact the overall results. The main idea here is that if a feasible solution to the linear system exists, applying any positive threshold in the sign nonlinearity block does not impede the feasibility of the system's solution. In other words, the actual size of the threshold is not important. Scaling the threshold will lead to an inverse scaling of the output of the linear system; therefore, since we are dealing with linear systems, it does not change the identification problem or overall results.

5.2.5.3 Data Processing

Data processing consisted of five general stages: correcting sample times, handling small intervals of missing data via linear interpolation, determining ending time of smoking episodes, dividing data into continuous pieces called data chunks, and excluding data chunks with less information is done. We now describe each step in detail.

First, the timing for each stress probability and smoking event is provided in timestamp format. Therefore, the primary step in processing the data is to convert timestamps to datetime. Datetime version represents the time and date information of the events more intuitively, making the results and their display more easily interpretable.

The sampling rate in this study is approximately one minute; however, the timing of some samples violated this criterion, such as when two probabilities were provided for a minute (e.g., with time difference of 59 seconds). To address this matter, the approach taken is to round time to the nearest minute. Therefore, in this context, a sample means one minute of information, and a chunk is a continuous series of samples.

Second, different durations of missing data occurred in the stress probability measure, ranging from one to about 120 minutes. If intervals of missing data were brief ($\leq$ 2 min), linear interpolation technique was used. The reason for this choice is that, given our dataset, two interpolated samples can still provide good consistency as well as maintaining the accuracy of the provided data. Also, these short intervals of missing data would mostly occur as the result of mis-attached sensors on the body rather than any kind of confounding activities which can interfere with stress probability estimation. If intervals were large ($>$ 2 min), there was not enough information to make any prediction/estimation

of missing stress probabilities at those time intervals.

Third, the puffMarker algorithm identified the start timing of each identified smoking episode and the timing of all detected smoking puffs, but did not identify when smoking episodes ended. A minimum of four puffs in a five-minute time interval was required to qualify as a smoking episode. To determine the duration of the smoking episodes, a sliding five-minute window was used beginning at the start of the episode. As long as the criterion of four puffs inside the considered window was met, the smoking episode was extended. Smoking episode durations for participants ranged from two to ten minutes.

Finally, given the fragmented nature of the stress probability dataset and the fact that no information was available to understand relations between stress and smoking during time gaps, we considered each continuous interval of data samples as one data chunk. Some data chunks in our dataset consisted of very small number of samples, as low as just one sample, which makes it hard for the system to understand the behavior and identify the meaningful relation between stress and smoking. To extract relevant information, chunks with less than five minutes of information were excluded. Removing these small data chunks from the analytic dataset had minimal impact on the number of minutes that could be modeled (on average, 68 minutes/participant).

5.3 Results

Participant characteristics are summarized in Table 5.1. A summary of processed and analyzed data for all participants can be found in Table 5.2 and Table 5.3. These quantities include the number of samples in the original dataset, samples after interpolation (with missing samples ≤ 2), chunks based on the interpolated dataset, chucks number after removing the small chunks (size < 5 samples), and samples after excluding the small chunks.

Prior to interpolation, the average total duration of data from each participant sampled in the dataset was 723.1 min (SD = 323.6; range = 79 - 1452) over 3 days; after interpolation, the average total duration of data from each participant increased to 887.9 min (SD = 385.5; range = 90 - 1776) over 3 days (wear time for many participants was less than 11.2 h/day). The interpolated samples were divided into chucks with a mean number of 76.2 chunks/participant (SD = 33.1; range = 3 - 150). After removing data chunks less than 5 minutes long, the mean number of data chunks/participant used for modeling was 40.5 (SD = 16.45; range = 3 – 80). The mean total duration of samples used for system identification was 819.9 minutes (SD = 375.8; range = 90 – 1716).

Table 5.1: Characteristics of the participants in stress-smoking study.

Characteristic	N (%)	Mean (SD)	Range
Age		42.6 (14)	20 - 64
Sex			
Female	22 (49%)		
Male	23 (51%)		
Race			
American Indian/Alaska Native	0 (0%)		
Asian	1 (2%)		
Native Hawaiian/ Other Pacific Islander	0 (0%)		
Black/African-American	23 (51%)		
White	14 (31%)		
Two or More Races	5 (11%)		
Other	2 (4%)		
Ethnicity			
Hispanic or Latino	5 (11%)		
Not Hispanic or Latino	40 (89%)		
Number of cigarettes per day			
10 or less	28 (62%)		
11-20	12 (27%)		
21-30	3 (7%)		
31 or more	2 (4%)		
Age of starting to smoke?		18.3 (6.5)	7 - 45

Applying modeling strategy developed for this analysis which was person-specific dynamical modeling, we report a single dynamic model estimated for a single participant to demonstrate the process of linking input and output through an identified system consisting of a response to the input, intrinsic response, and system response. This modeling strategy was then deployed on usable data from each participant separately. Next, we simulated how each participant would respond to a specific continuous stress episode lasting 10 minutes (an arbitrary value to standardize the comparison among participants), to illustrate how these response patterns vary across participants.

5.3.1 Deriving Person-Specific Model of Smoking

Data from a single participant are used to illustrate components of the dynamical system. Figure 5.2 and Figure 5.3 show changes in the candidate input, output, and responses of the identified system for one data chunk consisting of 15 samples. In all plots, the

Table 5.2: Data information for all the participants. "All samples" represents the data collected for each participant, "Interpolated" is the number of minutes of data after linearly interpolating the missing data of length ≤ 2 minutes, "Data Chunks" and "Used Chunks" are the number of chunks of data based on the interpolated sample and the ones after discarding chunks with size < 5, respectively. "Used Samples" are the interpolated samples after discarding data with chunk size < 5. All times are in minute scale.

Participant ID	All Samples	Interpolated	Data Chunks	Used Chunks	Used Samples
Participant 201	529	632	30	20	607
Participant 202	513	642	63	38	591
Participant 203	650	775	46	22	736
Participant 204	434	554	65	30	473
Participant 205	706	878	81	40	792
Participant 208	894	1169	121	64	1057
Participant 209	538	625	38	26	601
Participant 210	79	90	3	3	90
Participant 211	953	1182	85	51	1114
Participant 212	911	1076	89	45	989
Participant 213	782	913	63	33	860
Participant 214	768	976	113	50	851
Participant 215	1176	1380	51	31	1346
Participant 216	706	889	62	40	846
Participant 217	852	1043	90	48	957
Participant 219	766	933	55	37	898
Participant 220	553	673	66	33	598
Participant 222	625	770	89	47	699
Participant 226	1014	1253	101	67	1186
Participant 228	843	1063	90	50	992
Participant 229	1452	1776	90	60	1716
Participant 230	1077	1329	112	60	1237
Participant 231	1132	1402	148	80	1280
Participant 233	803	992	98	51	909
Participant 234	392	550	69	39	496
Participant 235	802	995	75	36	916
Participant 240	766	960	120	58	842
Participant 242	318	458	94	37	355
Participant 244	356	433	36	19	399
Participant 245	500	620	74	29	538
Participant 250	1169	1401	85	52	1345
Participant 251	1129	1336	95	52	1250
Participant 252	1221	1459	96	51	1365
Participant 253	1180	1408	78	56	1366
Participant 255	611	789	99	47	688
Participant 257	351	420	12	10	412
Participant 258	194	236	22	14	221
Participant 259	310	365	31	17	340
Participant 260	511	629	64	35	582
Participant 261	918	1103	56	37	1067
Participant 262	823	1023	111	60	914
Participant 264	377	529	150	40	335
Participant 265	1152	1353	88	55	1293
Participant 268	590	717	97	40	602
Participant 270	115	157	26	14	143

Table 5.3: Statistics of data used in this study.

Data Characteristic	Mean	SD	Median	Minimum	Maximum
Original Samples	723.13	323.6	766	79	1452
Interpolated	887.91	385.5	913	90	1776
Data Chunks	76.15	33.12	81	3	150
Used Chunks	40.53	16.46	40	3	80
Used Samples	819.86	375.8	846	90	1716

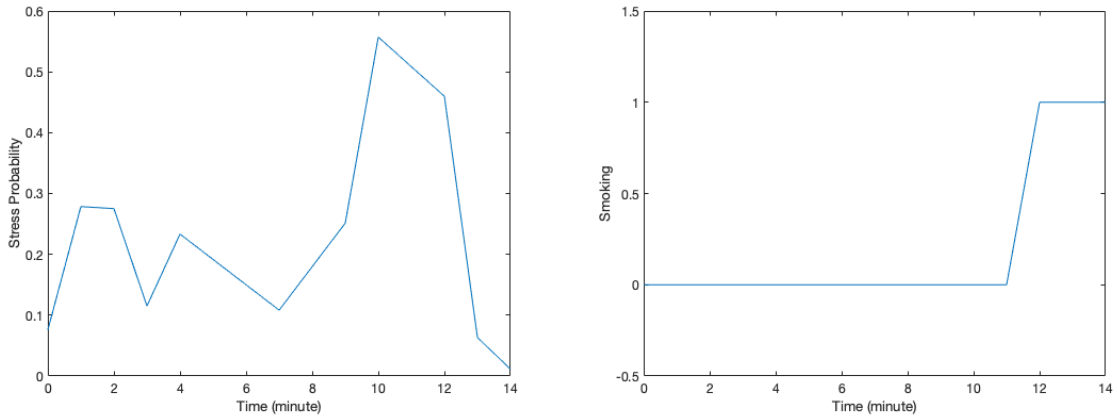

Figure 5.2: input (stress probability)(left) and output (smoking)(right) of the system for one data chunk.

horizontal axis shows time with a minute scale. Figure 5.2 (left) represents the candidate input (stress probability) and Figure 5.2 (right) shows the output (smoking) of the system for every minute. Stress probabilities in Figure 5.2 (left) ranged from 0 to 1; smoking values of 0 and 1 in Figure 5.2 (right) indicate non-smoking and smoking events at that minute. Respectively, Figure 5.3 (a) to (c) represent the input response, intrinsic response, and the overall response of the system for this data chunk.

As mentioned earlier, input response is a behavior of the system which is directly connected to stress (y_{input}, Figure 5.3 (a)), intrinsic response represents the odds of smoking when stress is zero (y_{int}, Figure 5.3 (b)), and the system response plot represents the summation of the response of the system to stress and intrinsic response (y, Figure 5.3 (c)). The concept represented in equation (5.1) is also depicted in (Figure 5.3 (c)). According to this criterion, whenever the value of $y(t)$ equals or exceeds the threshold of 1, there is a smoking minute in the output and if $y(t) < 1$, there is no smoking occurrence (Figure 5.2 (right)).

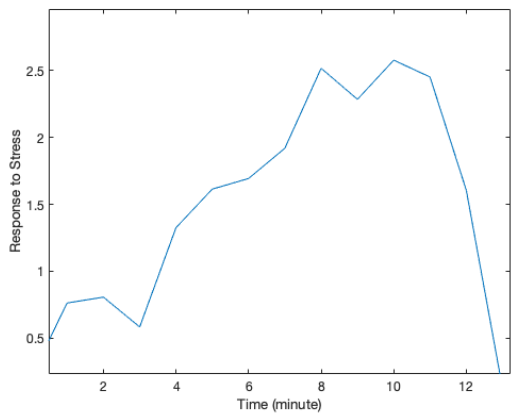

(a) Input response

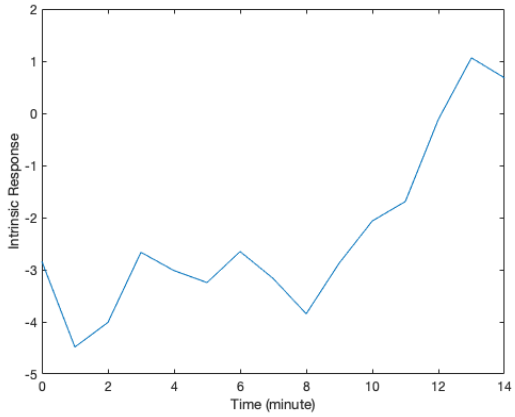

(b) Intrinsic response

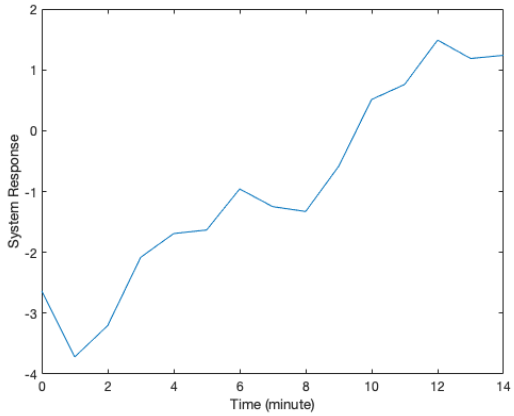

(c) System response

Figure 5.3: Different responses of the identified system for one data chunk, described in Figure 5.2: (a) Response of the system to input (stress), (b) Intrinsic response of system, (c) System response which is sum of input response and intrinsic response.

5.3.2 Simulated Smoking Responses to Stress

Another response of a system, pulse response, is used here to show the relation between stress and smoking. Pulse response is the response to a continuous stress episode for a given duration. For standardization, we simulate the responses to a presumed stress episode of length 10 minutes. This duration is arbitrary and allows us to standardize the comparison among participants. A stress episode of length 10 minutes is used to achieve the pulse response for all participants.

According to their respective pulse responses, results from the modeling of smoking behavior due to stress for all participants can be divided into five clusters. Due to

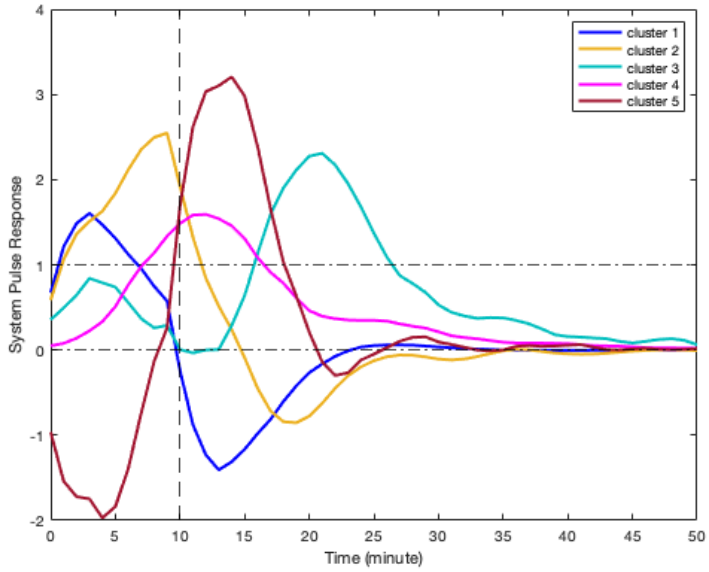

Figure 5.4: Pulse response of a representative of all clusters. The vertical line at the 10-min mark on the x-axis reflects the time when the stress probability returned to zero.

the limited sample size of this study, visual clustering is applied based on the shape of observed participants responses. Figure 5.4 illustrates the simulated pulse responses of a representative participant from each cluster to a 10-minute stress episode and Figure 5.5 (a) to (e) represent the pulse responses of individual participants in each cluster to the stress episode, respectively.

Cluster 1 was characterized by instantaneous or relatively rapid responses to stress as indicated by an immediate increase in the odds of smoking following by a sharp decrease in odds of smoking. Cluster 2 was characterized by a delayed response to stress, approximately 7 to 12 minutes after the start of stress episode. Participants in this cluster had shown an increase and subsequently a decrease in their odds of smoking. Cluster 3 was characterized by an instant increase followed by a second, delayed increase in the odds of smoking due to stress. Cluster 4 was characterized by a single delayed increase in response to stress without a subsequent sharp decrease in the odds of smoking. Finally, cluster 5 was characterized by an instant decrease in the odds of smoking following by a sharp delayed increase in its odds.

Table 5.4 summarizes the number of participants belonging to each cluster. It should be noted that the higher magnitudes of the pulse response do not necessarily imply a higher likelihood of smoking. In fact, the magnitude of the pulse response represents the estimated changes of propensity for smoking when stress happens, as a function of time.

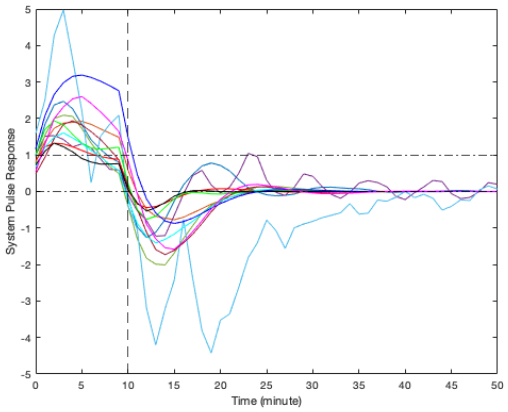

(a) Cluster 1

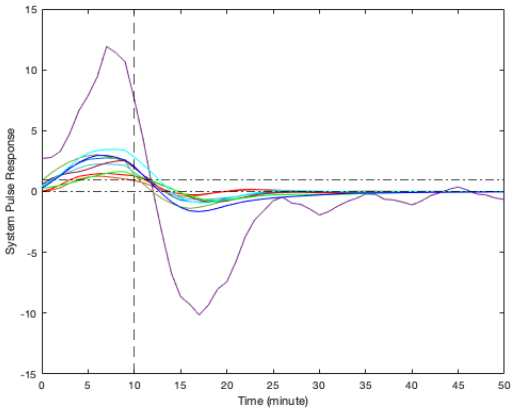

(b) Cluster 2

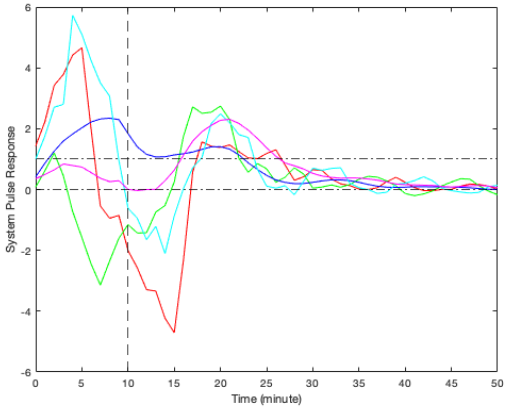

(c) Cluster 3

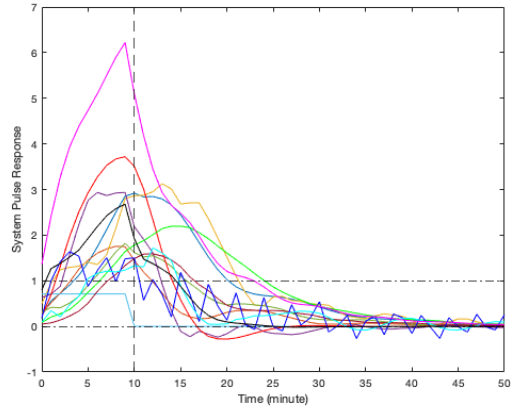

(d) Cluster 4

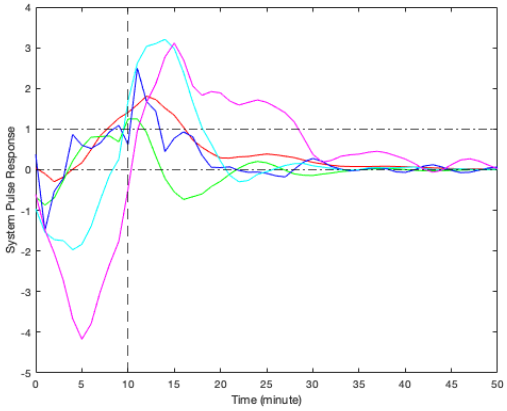

(e) Cluster 5

Figure 5.5: Pulse responses of all the participants to stress: (a) Instant increase following by a sharp decrease in smoking odds, (b) A delayed increase following by a sharp decrease in smoking odds, (c) Two rounds of increases in smoking odds, (d) Just one delayed increase in smoking odds in response to stress, (e) Instant decrease in the odds of smoking following by a sharp delayed increase. In all figures, the vertical line at the 10-min mark on the x-axis reflects the time when the stress probability returned to zero.

If the magnitude is positive, it represents an increase in the likelihood of smoking and if it is negative, it shows a decrease in the likelihood of smoking.

Table 5.4: Number of participants and the percentage for each detected cluster.

Cluster	**Number**	**Percentage**
Cluster 1: Immediate increase following by a decrease in odds of smoking	12	26.70%
Cluster 2: A delayed response to stress, an increase following by a decrease in odds of smoking	10	22.20%
Cluster 3: Two rounds of increase; an instant increase following by a delayed increase in odds of smoking	5	11.10%
Cluster 4: Just a delayed increase in odds of smoking	13	28.90%
Cluster 5: An instant decrease following by a sharp delayed increase in odds of smoking	5	11.10%

As shown by the results, all pulse responses to a continuous stress episode demonstrated an increase in the odds of smoking either immediately or with some delay. For the majority of participants (n = 25), the increase is followed by a sharp decrease in the tendency to smoke, down to negative probability. This can be interpreted as smoking due to stress leads to reducing the probability of further smoking in the near future for these participants. However, some participants (n = 12) did not follow the same trend, i.e., the increase in the odds of smoking did not proceed with a decrease in the smoking likelihood in the near future.

For a few individuals (n = 3), the early increase in the odds of smoking is followed by a second increase in its odds which shows that smoking in response to stress elevates the odds for further smoking for some people. For some participants (n = 5), the behavior is quite different. They represent a negative response to stress at the beginning which can be interpreted as a decrease in the chance of smoking at first moments of being under stress. The trend is followed by a sharp delayed increase in the odds of smoking. This can be an indicator of the effort of participants to prevent smoking at first; but eventually stress causes smoking to happen.

5.4 Discussion

This work makes two key contributions toward understanding relations between stress and smoking. First, it provides proof-of-concept for using system identification tools from

control systems engineering to identify person-specific dynamic models of stress-smoking responses for participants. In doing so, it applies a method developed in chapter 4 for combining a linear system with a sign nonlinearity to enable modeling of a continuous input (stress) and a binary output (smoking). Second, results of simulations based on person-specific models demonstrated heterogeneity in smoking responses to stress. For about half of the participants (49%), following an initial stress-induced increase in the likelihood of smoking, we expect to see an eventual reduction in the odds of smoking.

The work in this chapter demonstrated how dynamical systems modeling techniques can be applied to characterize the dynamics of stress and smoking. This modeling approach accounted for the influence of both recent stress and smoking to predict the odds of smoking in response to future stress. Prior efforts to link stress and smoking have been based on infrequent stress and smoking assessments for each smoking assessment [104, 168, 190, 191]. As sensing technology and digital markers improve, intensive longitudinal data will become more readily available to and important for researchers. Dynamical systems models can incorporate that information to predict the dynamics of smoking systems as a function of stress and other input variables.

5.4.1 Comparison of Approaches for Modeling Stress-Smoking Dynamics

Another tool for modeling longitudinal data is the time-varying effect model (TVEM) [54, 57–60, 62, 192]. This model has two noteworthy limitations. First, the TVEM cannot determine complex underlying within-time associations of variables [66], so it is not useful for investigating the long-term effect of inputs on an output. TVEM is limited to contemporaneous relations in a single model without considering the effect of delay in that association. That is, TVEM is not capable of exploring the memory effect of stress on smoking. Tools such as dynamical system modeling techniques from control systems engineering can fill this gap when investigators seek to understand the delayed effect of stress on smoking. Second, the TVEM represents bivariate associations as a function of time but requires an assumption that those time-varying associations are equivalent across people. The dynamical modeling technique applied in this chapter was used to generate person-specific models, and the results obtained would not support assumptions of equivalence across participants.

It is worth noting that the dynamical modeling approach applied here was a powerful technique considering the relatively limited amount of time series data, three days in

this dataset. Artificial intelligence techniques, including machine learning [193, 194] and deep learning methods [195], or statistical techniques such as Bayesian approaches and stochastic approximation expectation-maximization algorithms [68, 69] require a large volume of data. Additionally, the majority of these methods only provide the ultimate result not the dynamics of the system, that is, predicting whether the participant smokes or not by the end of the stress episode. With the three days of data available in this study, these alternative methods were not possible. Thus, control systems engineering tools strike a balance between capitalizing on intensive longitudinal data to reveal dynamics and being efficient in the volume of data required.

The person-specific models describing stress-smoking systems were used to simulate smoking dynamics following a 10-minute stress response. In those simulations, stress consistently increased the subsequent likelihood of smoking but there was considerable variation in how long it took for the likelihood of smoking to increase. In other words, although some participants did not show an immediate increase in smoking likelihood in response to stress, all participants were observed to increase smoking within some minutes of the stress episode. These findings are consistent with the hypothesis that some people use smoking to regulate stress [104, 168, 190, 191].

Although stress consistently increased the likelihood of smoking, participants varied in the delay between the onset of stress and observed smoking behavior. The latency of stress effects on smoking is an important contribution about which theories have been silent. For some individuals, stress responses have a relatively rapid effect on smoking behavior that may preclude intervention; for others, stress responses have a more delayed effect that represents a period of vulnerability when an intervention could be delivered. Data from this study do not indicate that participants learned to self-administer nicotine to regulate stress responses. Nevertheless, the approach demonstrated here can be extended to multiple time scales to test self-medication hypotheses – models on faster time scales can characterize stress effects on smoking and models on slower time scales can characterize how stress responses to smoking affect future stress-smoking dynamics (i.e., learning to self-administer nicotine to regulate stress (see [196, 197])).

Future research could also use n-of-1 or single-case research designs to compare system dynamics (e.g., latency of smoking following a stressor) following the introduction and removal of stress management interventions [198, 199]. These approaches would capitalize on the idiographic nature of the systems but allow quasi-experimental comparisons of clinically-meaningful outputs before and after introduction of an intervention. For example, n-of-1 trials could be applied to determine system properties that are amenable

or hostile to just-in-time stress-management prompts (e.g., how long of a delay between stress and smoking is required to intervene?).

5.4.2 Limitations

Participants in this study were smokers from large metropolitan area in a Western country. The stress-smoking systems identified here may not generalize to other contexts or populations. Additionally, the smokers in this study were preparing for a quit attempt. Stress-smoking system dynamics may differ for smokers who are not intending to quit or during a quit attempt when withdrawal symptoms present an additional demand. The small sample size was suitable for establishing proof-of-concept for modeling person-specific changes in smoking-responses to stress that can be used to develop person-specific decision rules for just-in-time stress management interventions; however, the sample size was insufficient to permit empirical clustering of participants based on their responses to stress. Future studies with larger samples can apply clustering algorithms and machine learning techniques like Shapelets to establish a robust typology of stress-smoking systems [200, 201].

The volume of missing data in the datasets was another limitation of this study. Some missing data was anticipated because the cStress marker cannot be estimated when the participant is moving. Other missing data was caused by human factors or device issues, such as device non-wear or poor attachment of sensors to the skin. One consequence of the missing data was that each participant's data was a collection of shorter chunks of data instead of a single long time series. This problem was partially mitigated in the modeling by considering different intrinsic responses for each chunk according to its own past; however, conclusions cannot be drawn about system dynamics between the available chunks, where data were not available.

A final modeling-related limitation was that we assumed the system is stationary. The dataset did not include information on situational factors that might alter dynamics (e.g., home versus work; weekday versus weekend). Given the relatively short period of three days of pre-quit data, we believe it was reasonable to assume that participant behavior would not change dramatically during this period. Accessing and analyzing more data including situational and contextual factors and exploring how they impact smoking should be a priority for the future studies.

5.5 Conclusion

This study provided proof-of-concept for using system identification tools from control systems engineering to identify relations between stress and smoking for regular smokers over time. The study made both substantive and methodological contributions to the addiction literature. From a substantive perspective, the identified person-specific dynamical models revealed a direct correlation between stress and subsequent increases in smoking risk. This general pattern was uniform but the latency between stress and smoking events varied from instantaneous to delayed.

Additionally, for about half of the participants, smoking in response to stress was followed by a marked reduction in the odds of smoking in the near future. From a methodological perspective, the system identification method yielded person-specific dynamical models that might have relatively consistent pattern for a given individual but different patterns for different people. This method provides a new approach for both (a) characterizing the dynamics of smoking risk at different stages (e.g., prior to a quit attempt), and (b) developing person-specific decision rules for just-in-time interventions that support smoking cessation.

Chapter 6
Logistic Regression for Dynamical Systems Modeling

In chapter 1, the regular form of logistic regression model and the state of the art in this regard was discussed. In such model, time does not play a role. That is, considering sample i as $(x^{(i)}, y^{(i)})$, the probability of $y^{(i)} = 1$ given $x^{(i)}$ is fixed. In this chapter, we develop a framework that allows to take into account the external stimuli that might affect how such probability changes not only at a specific time but also in the future times.

6.1 Dynamic Logistic Regression Model

Figure 6.1 depicts the configuration of the dynamical system modeling using time-varying logistic regression. As shown, the time-varying probability, $p_{y(k)}(k)$, that is the probability of $y(k)$ equal to 1 given the features at time k, is a function of the output of the linear system and is of the form

$$p_{y(k)}(k) = \sigma(z(k)), \tag{6.1}$$

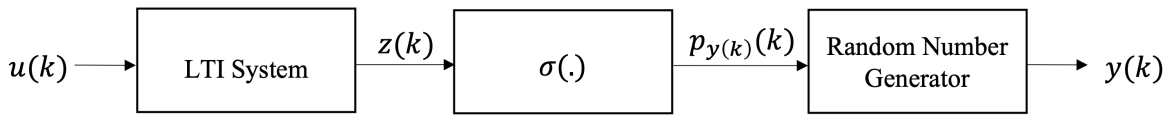

Figure 6.1: Time-varying logistic regression configuration.

where $z(k)$ is the output of the linear system and $u(k)$ is its input. Similar to the formulation described in chapter 4 for the output of the linear system, $z(k)$ is defined as

$$z(k) = (D + \sum_{j=1}^{n_p} C_{p_j} \alpha_{p_j} p_j^k) * u(k) + \sum_{j=1}^{n_p} C_{IC_{p_j}} \alpha_{p_j} p_j^k, \tag{6.2}$$

where the left side of the summation represents the input response and the right side describes the intrinsic response. C and C_{IC} are the coefficients of the input and intrinsic responses, respectively, p's are the poles of the system, and α is the scaling factor (as also described in chapter 4). n_p is the system order or the number of poles and D is the constant coefficient. It should be noted that the value of $u(0)$ is considered to be 1 to accommodate the effect of constant D in the model.

The random variables, $y(k)$'s, are independent binary values with Bernoulli distribution, that is $prob(y(k) = 1) = p_{y(k)}(k)$ and $prob(y(k) = 0) = 1 - p_{y(k)}(k)$. In order to get the $y(k)$'s, we have to start with generating random numbers with Uniform distribution, as shown. This way, the Bernoulli random variable $y(k)$ is equal to 1 if the probability of the uniform random variable is between 0 and $p_{y(k)}(k)$ and is 0 otherwise.

Considering $z(k)$ to be of the form $z(k) = \omega X(k)$ to match the usual logistic regression form (where ω represents the coefficients and X's are the features), $p_{y(k)}(k)$ will be of the form

$$p_{y(k)}(k) = \sigma\left(\omega X(k)\right) = \frac{e^{\omega X(k)}}{1 + e^{\omega X(k)}}. \tag{6.3}$$

In this case and considering the following assumption, the maximum likelihood estimators can be identified.

Assumption 6.1 The outputs of the system, $y(1), \cdots, y(k), \cdots, y(m)$, are conditionally independent given the features X, while the X's, as defined above, are the time-varying variables and are not independent from each other.

6.1.1 Time-varying Logistic Regression

While the ultimate objective is to develop an algorithm that incorporates sparsity and handles data fragmentation, here, we build that algorithm step by step. First, we start with an algorithm that does not account for the data fragmentation or consider sparsity. Then, we progress toward adding each concept at a time.

With that, the optimization problem for the time-varying logistic regression without

sparsity or data fragmentation can be formulated as the following

$$\begin{aligned}
&\min_{C,C_{IC}} \quad J \\
&\text{subject to } J = -\frac{1}{m}\sum_{k=1}^{m}(y(k)\omega X(k) - log(1+e^{\omega X(k)})) \\
&\qquad \omega X(k) = (D + \sum_{j=1}^{n_p} C_{p_j}\alpha_{p_j}p_j^k) * u(k) + \sum_{j=1}^{n_p} C_{IC_{p_j}}\alpha_{p_j}p_j^k \\
&\qquad C_{p_j} = C^*_{p_j^*}, \quad C_{IC_{p_j}} = C^*_{IC p_j^*}
\end{aligned} \tag{6.4}$$

The cost function J is formulated in this form to make it implementable using MATLAB® software. It should be noted that in this optimization problem, the order of the system has to be fixed. That is, the dynamics involved in predicting the output at present, i.e., how far to look back in time or how many samples from the past to be included, should be predefined. This is not an easy choice, since not all systems respond the same, and an arbitrary choice of the model complexity might result in a model that does not provide a good description of the data Therefore, in the next section, we introduce the concept of sparsity to the optimization problem. That way, the algorithm chooses the satisfying poles from the poles on a gridded unit circle (the same concept as in chapter 4) and accordingly reflects the model order, based on conditions of the problem. To do so, the unit circle has been gridded uniformly and random poles were picked to check as candidates for the system.

6.1.2 Time-varying Logistic Regression with Sparsity

Considering a continuous dataset, and inducing sparsity to the time-varying logistic regression, the optimization problem can be formulated as

$$\begin{aligned}
&\min_{C,C_{IC}} \quad \lambda\|t\|_1 + J \\
&\text{subject to } J = -\frac{1}{m}\sum_{k=1}^{m}(y(k)\omega X(k) - log(1+e^{\omega X(k)})) \\
&\qquad \omega X(k) = (D + \sum_{j=1}^{n_p} C_{p_j}\alpha_{p_j}p_j^k) * u(k) + \sum_{j=1}^{n_p} C_{IC_{p_j}}\alpha_{p_j}p_j^k \\
&\qquad C_{p_j} = C^*_{p_j^*}, \quad C_{IC_{p_j}} = C^*_{IC p_j^*} \\
&\qquad |C_{p_j}| \le t_{p_j}, \quad |C_{IC_{p_j}}| \le t_{p_j}
\end{aligned} \tag{6.5}$$

where the objective function is the summation of two parts; in the first part, $\|t\|_1$ is the l_1-norm relaxation that is the summation of absolute values of t and introduces the sparsity to the system. The second part of the objective function is the cost function for the time-varying logistic regression. λ is the regularization parameter to be predefined and its value is considered between 0 and 1.

The regularization parameter λ provides a trade-off between the two parts of the objective function and its optimal value depends on the data set and the problem. Smaller values of λ provide less weight on the sparsity and consequently cause a higher order of the system, while its higher values push coefficients down, make them and accordingly the system order smaller. Extremely high values of λ might even result in zero-order systems.

6.1.3 Time-varying Logistic Regression with Sparsity - Incorporating Data Fragmentation

This section represents a slight change from the previous one to incorporate the times when the data set is fragmented or a lot of missing data is present. To do so, the optimization problem should be modified to handle different intervals of available continuous data i.e., data chunks. Considering the dataset to include different chunks (continuous intervals) of data, the optimization problem can be formulated as

$$
\begin{aligned}
&\min_{C,C_{IC}} \quad \lambda\|t\|_1 + J \\
&\text{subject to } J = -\frac{1}{m}\sum_{k=1}^{m}(y(k)\omega X(k) - log(1+e^{\omega X(k)})) \\
&\qquad \omega X(k) = (D + \sum_{j=1}^{n_p} C_{p_j}\alpha_{p_j}p_j^{N_{ch}}) * u(k) + \sum_{j=1}^{n_p} C^l_{IC_{p_j}}\alpha_{p_j}p_j^{N_{ch}} \\
&\qquad |C_{p_j}| \leq t_{p_j} \quad \text{for all } p \in \text{Grid} \\
&\qquad |C^l_{IC_{p_j}}| \leq t_{p_j} \quad \text{for all data chunks } l; \text{for all } p \in \text{Grid} \\
&\qquad C_{p_j} = C^*_{p_j^*} \\
&\qquad C^l_{IC_{p_j}} = C^{l^*}_{IC_{p_j^*}} \quad \text{for all data chunks } l
\end{aligned}
\tag{6.6}
$$

where N_{ch} is the number of samples in each chunk. It should be noted that for this analysis, considering different data chunks, the intrinsic response of linear system is different for each chunk and should be calculated separately. The reason behind that is the information regarding the moments before starting each chunk is not provided and

the information from the prior chunk cannot reflect in such response. This way, for each data chunk the coefficients related to intrinsic response, C_{IC}^{l}, is different but the input response remains the same.

6.1.4 Sparsity and System Order

Solving the optimization problem 6.5 or 6.6 and identifying the coefficients related to the input response, each coefficient C_{p_j} is associated with the pole p_j. An input response coefficient is considered significant and contributed to the order of the system only if

$$|C_{p_j}| \geq threshold. \tag{6.7}$$

Therefore, the order of the system is computed based on the number of poles which their corresponding input response coefficients are valued above the assigned threshold, that is considered to be 0.01 here. This choice of threshold provided a reasonable distinction between the significant and non-significant coefficients. It should be noted that this choice is one of the possible choices. Depending on the application, one might end up using a different threshold, or different ways for inducing sparsity.

6.1.5 Second Optimization Problem to Estimate the Parameters

As discussed in the last part of the introduction, using data splitting technique, after model selection on the first data half, we need to estimate the parameters on a separate new data, the second half of the entire data set. That is, a second optimization problem should be solved. After implementing the first optimization problem and identifying the model and features contributing to the output, the corresponding poles and system order can be used as prior information to implement a second optimization problem and identify a model for the unseen data. Defining the satisfying poles obtained from solving the first optimization problem as p_{incl} and correspondingly, $\alpha_{p_{incl\,j}}$ and $n_{p_{incl}}$, the second

optimization problem can be formulated as

$$
\begin{aligned}
&\min_{\beta,\beta_{IC}} \quad J_{sec} \\
&\text{subject to } J_{sec} = -\frac{1}{m_{sec}} \sum_{k=1}^{m_{sec}} (y_{sec}(k)\omega X_{sec}(k) - log(1 + e^{\omega_{sec} X_{sec}(k)})) \\
&\qquad \omega_{sec} X_{sec}(k) = (\beta_0 + \sum_{j=1}^{n_{p_{incl}}} \beta_{p_{incl\,j}} \alpha_{p_{incl\,j}} {p_{incl\,j}}^{N_{ch-sec}}) * u_{sec}(k) \\
&\qquad + \sum_{j=1}^{n_{p_{incl}}} \beta^l_{IC_{p_{incl\,j}}} \alpha_{p_{incl\,j}} {p_{incl\,j}}^{N_{ch-sec}} \\
&\qquad \beta_{p_{incl\,j}} = \beta^*_{p_{incl\,j}^*} \\
&\qquad \beta^l_{IC_{p_{incl\,j}}} = \beta^{l^*}_{IC_{p_{incl\,j}^*}} \quad \text{for all data chunks } l
\end{aligned}
\tag{6.8}
$$

where J_{sec} is the objective function to be minimized, m_{sec} and N_{ch-sec} are the number of entire samples (unseen data) and the samples in each chunk used to identify the coefficients, respectively. β_0, β, and β_{IC} are the constant parameter and the coefficients related to the input and intrinsic responses, respectively. The term $n_{p_{incl}}$ is equivalent to the order of the system. For simplicity, hereafter, X refers to X_{sec} and ω refers to ω_{sec} in equation (6.8) where ω contains all the coefficients of the identified system including β_0, β, and β_{IC}.

This should be noted that the heuristic here is that we have assumed that the first optimization problem identifies the right poles and that provides a good approximation of the model. Using those identified poles, the objective of the second optimization problem is to further tune the estimates and asymptotic results.

6.2 Statistical Inference

In order to investigate the significance of the identified coefficients, a few steps have to be taken

- Estimating the coefficients β_0, β, and β_{IC}.
- Estimating the probabilities $p_{y(k)}(k) = \sigma(\omega X(k))$.
- Testing whether the confidence around β_j contains origin or zero.

6.2.1 Confidence Interval

Considering a 95% confidence interval, $Z_{\alpha/2}$ is equal to $Z_{0.025} = 1.96$, and therefore the 95% confidence interval for the coefficient β_j can be calculated as

$$\beta_j \pm 1.96 \times SE(\beta_j), \tag{6.9}$$

where $SE(\beta_j)$, the standard error for the coefficient β_j, can be computed as

$$SE = \sqrt{((X^T \hat{W} X)^{-1})_{jj}}. \tag{6.10}$$

where X is what multiplies the coefficients, and $\hat{W}$ is a $m \times m$ diagonal matrix. This should be noted that although the system's coefficients are complex numbers, for the purpose of confidence analysis, if the imaginary part is non-zero, the real and imaginary parts of each system's coefficients is considered two real-valued coefficients. That is, all β_j are real-valued coefficients containing the real and imaginary parts of original coefficients and the covariance matrix and standard errors are computed based on this criterion. Therefore, we compute the confidence interval for the real and imaginary parts of the system's coefficients separately.

Although method described in (6.9) has been mostly used by the statistical computing packages, the efficiency of it in interpreting the significance of complex coefficients is under question. Following section describes the other technique used here to investigate and compute this significance.

6.2.2 Confidence Ellipsoids

***q*-dimensional Ellipsoids** Considering that the assumptions on asymptotic normality of the maximum likelihood estimators are satisfied and the sample m is sufficiently large, the $1 - \alpha$ confidence ellipsoid for β can be computed as

$$p[(\hat{\beta} - \beta)^T J(\hat{\beta} - \beta) \leq \chi^2_{q+1,\alpha}] = 1 - \alpha, \tag{6.11}$$

where $\chi^2_{q+1,\alpha}$ denotes the upper α percentage point of the χ^2_{q+1} distribution, q is the number of input coefficients β, and the jf-th element of J, the sample information matrix can be computed as

$$J_{jf} = -\frac{\partial^2}{\partial\beta_j \partial\beta_f} l(\beta | X_1, \ldots, X_m)|_{\beta-\hat{\beta}}, j, f = 0, \ldots, q. \tag{6.12}$$

Lower Dimensional Ellipsoids Through Marginalization The above formulation is for the q-dimensional case where the confidence ellipsoid is computed for all q coefficients at once. Here, we propose another approach to compute the confidence ellipsoid for each coefficient separately. In other words, going from a q-dimensional ellipsoid to a lower dimensional ellipsoid by marginalizing it. The following definition and theorems by Muirhead represent the theory behind and the process used for marginalization [202].

Definition 6.1 The $m \times 1$ random vector X is said to have a m-variate normal distribution if, for every $a \in \mathbb{R}^m$, the distribution of $a'X$ is univariate normal.

Theorem 6.1 If X has a m-variate normal distribution, then both $\mu \equiv E(X)$ and $\Sigma \equiv Cov(X)$ exist and the distribution of X is determined by μ and Σ.

Theorem 6.2 If X is $\mathcal{N}_m(\mu, \Sigma)$, B is $k \times m$, and b is $k \times 1$ then

$$Y = BX + b \ \sim \ \mathcal{N}_k(B\mu + b, B\Sigma B'). \tag{6.13}$$

The fact that Y is k-variate normal is a direct consequence of `Theorem 6.1`.

This leads to the theorem on the very important property of the multivariate normal distribution that all marginal distributions are also normal, as follows:

Theorem 6.3 If X is $\mathcal{N}_m(\mu, \Sigma)$, then the marginal distribution of any subset of k (that is less than m) components of X is k-variate normal.

As an example, considering X, μ and Σ of the form

$$X = \begin{bmatrix} X_1 \\ X_2 \end{bmatrix}, \mu = \begin{bmatrix} \mu_1 \\ \mu_2 \end{bmatrix}, \Sigma = \begin{bmatrix} \Sigma_{11} & \Sigma_{12} \\ \Sigma_{21} & \Sigma_{22} \end{bmatrix} \tag{6.14}$$

and putting $B_{k \times m} = [I_k : 0]$ and $b = 0$ in `Theorem 6.2`, shows that $X_1 \sim \mathcal{N}(\mu_1, \Sigma_{11})$ and so on.

The results of theorems above are used to investigate the marginal associations of complex coefficients, as explained and interpreted in the following.

Marginalization for complex coefficients Suppose we have a complex coefficient with a non-zero imaginary part. The confidence ellipsoid for this coefficient can be obtained as if we have a two-dimensional ellipsoid where the vertical axis represents the imaginary axis and the horizontal one represents the real axis and the real and imaginary

parts of the coefficient are two real-valued coefficients that we are going to find the confidence ellipsoid around that point in the plot.

Similar to the example derived from `Theorem 6.3`, the covariance matrix for this complex coefficient that is considered as two real coefficients (real and imaginary parts of the coefficient are considered each as one coefficient), i.e., coefficients j and f, is a subset of the original covariance matrix related to coefficients j and f. Since we are computing the confidence ellipsoid for the two coefficients j and f, that leads to considering $q = 2$ and as such, the χ^2_{q+1} will be χ^2_3. Again, it should be noted that the covariance matrix is computed as if all the coefficients are real. That is, each real and imaginary parts is considered a coefficient for those purposes.

Similarly, for the case that the imaginary part of the coefficients is equal to zero, we use the relevant subset of the covariance matrix and χ^2_2.

6.3 Results and Discussion

6.3.1 Dataset

Various datasets were simulated to investigate the results of the developed algorithms and assess the validity of them. Data fragmentation is induced since real datasets often suffer from fragmented data in between, as this effect is described in detail in chapters 1 and 4. For simplicity, each dataset contains four data chunks with various number of samples in each. The order of the true system is considered four. To illustrate the results in this section, a dataset containing 5000 samples is used.

6.3.2 λ and the Relation Between Cost and Sparsity

The algorithm developed and explained in the equation (6.6) is used to identify the dynamical models in this section. Considering a dataset of 5000 samples, Figure 6.2 illustrates how the order of the system changes as the value of λ increases. As shown, for higher values of λ, the algorithm applies more weight on sparsity, pushing the objective function of the l_1-norm to be smaller and consequently pushing the coefficients too down, all close to zero. For this dataset, values of $\lambda \geq 0.11$ represent a zero-order system which means $z = \beta_0$, a constant, all the time. Therefore, choosing $\lambda \geq 0.11$ is a poor choice and does not provide a good fit to the data. This should be noted that the reason for not having a monotonically descreasing plot is simply because we are working with approximations.

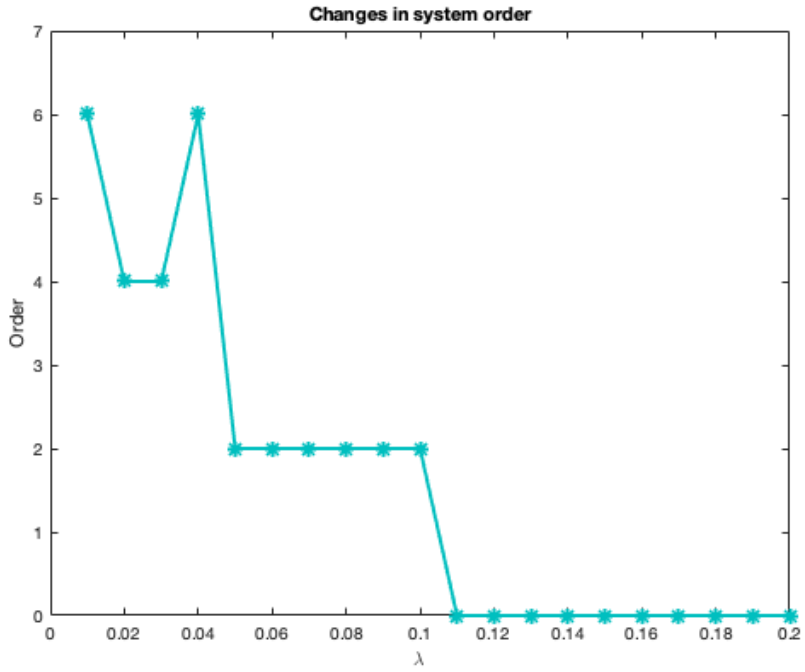

Figure 6.2: Change in system order as λ increases.

Figure 6.3 shows the change in values of the l_1-norm objective function, logistic regression cost function, and the overall objective function that are respected in the figure as Order objective, Cost objective, and Total objective, with an increase in the value of λ. As shown in this figure, with an increase in the value of λ, the l_1-norm objective decreases, getting down to almost zero for values of $\lambda \geq 0.11$ that implies a zero-order system.

For the values of $\lambda < 0.11$, the total objective increases slightly for each incremental change in λ value and the order of system changes accordingly. Again, this should be in mind that the value of λ provides a trade-off between the model order and cost. Therefore, for this dataset and according to Figures 6.2 and 6.3, $\lambda = 0.02$ is a reasonable choice since it provides the sparsest model with a slightly higher overall cost in comparison to the case where $\lambda = 0.01$.

6.3.3 Comparing the Identified Versus True System

The true system contains four complex poles of which 2 have their imaginary part equal to zero. The overall dataset includes 5000 samples with 4 data chunks and is equally divided to two datasets each with two chunks of different sizes, to be used for each optimization

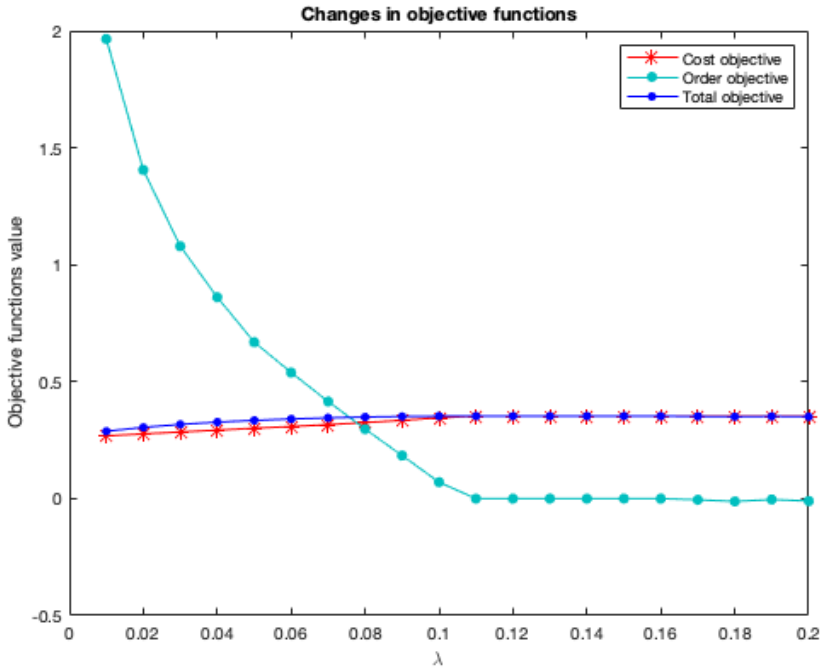

Figure 6.3: Change in the objective function values as λ increases.

problem. The first dataset, containing 2500 samples and 2 data chunks of different size, is used to identify the sparsest model that can fit that data well, implementing the first optimization problem formulated at (6.6). Using the method described in the previous section, for this dataset, $\lambda = 0.01$ provided the sparsest model with lowest cost and therefore considered in solving this problem.

A grid of 90 poles were provided for algorithm as the candidate poles. Solving the first optimization problem and applying a threshold of 0.01 for the coefficients as in (6.7), a model of order 6 was identified. The corresponding poles and model order were used as the prior information for solving the second optimization problem, formulated at (6.8). Considering the second half of the data which was 2500 samples with 2 chunks of different size, the coefficients of the system were identified.

Figure 6.4 illustrates the impulse responses of the true system and the two identified ones. As shown, the identified system 2 more closely follows the pattern of the true system. This indicates that the approach of developing the algorithms and implementing them in order to divide the dataset into two sets and solve two optimization problems, results in a greater fit that is closer to the original model, a model that follows closely the characteristics of the true system.

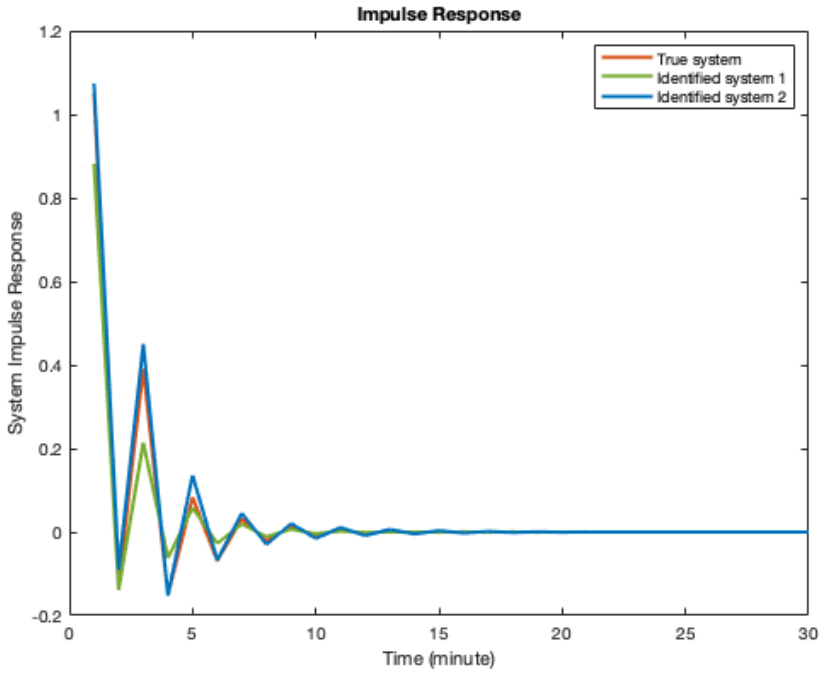

Figure 6.4: Comparing the impulse responses of the true versus identified systems.

Figure 6.5 shows the pole-zero map of the identified model. Additionally, the identified constant parameter and input response coefficients for this system are as follows

```
Coefficients =

-0.4232 + 0.0000i
-0.2877 + 0.9426i
 0.6936 + 5.5719i
 1.4760 + 0.1291i
-0.2877 - 0.9426i
 0.6936 - 5.5719i
 1.4760 - 0.1291i
```

Next section investigates the confidence of the identified coefficients via the optimization problem (6.8).

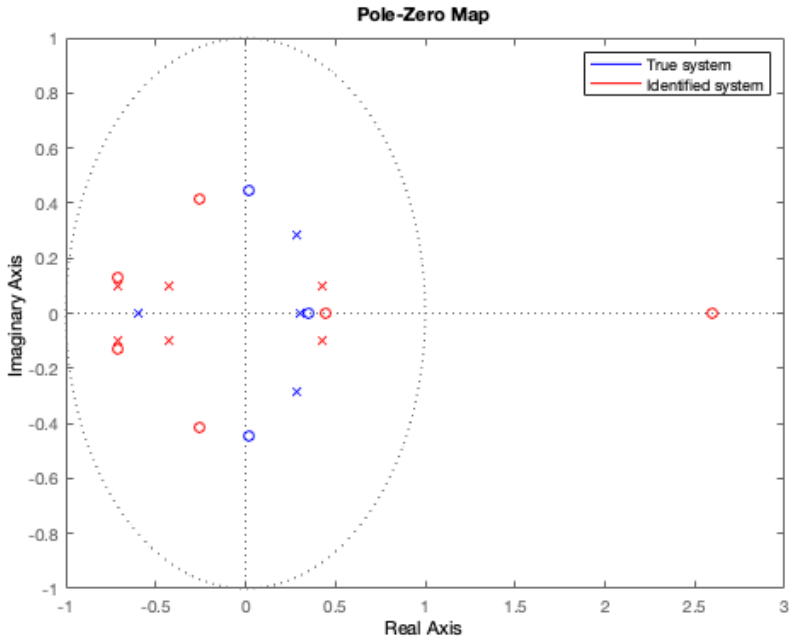

Figure 6.5: pole-zero map of the true and identified system.

6.3.4 Confidence of the Coefficients

In this section, using techniques described in the method section, the identified coefficients are evaluated. To do so, confidence ellipsoids for the input coefficients and confidence curve for the constant parameter were plotted using the equation (1.24) and the confidence intervals were computed using equation (6.9).

6.3.4.1 Confidence Ellipsoid

The confidence curve and ellipsoids were computed using equation (1.24) and plotted in Figure 6.6 (a) to (d) for the constant β_0 and input coefficients, β, respectively. As mentioned, in figures related to confidence ellipsoids of the input coefficients β, the vertical and horizontal axes present the imaginary and real axes, respectively.

As shown in the plots, the confidence of the constant parameter and each set of complex coefficients were computed separately and illustrated in different plots. Therefore, the χ^2_{q+1} was considered 5.991 for the β_0 as $q+1=2$ and 7.815 for input coefficients β, as $q+1=3$, for $\alpha=0.05$.

The reason for this choice for the input coefficients β is that, for this specific dataset,

all the input coefficients are complex values with non-zero imaginary parts. Therefore, $q = 2$, since each real and imaginary part is considered as one coefficient for the purpose of plotting the confidence ellipsoids. Note that, since the half of the input coefficients are complex conjugate of the other half, it is sufficed to only compute the confidence ellipsoid for one set.

As mentioned before, the covariance matrix is computed as if all the coefficients are real numbers. Therefore, since the identified model is of order 6 with 2 data chunks, the covariance matrix is of the size 19×19 where the 19 coefficients are the constant (1), real and imaginary parts of the input responses (6 - 3 real, 3 imaginary) and real and imaginary parts of the intrinsic responses (12 - 6 real, 6 imaginary, double of input response coefficients since we have two data chunks).

The way to interpret these plots is that if the origin is inside the ellipsoid, then the coefficient does not play an important role in the model and its effect is not significant. For example, although pretty close to the edge, the point $(0, 0)$ is located inside the ellipsoid in Figure 6.6 (d). These set of coefficients are the ones corresponding to the poles at the very left side of the plot shown in figure 6.5. Those complex poles are pretty close to the zeros in the pole-zero plot, suggesting a pole-zero cancellation and that explains the confidence ellipsoid case.

6.3.4.1.1 Special case Lets go through the steps of calculating the confidence interval for one input coefficient, i.e., $\beta = -0.2877 + 0.9426i$. First step is to consider the real and imaginary parts as two coefficients with real values. This leads to having two coefficients as

```
coef_complex_1 =

-0.2877
0.9426
```

with the covariance matrix that is a subset of the overall 19×19 matrix related to these coefficients as

```
var_covar_complex_1 =

 4.3328   -2.7201
-2.7201    2.0476
```

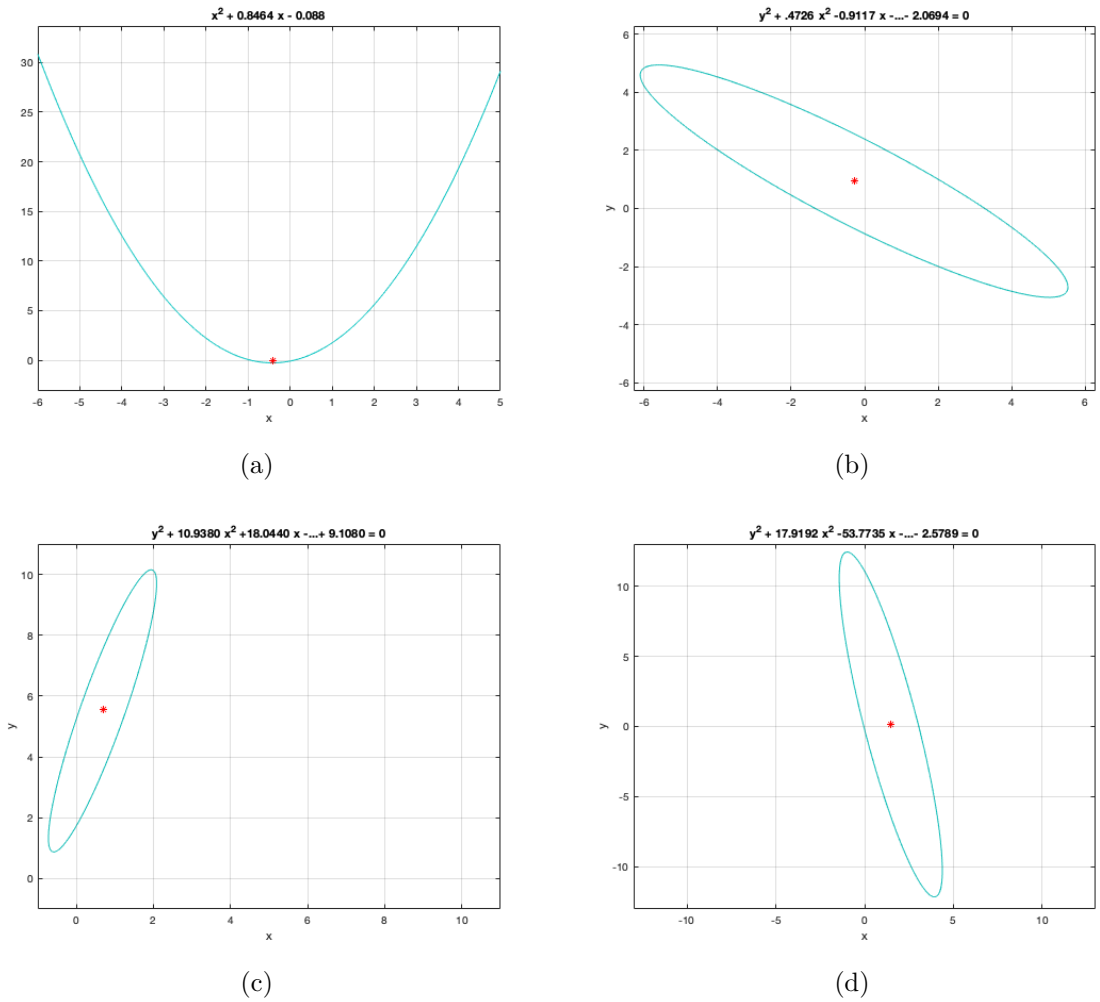

(a) (b)

(c) (d)

Figure 6.6: Confidence curve and ellipsoid for the constant parameter and input coefficients. In each plot, the red star presents the location of the coefficient.

Incorporating this information into the equation (6.11) where $\chi_3^2 = 7.815$, the confidence ellipsoid will be of the form of $y^2+0.4726x^2-0.9117x-1.5240y+1.2556xy = 2.0694$. As shown in Figure 6.6 (b), the red $*$ illustrates the location of the coefficient and the ellipse is plotted according to the acquired formula above. The same process has repeated for all the coefficients.

Next section represents the results of applying the confidence interval method to investigate the confidence of the identified coefficients. At the end, the two methods used are compared.

6.3.4.2 Confidence Interval

95% confidence interval is computed for the identified coefficients of the system. Real and imaginary parts of each coefficient treated separately as real values and all are depicted in table 6.1. In this table, from left to right, the columns represent the lower confidence interval, coefficients, and upper confidence interval, respectively.

Table 6.1: 95% confidence interval of the coefficients.

CI_Lower	Coefficients	CI_Upper
-0.8371	-0.4232	-0.0094
-4.3675	-0.2877	3.7922
-1.8621	0.9426	3.7472
0.0219	0.6936	1.3654
3.3503	5.5719	7.7934
-0.5636	1.476	3.5156
-8.5009	0.1291	8.7591

By comparing the two methods to evaluate the coefficients and compute their confidence, this is clear that the confidence ellipsoid technique provides a better representation of the result. As such, since we are dealing with complex coefficients, the confidence interval method presented that has been used by most logistic regression software to evaluate the coefficients does not work well.

6.3.5 Conclusion

This chapter represents the progress from usual logistic regression to developing algorithms that take into account dynamics, sparsity, and data fragmentation, and emphasizes how the new approaches help understanding the dynamics of the system and predict more accurate results. Developing the algorithms, we not only took advantage of benefits of the logistic regression technique, but also we incorporated the dynamics of behavior into the models to take into account the memory effect. Additionally, considering parsimonious system identification techniques, we implemented the algorithms to achieve the least complex model that can describe the data well.

Chapter 7
Conclusion and discussions

Dynamical system modeling is a strong tool to investigate human behavior over time and it provides powerful techniques to analyze them. Such behavior can be considered as complex dynamic models which varies by time, degree, type, and stage of concepts of interest such as an intervention or a disease. Applying dynamical system modeling tools to model these systems under different conditions provides the basis for predicting conditions like moments of vulnerability and applying potential treatments and interventions when and where they are needed. That motivates one of the main objectives of this work that has been to develop algorithms using tools from control systems engineering to effectively analyze different problems associated with health and behavioral medicine.

System identification of linear systems with some a priori information is a central concept in control systems engineering. There have been a number of studies targeting identification of linear and nonlinear systems each with its own difficulties. The problem of computational complexity and no guarantee for identifying simplest model representing the data in prior works has led us to develop identification algorithms that consider sparsity using the atomic norm concept in this dissertation. Therefore, to identify the dynamical models, a new parsimonious model identification algorithm is developed to identify models that provide a desired explanation of the data with as few parameters as possible.

From the behavioral science standpoint, since we have developed dynamical systems relating the inputs to outputs, we have computational models of interactions that can use it to simulate responses to different inputs. The computational complexity of developed models, even for large data sets, is very low and they are capable of characterizing complex change patterns. The models obtained can be used not only to study how an individual responds to different inputs but also as a first step in the process of designing just-in-time adaptive interventions.

Economic burden of the physical inactivity on one hand and health issues caused by it on the other hand necessitate some actions. Therefore, designing intervention programs to help increase physical activity and reduce the sedentary behavior in early adulthood has been of great value. That motivated us to design intervention programs targeting promotion of physical activity in young adults. Analyzing the data and investigating the effectiveness of treatment has led to developing new methodologies for identifying switched models.

In this regard, we focused on intervention plan according to sending random daily messages from a content library for 6-month study period. We developed dynamical, piecewise affine models of physical activity based on historical responses to treatment (intervening messages), recent behavior, and location-specific weather conditions. This process involved identifying the parameters of sub-models based on noisy, potentially fragmented input data provided by different sensors. Additionally, the effect of contextual changes such as life stressors, i.e., a pandemic on the physical activity responses has been investigated using the developed models.

Identified person-specific dynamical models represented a significant heterogeneity in physical activity responses to different intervention messages, and according to the type of day and external contextual changes. These analyses suggested that personalizing messages for participants in an intervention may be a worthy endeavor for generating greater step responses over time. Personalization approaches that identify optimal times and content for message delivery may be especially valuable on weekdays.

Models developed to investigate the physical activity responses of participants to digital messages all consider the same order to model the behavior as a trade-off between model complexity and accuracy. Future work will need to investigate the optimal model complexity for reducing uncertainty in the model while maintaining an acceptable user experience and modeling the behavior effectively. Also, efforts can be put to model the behavior as nonlinear models.

The heterogeneity between participants indicates that future interventions can benefit from methods that can both explore the effects of multiple message types on physical activity and exploit the most effective message types for an individual once identified. Given that messages have proximal effects on behavior in the minutes and hours after message delivery, the use of wearables for measuring physical activity behavior provides a rich source of information about behavioral dynamics.

In future studies, taking advantage of this technology, system identification and dynamical modeling used here can be extended to design effective controllers (decision

rules) that maximize the probability of achieving a desired goal while avoiding unsafe or ineffective operating regions by continuously tuning interventions based on participants' responses over time. Furthermore, future studies should extend the system identification work for behavior changes, by applying robust control tools for effective control design in the presence of uncertainty.

Another main contribution in this dissertation has been addressing the problem of data fragmentation and memory effect. As a real-world example, the developed models account for the past moments of stress and smoking and handle missing data that are often present in real data. That is, the developed models consider memory effect, handle data fragmentation, and provide the identified parameters needed to develop decision rules in designing and adapting the delivery of just-in-time smoking cessation interventions based on person-specific moments of vulnerability, in future studies. More precisely, once the person-specific response model is available based on the developed algorithms, an effective robust intervention can be designed.

As an example, identified person-specific models of smoking in response to stress can be used to inform the selection and timing of just-in-time intervention approaches in future. For participants who responds to stress so quickly, there may not be sufficient time to implement a stress-management intervention before a smoking response is initiated. For such participants, it may be more effective to implement an intervention aimed at developing stress-management skills that could be employed without a prompt or to tailor just-in-time interventions on other advanced triggers for smoking, such as location or social context.

In contrast, for participants with somewhat slower responses to stress, the delay may provide enough time to detect stress, deliver a prompt to engage in a stress-management exercise (perhaps mediated by an app on the user's device), improve their regulation, and reduce smoking risk. For participants with a more complex response, there may be a need for a more complex intervention with multiple tailoring variables.

As shown by the identified models of category 3 in the analysis of chapter 5, one example of such complex behavior is if the risk of smoking increases quickly after the beginning of a stress episode, but it then subsides before increasing again long after the stress episode ends. This behavior may require a more complex intervention with multiple tailoring variables. For example, one tailoring variable could be used to identify moments of anticipated vulnerability and trigger intervention options that reduce the risk of smoking expected shortly after the onset of(anticipated) stressful experiences (e.g., upon arriving at work, sending the user a reminder to seek out supportive coworkers). A

second tailoring variable could be used to trigger an intervention option that reduces the risk of smoking after a detected stressful experience has ended (e.g., after detecting a stress response from an upsetting interaction with coworkers, prompting the user to engage in mindfulness practice).

This approach of system identification provides a complement to micro-randomized trials for determining the optimal level of individual tailoring variables for triggering different intervention options. Future work should extend the system identification approaches for behavioral change by considering the influence of more factors on the output and modeling the systems with multiple outputs.

The tools discussed in this dissertation to identify the models describing the relation between continuous input variables and binary output does not directly consider the fact that there might be external perturbations influencing the output. This can be addressed in multiple ways in future work. If the perturbation is known, it can be incorporated in the model as another input (i.e., we can extend this framework to deal with multiple inputs). If the perturbation is not known, it can be modeled as noise and also be incorporated in the model in a way similar to the noise parameter in the validation procedure described.

Appendix A
Publications

A.1 Journal Papers

- Turrisi, Taylor B., Kelsey M. Bittel, Ashley B. West, Sarah Hojjatinia, Sahar Hojjatinia, Scherezade K. Mama, Constantino M. Lagoa, and David E. Conroy. "Seasons, weather, and device-measured movement behaviors: a scoping review from 2006 to 2020." International Journal of Behavioral Nutrition and Physical Activity 18, no. 1 (2021): 1-26.

- Hojjatinia, Sarah, Sahar Hojjatinia, Constantino M. Lagoa, Deborah Brunke-Reese, and David E. Conroy. "Person-specific dose-finding for a digital messaging intervention to promote physical activity." Health Psychology 40, no. 8 (2021): 502-512.

- Hojjatinia, Sahar, Elyse R. Daly, Timothy Hnat, Syed Monowar Hossain, Santosh Kumar, Constantino M. Lagoa, Inbal Nahum-Shani, Shahin Alan Samiei, Bonnie Spring, and David E. Conroy. "Dynamic models of stress-smoking responses based on high-frequency sensor data." NPJ digital medicine 4, no. 1 (2021): 1-11.

- Hojjatinia, Sahar, Alexandra M. Lee, Sarah Hojjatinia, Constantino M. Lagoa, Deborah Brunke-Reese, and David E. Conroy. "Physical activity dynamics during a digital messaging intervention changed after the pandemic declaration." In Annals of Behavioral Medicine, kaac051 (2022).

- Lagoa, Constantino M., Sahar Hojjatinia, and David E. Conroy. "dynamical outcome modeling of fragmented intensive longitudinal data." In Multivariate Behavioral Research *submitted* (2022).

- Lee, Alexandra M., Sahar Hojjatinia, Jimikaye Courtney, Deborah Brunke-Reese, Sarah Hojjatinia, Constantino M. Lagoa, and David E. Conroy. "Motivational message framing effects on physical activity dynamics in a digital messaging intervention: A secondary analysis." In Journal of Medical Internet Research *submitted* (2022).

A.2 Conference Papers and Posters

- Bardakci, Ibrahim E., Sahar Hojjatinia, Sarah Hojjatinia, Constantino M. Lagoa, David E. Conroy. "Model predictive control approach to adaptive messaging intervention for physical activity." arXiv preprint arXiv:2108.11499 (2021).

- Hojjatinia, Sarah, Constantino M. Lagoa, Ashley B. West, Sahar Hojjatinia, Taylor Turrisi, Deborah Brunke-Reese, and David E. Conroy. "Abstract P196: Personalized dynamical system models of individual text message effects on changes in physical activity." Circulation 141, no. Suppl-1 (2020): AP196-AP196.

- Turrisi Taylor B., Ashley B. West, Kelsey M. Bittel, Scherezade K. Mama, Sahar Hojjatinia, Sarah Hojjatinia, Constantino M. Lagoa, and David E. Conroy. "Physical activity, seasonality, and weather: A scoping review of research with device-based measures of physical activity." Society of Behavioral Medicine's 41st Annual Meeting & Scientific Sessions, vol. 54, no. SUPP 1 (2020): S640-S640.

- Hojjatinia, Sahar, Elyse R. Daly, Timothy Hnat, Syed Monowar Hossain, Santosh Kumar, Constantino M. Lagoa, Inbal Nahum-Shani, Shahin Alan Samiei, Bonnie Spring, and David E. Conroy. "Dynamical system modeling to identify moments of vulnerability based on stress-smoking responses in daily smokers." Society of Behavioral Medicine's 43rd Annual Meeting & Scientific Sessions, vol. 56, no. SUPP 1 (2022): S167-S167.

- Hojjatinia, Sahar, Alexandra M. Lee, Sarah Hojjatinia, Constantino M. Lagoa, Deborah Brunke-Reese, and David E. Conroy. "Using dynamic modeling to understand physical activity change after COVID-19 pandemic declaration in a messaging intervention." Society of Behavioral Medicine's 43rd Annual Meeting & Scientific Sessions, vol. 56, no. SUPP 1 (2022): S667-S667.

- Lagoa, Constantino M., Sahar Hojjatinia, and David E. Conroy. "Dynamical outcome modeling of fragmented intensive longitudinal data." In ISRII (2022).

- Conroy, David E., Omar Sleem, Sahar Hojjatinia, Deborah Brunke-Reese, and Constantino M. Lagoa. "Person-specific dynamic models of wearable-based self-monitoring and behavioral feedback prompt effects on physical activity." In ISRII (2022).

A.3 Extras

- Hojjatinia, Sahar, and Constantino M. Lagoa. "Comparison of different spike sorting subtechniques based on rat brain basolateral amygdala neuronal activity." In 2019 IEEE International Conference on Bioinformatics and Biomedicine (BIBM), (2019): 2251-2258.

- Subramanian, T., K. Le, S. Hojjatinia, K. Venkiteswaran, M. Subramanian, L. Anselmi, C. Bove, and R. Travagli. "Maladaptive Nigrovagal neuronal plasticity causes ascending Alpha-Synucleinopathy in a novel environmental toxin based rat model of parkinsonism." Mov Disord. vol. 34, no. suppl 2 (2019): S733-S733.

Bibliography

[1] Conroy, D. E., S. Hojjatinia, C. M. Lagoa, C. H. Yang, S. T. Lanza, and J. M. Smyth (2019) "Personalized Models of Physical Activity Responses to Text Message Micro-Interventions: A Proof-of-Concept Application of Control Systems Engineering Methods," *Psychology of Sport and Exercise*, **41**, pp. 172–180.

[2] Hojjatinia, S., C. M. Lagoa, A. B. West, S. Hojjatinia, T. Turrisi, D. Brunke-Reese, and D. E. Conroy (2020) "Abstract P196: Personalized Dynamical System Models Of Individual Text Message Effects On Changes In Physical Activity," *Circulation*, **141**(Suppl_1), pp. AP196–AP196.

[3] Thomaz, E., C. Zhang, I. A. Essa, and G. D. Abowd (2015) "Inferring Meal Eating Activities in Real World Settings from Ambient Sounds: A Feasibility Study," in *Proceedings of the 20th International Conference on Intelligent User Interfaces, IUI 2015, Atlanta, GA, USA, March 29 - April 01, 2015* (O. Brdiczka, P. Chau, G. Carenini, S. Pan, and P. O. Kristensson, eds.), ACM, pp. 427–431.

[4] Kumar, S., W. J. Nilsen, A. Abernethy, A. Atienza, K. Patrick, M. Pavel, W. T. Riley, A. Shar, B. Spring, D. Spruijt-Metz, et al. (2013) "Mobile health technology evaluation: the mHealth evidence workshop," *American journal of preventive medicine*, **45**(2), pp. 228–236.

[5] Kumar, S., W. Nilsen, M. Pavel, and M. Srivastava (2012) "Mobile health: Revolutionizing healthcare through transdisciplinary research," *Computer*, **46**(1), pp. 28–35.

[6] McGarraugh, G. (2009) "The chemistry of commercial continuous glucose monitors," *Diabetes technology & therapeutics*, **11**(11), pp. S17–S24.

[7] Fairbairn, C. E. and D. Kang (2019) "Temporal dynamics of transdermal alcohol concentration measured via new-generation wrist-worn biosensor," *Alcoholism: Clinical and Experimental Research*, **43**(10), pp. 2060–2069.

[8] Trister, A. D., E. R. Dorsey, and S. H. Friend (2016) "Smartphones as new tools in the management and understanding of Parkinson's disease," *npj Parkinson's Disease*, **2**(1), pp. 1–2.

[9] Canzian, L. and M. Musolesi (2015) "Trajectories of depression: unobtrusive monitoring of depressive states by means of smartphone mobility traces analysis," in *Proceedings of the 2015 ACM international joint conference on pervasive and ubiquitous computing*, pp. 1293–1304.

[10] Saeb, S., M. Zhang, C. J. Karr, S. M. Schueller, M. E. Corden, K. P. Kording, and D. C. Mohr (2015) "Mobile phone sensor correlates of depressive symptom severity in daily-life behavior: an exploratory study," *Journal of medical Internet research*, **17**(7), p. e175.

[11] Wyatt, D., T. Choudhury, and J. Bilmes (2007) "Conversation detection and speaker segmentation in privacy-sensitive situated speech data," in *Eighth Annual Conference of the International Speech Communication Association*.

[12] Choudhury, T., G. Borriello, S. Consolvo, D. Haehnel, B. Harrison, B. Hemingway, J. Hightower, P. Pedja, K. Koscher, A. LaMarca, et al. (2008) "The mobile sensing platform: An embedded activity recognition system," *IEEE Pervasive Computing*, **7**(2), pp. 32–41.

[13] Lu, H., D. Frauendorfer, M. Rabbi, M. S. Mast, G. Chittaranjan, A. T. Campbell, D. Gatica-Perez, and T. Choudhury (2012) "StressSense: detecting stress in unconstrained acoustic environments using smartphones," in *The 2012 ACM Conference on Ubiquitous Computing* (A. K. Dey, H. Chu, and G. R. Hayes, eds.), ACM, pp. 351–360.

[14] Choudhury, T. (2014) "Using Smartphones to Sense, Assess, and Improve Well-Being," in *Proceedings of the 2014 Workshop on Physical Analytics*, WPA '14, Association for Computing Machinery, New York, NY, USA, p. 15.

[15] Hojjatinia, S., S. Hojjatinia, C. M. Lagoa, D. Brunke-Reese, and D. E. Conroy (2021) "Person-Specific Dose-Finding for a Digital Messaging Intervention to Promote Physical Activity," *Health Psychology*, **40**(8), pp. 502–512.

[16] Hamaker, E. L. and R. P. Grasman (2015) "To center or not to center? Investigating inertia with a multilevel autoregressive model," *Frontiers in psychology*, **5**, p. 1492.

[17] Gistelinck, F., T. Loeys, and N. Flamant (2020) "Multilevel Autoregressive Models when the Number of Time Points is Small," *Structural Equation Modeling: A Multidisciplinary Journal*, pp. 1–13.

[18] Goldstein, H., M. J. Healy, and J. Rasbash (1994) "Multilevel time series models with applications to repeated measures data," *Statistics in medicine*, **13**(16), pp. 1643–1655.

[19] Kumar, S., G. D. Abowd, W. T. Abraham, M. al'Absi, J. Gayle Beck, D. H. Chau, T. Condie, D. E. Conroy, E. Ertin, D. Estrin, et al. (2015)

"Center of excellence for mobile sensor data-to-knowledge (MD2K)," *Journal of the American Medical Informatics Association*, **22**(6), pp. 1137–1142.

[20] Cho, S., I. Ensari, C. Weng, M. G. Kahn, and K. Natarajan (2021) "Factors Affecting the Quality of Person-Generated Wearable Device Data and Associated Challenges: Rapid Systematic Review," *JMIR Mhealth Uhealth*, **9**(3), p. e20738.

[21] Ljung, L. (1998) *System Identification: Theory for the User*, Pearson Education.

[22] Box, G. E., G. M. Jenkins, and G. C. Reinsel (2008) *Time series analysis: forecasting and control*, John Wiley & Sons.

[23] Åström, K. J. and P. Eykhoff (1971) "System identification—a survey," *Automatica*, **7**(2), pp. 123–162.

[24] Wellstead, P. E. (1981) "Non-parametric methods of system identification," *Automatica*, **17**(1), pp. 55–69.

[25] Rake, H. (1979) "Step response and frequency response methods," *IFAC Proceedings Volumes*, **12**(8), pp. 519–526.

[26] Van Overschee, P. and B. De Moor (2012) *Subspace identification for linear systems: Theory—Implementation—Applications*, Springer Science & Business Media.

[27] Sznaier, M., M. Ayazoglu, and T. Inanc (2014) "Fast structured nuclear norm minimization with applications to set membership systems identification," *IEEE Transactions on Automatic Control*, **59**(10), pp. 2837–2842.

[28] Mohan, K. and M. Fazel (2010) "Reweighted nuclear norm minimization with application to system identification," in *Proceedings of the 2010 American Control Conference*, IEEE, pp. 2953–2959.

[29] Fazel, M., T. K. Pong, D. Sun, and P. Tseng (2013) "Hankel matrix rank minimization with applications to system identification and realization," *SIAM Journal on Matrix Analysis and Applications*, **34**(3), pp. 946–977.

[30] Liu, Z. and L. Vandenberghe (2009) "Interior-point method for nuclear norm approximation with application to system identification," *SIAM Journal on Matrix Analysis and Applications*, **31**(3), pp. 1235–1256.

[31] Mohan, K. and M. Fazel (2010) "Reweighted nuclear norm minimization with application to system identification," *Proceedings of the 2010 American Control Conference*, (5), pp. 2953–2959.

[32] Shah, P., B. N. Bhaskar, G. Tang, and B. Recht (2012) "Linear system identification via atomic norm regularization," in *2012 IEEE 51st IEEE conference on decision and control (CDC)*, IEEE, pp. 6265–6270.

[33] Chandrasekaran, V., B. Recht, P. A. Parrilo, and A. S. Willsky (2012) "The convex geometry of linear inverse problems," *Foundations of Computational Mathematics*, **12**(6), pp. 805–849, 1012.0621.

[34] Yilmaz, B., K. Bekiroglu, C. Lagoa, and M. Sznaier (2018) "A randomized algorithm for parsimonious model identification," *IEEE Transactions on Automatic Control*, **63**(2), pp. 532–539.

[35] Bekiroglu, K., B. Yilmaz, C. Lagoa, and M. Sznaier (2014) "Parsimonious model identification via atomic norm minimization," in *2014 European Control Conference (ECC)*, IEEE, pp. 2392–2397.

[36] Hojjatinia, S., K. Bekiroglu, and C. M. Lagoa (2018) "Parsimonious volterra system identification," *2018 American Control Conference (ACC)*, pp. 1933–1938.

[37] Lagoa, C. M., S. Hojjatinia, and D. E. Conroy (2021) "Dynamical Outcome Modeling of Fragmented Intensive Longitudinal Data," .

[38] Laney, D. et al. (2001) "3D data management: Controlling data volume, velocity and variety," *META group research note*, **6**(70), p. 1.

[39] Nahum-Shani, I., S. N. Smith, K. Witkiewitz, L. M. Collins, B. Spring, and S. A. Murphy (2014) "Just-in-time adaptive interventions (JITAIs): An organizing framework for ongoing health behavior support." (14), pp. 1–37.

[40] Spruijt-Metz, D. and W. Nilsen (2014) "Dynamic models of behavior for just-in-time adaptive interventions," *IEEE Pervasive Computing*, **13**(3), pp. 13–17.

[41] Hardeman, W., J. Houghton, K. Lane, A. Jones, and F. Naughton (2019) "A systematic review of just-in-time adaptive interventions (JITAIs) to promote physical activity," *International Journal of Behavioral Nutrition and Physical Activity*, **16**(1).

[42] Sarker, H., M. Tyburskir, M. D. Rahman, K. Hovsepian, M. Sharmin, D. H. Epsteinr, K. L. Prestonr, C. D. Furr-Holden, A. Milam, I. Nahum-Shani, M. Al'Absi, and S. Kumar (2016) "Finding significant stress episodes in a discontinuous time series of rapidly varying mobile sensor data," *Conference on Human Factors in Computing Systems - Proceedings*, pp. 4489–4501.

[43] Conroy, D. E., A. B. West, D. Brunke-Reese, E. Thomaz, and N. M. Streeper (2020) "Just-in-time adaptive intervention to promote fluid consumption in patients with kidney stones." *Health Psychology*, **39**(12), p. 1062.

[44] Forman, E. M., S. P. Goldstein, R. J. Crochiere, M. L. Butryn, A. S. Juarascio, F. Zhang, and G. D. Foster (2019) "Randomized controlled trial of OnTrack, a just-in-time adaptive intervention designed to enhance weight loss," *Translational behavioral medicine*, **9**(6), pp. 989–1001.

[45] Huh, J., K. J. Lee, W. Roldan, Y. Castro, S. Kshirsagar, P. Rastogi, I. Kim, K. A. Miller, M. Cockburn, and J. Yip (2021) "Making of Mobile SunSmart: Co-designing a Just-in-Time Sun Protection Intervention for Children and Parents," *International journal of behavioral medicine*, pp. 1–11.

[46] Goldstein, S. P., B. C. Evans, D. Flack, A. Juarascio, S. Manasse, F. Zhang, and E. M. Forman (2017) "Return of the JITAI: Applying a Just-in-Time Adaptive Intervention Framework to the Development of m-Health Solutions for Addictive Behaviors," *International Journal of Behavioral Medicine*, **24**(5), pp. 673–682.

[47] McClernon, F. J. and R. R. Choudhury (2013) "I am your smartphone, and i know you are about to smoke: The application of mobile sensing and computing approaches to smoking research and treatment," *Nicotine and Tobacco Research*, **15**(10), pp. 1651–1654.

[48] Ben-Zeev, D., C. J. Brenner, M. Begale, J. Duffecy, D. C. Mohr, and K. T. Mueser (2014) "Feasibility, acceptability, and preliminary efficacy of a smartphone intervention for schizophrenia," *Schizophrenia bulletin*, **40**(6), pp. 1244–1253.

[49] Kim, J., D. Marcusson-Clavertz, F. Togo, and H. Park (2018) "A Practical Guide to Analyzing Time-Varying Associations between Physical Activity and Affect Using Multilevel Modeling," *Computational and Mathematical Methods in Medicine*, **2018**.

[50] Schwartz, J. E. and A. A. Stone (1998) "Strategies for analyzing ecological momentary assessment data," *Health Psychology*, **17**(1), pp. 6–16.

[51] Snijders, T. A. and R. J. Bosker (2011) *Multilevel analysis: An introduction to basic and advanced multilevel modeling*, Sage.

[52] Grimm, K. J., N. Ram, and R. Estabrook (2016) *Growth modeling: Structural equation and multilevel modeling approaches*, Guilford Publications.

[53] Liu, S. (2017) "Person-specific versus multilevel autoregressive models: Accuracy in parameter estimates at the population and individual levels," *British Journal of Mathematical and Statistical Psychology*, **70**(3), pp. 480–498.

[54] Shiyko, M. P., S. T. Lanza, X. Tan, R. Li, and S. Shiffman (2012) "Using the Time-Varying Effect Model (TVEM) to Examine Dynamic Associations between Negative Affect and Self Confidence on Smoking Urges: Differences between Successful Quitters and Relapsers," *Prevention Science*, **13**(3), pp. 288–299.

[55] Lanza, S. T. and A. N. Linden-Carmichael (2021), "Time-Varying Effect Modeling for the Behavioral, Social, and Health Sciences," .

[56] Li, R., J. J. Dziak, X. Tan, L. Huang, A. T. Wagner, and J. Yang (2017) "TVEM (Time-Varying Effect Modeling) SAS Macro Users ' Guide (Version 3.1.1)," *University Park: The Methodology Center, Penn State. Retrieved from http:methodology.psu.edu*.

[57] Merrill, J. E., S. R. Kenney, and N. P. Barnett (2017) "A time-varying effect model of the dynamic association between alcohol use and consequences over the first two years of college," *Addictive Behaviors*, **73**(January), pp. 57–62.

[58] Koslovsky, M. D., E. T. Hébert, M. S. Businelle, M. Vannucci, et al. (2020) "A Bayesian time-varying effect model for behavioral mHealth data," *Annals of Applied Statistics*, **14**(4), pp. 1878–1902.

[59] Lanza, S. T. and S. A. Vasilenko (2015) "New methods shed light on age of onset as a risk factor for nicotine dependence," *Addictive Behaviors*, **50**, pp. 161–164.

[60] Lanza, S. T., S. A. Vasilenko, X. Liu, R. Li, and M. E. Piper (2014) "Advancing the understanding of craving during smoking cessation attempts: A demonstration of the time-varying effect model," *Nicotine and Tobacco Research*, **16**(SUPPL2), pp. 127–134.

[61] Flannery, K. M., A. Vannucci, and C. M. C. Ohannessian (2018) "Using Time-Varying Effect Modeling to Examine Age-Varying Gender Differences in Coping Throughout Adolescence and Emerging Adulthood," *Journal of Adolescent Health*, **62**(3), pp. S27–S34.

[62] Snippe, E., J. J. Dziak, S. T. Lanza, I. Nyklíček, and M. Wichers (2017) "The Shape of Change in Perceived Stress, Negative Affect, and Stress Sensitivity During Mindfulness-Based Stress Reduction," *Mindfulness*, **8**(3), pp. 728–736.

[63] Maher, J. P., E. Dzubur, J. Huh, S. Intille, and G. F. Dunton (2016) "Within-day time-varying associations between behavioral cognitions and physical activity in adults," *Journal of Sport and Exercise Psychology*, **38**(4), pp. 423–434.

[64] Maher, J. P. and G. F. Dunton (2020) "Within-day time-varying associations between motivation and movement-related behaviors in older adults," *Psychology of Sport and Exercise*, **47**, p. 101522.

[65] Dziak, J. J., R. Li, X. Tan, S. Shiffman, and M. P. Shiyko (2015) "Modeling intensive longitudinal data with mixtures of nonparametric trajectories and time-varying effects," *Psychological Methods*, **20**(4), pp. 444–469.

[66] Lanza, S. T., S. A. Vasilenko, and M. A. Russell (2016) "Time-varying effect modeling to address new questions in behavioral research: Examples in marijuana use." *Psychology of Addictive Behaviors*, **30**(8), pp. 939–954.

[67] Jacobson, N. C., S. M. Chow, and M. G. Newman (2019) "The Differential Time-Varying Effect Model (DTVEM): A tool for diagnosing and modeling time lags in intensive longitudinal data," *Behavior Research Methods*, **51**(1), pp. 295–315.

[68] Lu, Z. H., S. M. Chow, A. Sherwood, and H. Zhu (2015) "Bayesian analysis of ambulatory blood pressure dynamics with application to irregularly spaced sparse data," *Annals of Applied Statistics*, **9**(3), pp. 1601–1620.

[69] Chow, S. M., Z. Lu, A. Sherwood, and H. Zhu (2016) "Fitting Nonlinear Ordinary Differential Equation Models with Random Effects and Unknown Initial Conditions Using the Stochastic Approximation Expectation–Maximization (SAEM) Algorithm," *Psychometrika*, **81**(1), pp. 102–134.

[70] Chow, S.-M., J. R. Nesselroade, K. Shifren, and J. J. McArdle (2004) "Dynamic Structure of Emotions Among Individuals with Parkinson's Disease," *Structural Equation Modeling*, **11**(4), pp. 560–582.

[71] Houtveen, J. H. and P. C. Molenaar (2001) "Comparison between the Fourier and Wavelet methods of spectral analysis applied to stationary and nonstationary heart period data," *Psychophysiology*, **38**(5), pp. 729–735.

[72] Liao, P., K. Greenewald, P. Klasnja, and S. Murphy (2020) "Personalized heartsteps: A reinforcement learning algorithm for optimizing physical activity," *Proceedings of the ACM on Interactive, Mobile, Wearable and Ubiquitous Technologies*, **4**(1), pp. 1–22.

[73] Silvia, P. J., T. R. Kwapil, M. A. Walsh, and I. Myin-Germeys (2014) "Planned missing-data designs in experience-sampling research: Monte Carlo simulations of efficient designs for assessing within-person constructs," *Behavior Research Methods*, **46**(1), pp. 41–54.

[74] Agresti, A. (2003) *Categorical data analysis*, John Wiley & Sons.

[75] Collett, D. (2002) *Modelling binary data*, CRC press.

[76] Myung, I. J. (2003) "Tutorial on maximum likelihood estimation," *Journal of mathematical Psychology*, **47**(1), pp. 90–100.

[77] Christodoulou, E., J. Ma, G. S. Collins, E. W. Steyerberg, J. Y. Verbakel, and B. Van Calster (2019) "A systematic review shows no performance benefit of machine learning over logistic regression for clinical prediction models," *Journal of clinical epidemiology*, **110**, pp. 12–22.

[78] Gourieroux, C. and A. Monfort (1981) "Asymptotic properties of the maximum likelihood estimator in dichotomous logit models," *Journal of Econometrics*, **17**(1), pp. 83–97.

[79] Hauck, W. W. (1983) "A note on confidence bands for the logistic response curve," *The American Statistician*, **37**(2), pp. 158–160.

[80] Hinkley, D. V. and G. Runger (1984) "The analysis of transformed data," *Journal of the American Statistical Association*, **79**(386), pp. 302–309.

[81] Draper, D. (1995) "Assessment and propagation of model uncertainty," *Journal of the Royal Statistical Society: Series B (Methodological)*, **57**(1), pp. 45–70.

[82] Faraway, J. J. (1992) "On the cost of data analysis," *Journal of Computational and Graphical Statistics*, **1**(3), pp. 213–229.

[83] Cox, D. R. (1975) "A note on data-splitting for the evaluation of significance levels," *Biometrika*, **62**(2), pp. 441–444.

[84] Lee, J. D., D. L. Sun, Y. Sun, and J. E. Taylor (2016) "Exact post-selection inference, with application to the lasso," *The Annals of Statistics*, **44**(3), pp. 907–927.

[85] Faraway, J. J. (2016) "Does data splitting improve prediction?" *Statistics and computing*, **26**(1), pp. 49–60.

[86] Hojjatinia, S., E. R. Daly, T. Hnat, S. M. Hossain, S. Kumar, C. M. Lagoa, I. Nahum-Shani, S. A. Samiei, B. Spring, and D. E. Conroy (2021) "Dynamic Models of Stress-Smoking Responses Based on High-Frequency Sensor Data," *npj Digital Medicine*, pp. 1–11.

[87] Hojjatinia, S., E. R. Daly, T. Hnat, S. M. Hossain, S. Kumar, C. Lagoa, I. B. Nahum-Shani, S. A. Samiei, B. Spring, and D. E. Conroy (2022) "Dynamical system modeling to identify moments of vulnerability based on stress-smoking responses in daily smokers," in *Society of Behavioral Medicine's 43rd Annual Meeting & Scientific Sessions*, vol. 56, pp. S167–S167.

[88] Hojjatinia, S., A. M. Lee, C. Lagoa, D. Brunke-Reese, and D. Conroy (2022) "Using dynamic modeling to understand physical activity change after COVID-19 pandemic declaration in a messaging intervention," *Society of Behavioral Medicine's 43rd Annual Meeting & Scientific Sessions*, **56**(SUPP 1), pp. S667–S667.

[89] Hojjatinia, S., A. M. Lee, S. Hojjatinia, C. M. Lagoa, D. Brunke-Reese, and D. E. Conroy (2022) "Physical Activity Dynamics During a Digital Messaging Intervention Changed After the Pandemic Declaration," *Annals of behavioral medicine: a publication of the Society of Behavioral Medicine*.

[90] of Health, U. D. and H. Services (2018), "Physical Activity Guidelines for Americans," `https://health.gov/sites/default/files/2019-09/Physical_Activity_Guidelines_2nd_edition.pdf`.

[91] Troiano, R. P., D. Berrigan, K. W. Dodd, L. C. Masse, T. Tilert, and M. McDowell (2008) "Physical activity in the United States measured by accelerometer," *Medicine & Science in Sports & Exercise*, **40**(1), pp. 181–188.

[92] Ussery, E. N., J. D. Omura, K. McCain, and K. B. Watson (2021) "Change in Prevalence of Meeting the Aerobic Physical Activity Guideline Among US Adults, by States and Territories—Behavioral Risk Factor Surveillance System, 2011 and 2019," *Journal of Physical Activity and Health*, **18**(S1), pp. S84–S85.

[93] Smith, D. M., L. Duque, J. C. Huffman, B. C. Healy, and C. M. Celano (2020) "Text Message Interventions for Physical Activity: A Systematic Review and Meta-Analysis," *American Journal of Preventive Medicine*, **58**(1), pp. 142–151.

[94] Chevance, G., D. Baretta, M. Heino, O. Perski, M. Olthof, P. Klasnja, E. Hekler, and J. Godino (2021) "Characterizing and Predicting Person-Specific, Day-to-Day, Fluctuations in Walking Behavior," *PLoS ONE*, **16**(5), p. e0251659.

[95] Martin, K. R., A. Koster, R. A. Murphy, D. R. Van Domelen, M. Y. Hung, R. J. Brychta, K. Y. Chen, and T. B. Harris (2014) "Changes in Daily Activity Patterns with Age in U.S. Men and Women: National Health and Nutrition Examination Survey 2003-04 and 2005-06," *Journal of the American Geriatrics Society*, **62**(7), pp. 1263–1271.

[96] "Centers for Disease Control and Prevention National Center for Chronic Disease Prevention and Health Promotion, Smoking and Tobacco Use, Fast Facts," . URL `https://www.cdc.gov/tobacco/data_statistics/fact_sheets/fast_facts/`

[97] Hall, W. and C. Doran (2016) "How much can the USA reduce health care costs by reducing smoking?" *PLoS Medicine*, **13**(5), p. e1002021.

[98] Xu, X., E. Bishop, S. Kennedy, S. Simpson, and T. Pechacek (2015) "Annual healthcare spending attributable to cigarette smoking: an update," *American Journal of Preventive Medicine*, **48**(3), pp. 326–333.

[99] McEwen, A., R. West, and H. McRobbie (2008) "Motives for smoking and their correlates in clients attending Stop Smoking treatment services," *Nicotine and Tobacco Research*, **10**(5), pp. 843–850.

[100] Byrne, D. G., A. E. Byrne, and M. I. Reinhart (1995) "Personality, stress and the decision to commence cigarette smoking in adolescence," *Journal of Psychosomatic Research*, **39**(1), pp. 53–62.

[101] Torres, O. V. and L. E. O'Dell (2016) "Stress is a principal factor that promotes tobacco use in females," *Progress in Neuro-Psychopharmacology and Biological Psychiatry*, **65**, pp. 260–268.

[102] Pomerleau, O. F. and C. S. Pomerleau (1991) "Research on stress and smoking: progress and problems," *British Journal of Addiction*, **86**(5), pp. 599–603.

[103] Jahnel, T., S. G. Ferguson, S. Shiffman, and B. Schüz (2019) "Daily stress as link between disadvantage and smoking: an ecological momentary assessment study," *BMC Public Health*, **19**(1), pp. 1–8.

[104] Pesko, M. F. and C. F. Baum (2016) "The self-medication hypothesis: evidence from terrorism and cigarette accessibility," *Economics and Human Biology*, **22**, pp. 94–102.

[105] Center, P. R. (2019) "Mobile fact sheet," *Pew Research Center*.

[106] Monroe, C. M., D. L. Thompson, D. R. Bassett Jr, E. C. Fitzhugh, and H. A. Raynor (2015) "Usability of mobile phones in physical activity–related research: a systematic review," *American Journal of Health Education*, **46**(4), pp. 196–206.

[107] Wright, C. E., R. E. Rhodes, E. W. Ruggiero, and P. Sheeran (2021) "Benchmarking the effectiveness of interventions to promote physical activity: A metasynthesis." *Health Psychology*, **40**(11), p. 811.

[108] Williamson, C., G. Baker, N. Mutrie, A. Niven, and P. Kelly (2020) "Get the message? A scoping review of physical activity messaging," *International Journal of Behavioral Nutrition and Physical Activity*, **17**(1), pp. 1–15.

[109] Rhodes, R. E. and C. R. Nigg (2011) "Advancing physical activity theory: A review and future directions," *Exercise and sport sciences reviews*, **39**(3), pp. 113–119.

[110] Zhang, C.-Q., R. Zhang, R. Schwarzer, and M. S. Hagger (2019) "A meta-analysis of the health action process approach." *Health Psychology*, **38**(7), p. 623.

[111] Ajzen, I. (1991) "The theory of planned behavior," *Organizational behavior and human decision processes*, **50**(2), pp. 179–211.

[112] Williams, D. M. and D. R. Evans (2014) "Current emotion research in health behavior science," *Emotion Review*, **6**(3), pp. 277–287.

[113] Stevens, C. J., A. S. Baldwin, A. D. Bryan, M. Conner, R. E. Rhodes, and D. M. Williams (2020) "Affective determinants of physical activity: a conceptual framework and narrative review," *Frontiers in Psychology*, **11**, p. 3366.

[114] Sheeran, P., A. Maki, E. Montanaro, A. Avishai-Yitshak, A. Bryan, W. M. Klein, E. Miles, and A. J. Rothman (2016) "The impact of changing attitudes, norms, and self-efficacy on health-related intentions and behavior: A meta-analysis." *Health psychology*, **35**(11), p. 1178.

[115] Lawton, R., M. Conner, and R. McEachan (2009) "Desire or reason: predicting health behaviors from affective and cognitive attitudes." *Health Psychology*, **28**(1), p. 56.

[116] Conner, M., R. E. Rhodes, B. Morris, R. McEachan, and R. Lawton (2011) "Changing exercise through targeting affective or cognitive attitudes," *Psychology and Health*, **26**(2), pp. 133–149.

[117] Morris, B., R. Lawton, R. McEachan, R. Hurling, and M. Conner (2016) "Changing self-reported physical activity using different types of affectively and cognitively framed health messages, in a student population," *Psychology, health & medicine*, **21**(2), pp. 198–207.

[118] Sirriyeh, R., R. Lawton, and J. Ward (2010) "Physical activity and adolescents: an exploratory randomized controlled trial investigating the influence of affective and instrumental text messages," *British journal of health psychology*, **15**(4), pp. 825–840.

[119] Bassett, D. R., L. P. Toth, S. R. LaMunion, and S. E. Crouter (2017) "Step counting: a review of measurement considerations and health-related applications," *Sports Medicine*, **47**(7), pp. 1303–1315.

[120] Conroy, D. E., S. Elavsky, A. L. Hyde, and S. E. Doerksen (2011) "The dynamic nature of physical activity intentions: a within-person perspective on intention-behavior coupling," *Journal of Sport & Exercise Psychology*, **33**(6), p. 807.

[121] Conroy, D. E., S. Elavsky, S. E. Doerksen, and J. P. Maher (2013) "A Daily Process Analysis of Intentions and Physical Activity in College Students," *Journal of Sport and Exercise Psychology*, **35**(5), pp. 493–502.

[122] Dunton, G. F., A. A. Atienza, C. M. Castro, and A. C. King (2009) "Using ecological momentary assessment to examine antecedents and correlates of physical activity bouts in adults age 50+ years: a pilot study," *Annals of Behavioral Medicine*, **38**(3), pp. 249–255.

[123] Ashour, M., K. Bekiroglu, C.-H. Yang, C. Lagoa, D. Conroy, J. Smyth, and S. Lanza (2016) "On the mathematical modeling of the effect of treatment on human physical activity," in *2016 IEEE conference on control applications (CCA)*, IEEE, pp. 1084–1091.

[124] Troiano, R. P. (2007) "Large-Scale Applications of Accelerometers: New Frontiers and New Questions," *Medicine and Science in Sports and Exercise*, **39**(9), p. 1501.

[125] Freedson, P. S., E. Melanson, and J. Sirard (1998) "Calibration of the Computer Science and Applications, Inc. Accelerometer," *Medicine and Science in Sports and Exercise*, **30**(5), pp. 777–781.

[126] Feehan, L. M., J. Geldman, E. C. Sayre, C. Park, A. M. Ezzat, J. Young Yoo, C. B. Hamilton, and L. C. Li (2018) "Accuracy of Fitbit Devices: Systematic Review and Narrative Syntheses of Quantitative Data," *JMIR mHealth and uHealth*, **6**(8), p. e10527.

[127] Imboden, M. T., M. B. Nelson, L. A. Kaminsky, and A. H. Montoye (2018) "Comparison of Four Fitbit and Jawbone Activity Monitors with a Research-Grade ActiGraph Accelerometer for Estimating Physical Activity and Energy Expenditure," *British journal of sports medicine*, **52**(13), pp. 844–850.

[128] Van Rossum, G. and F. L. Drake (2009) *Python 3 Reference Manual*, CreateSpace, Scotts Valley, CA.

[129] Phatak, S. S., M. T. Freigoun, C. A. Martín, D. E. Rivera, E. V. Korinek, M. A. Adams, M. P. Buman, P. Klasnja, and E. B. Hekler (2018) "Modeling Individual Differences: A Case Study of the Application of System Identification for Personalizing a Physical Activity Intervention," *Journal of Biomedical Informatics*, **79**, pp. 82–97.

[130] Mischel, W. and Y. Shoda (1995) "A cognitive-affective system theory of personality: reconceptualizing situations, dispositions, dynamics, and invariance in personality structure." *Psychological review*, **102**(2), p. 246.

[131] Fredrickson, B. L. (2004) "The broaden-and-build theory of positive emotions," *Philosophical transactions of the royal society of London. Series B: Biological Sciences*, **359**(1449), pp. 1367–1377.

[132] Conroy, D. E., C. M. Lagoa, E. Hekler, and D. E. Rivera (2020) "Engineering Person-Specific Behavioral Interventions to Promote Physical Activity," *Exercise & Sport Sciences Reviews*, **48**(4), pp. 170–179.

[133] Bardakci, I. E., S. Hojjatinia, S. Hojjatinia, C. M. Lagoa, and D. E. Conroy (2021) "Model predictive control approach to adaptive messaging intervention for physical activity," *arXiv preprint arXiv:2108.11499*, 2108.11499.

[134] Report, . P. A. G. A. C. S. (2018) *2018 Physical Activity Guidelines Advisory Committee*, *Tech. rep.*

[135] Piercy, K. L., R. P. Troiano, R. M. Ballard, S. A. Carlson, J. E. Fulton, D. A. Galuska, S. M. George, and R. D. Olson (2018) "The Physical Activity Guidelines for Americans," *Jama*, **320**(19), pp. 2020–2028.

[136] Turrisi, T. B., K. M. Bittel, A. B. West, S. Hojjatinia, S. Hojjatinia, S. K. Mama, C. M. Lagoa, and D. E. Conroy (2021) "Seasons, Weather, and Device-Measured Movement Behaviors: A Scoping Review from 2006 to 2020," *International Journal of Behavioral Nutrition and Physical Activity*, **18**(1), pp. 1–26.

[137] Bauman, A. E., R. S. Reis, J. F. Sallis, J. C. Wells, R. J. Loos, and B. W. Martin (2012) "Correlates of Physical Activity: Why Are Some People Physically Active and Others Not?" *The Lancet*, **380**(9838), pp. 258–271.

[138] Turrisi, T. B., A. B. West, K. M. Bittel, S. K. Mama, S. Hojjatinia, S. Hojjatinia, C. Lagoa, and D. E. Conroy (2020) "Physical activity, seasonality, and weather: A scoping review of research with device-based measures of physical activity," in *Society of Behavioral Medicine's 41st Annual Meeting & Scientific Sessions*, vol. 54, pp. S640–S640.

[139] Tison, G. H., R. Avram, P. Kuhar, S. Abreau, G. M. Marcus, M. J. Pletcher, and J. E. Olgin (2020) "Worldwide Effect of COVID-19 on Physical Activity: A Descriptive Study," *Annals of internal medicine*, **173**(9), pp. 767–770.

[140] Pollard, M. S., J. S. Tucker, and H. D. Green (2020) "Changes in Adult Alcohol Use and Consequences During the COVID-19 Pandemic in the US," *JAMA network open*, **3**(9), p. e2022942.

[141] Horigian, V. E., R. D. Schmidt, and D. J. Feaster (2021) "Loneliness, Mental Health, and Substance Use among US Young Adults during COVID-19," *Journal of Psychoactive Drugs*, **53**(1), pp. 1–9.

[142] Rezaei, N. and M. A. Grandner (2021) "Changes in Sleep Duration, Timing, and Variability During the COVID-19 Pandemic: Large-Scale Fitbit Data from 6 Major US Cities," *Sleep Health*, **7**, pp. 303–313.

[143] Cardel, M. I., S. Manasse, R. A. Krukowski, K. Ross, R. Shakour, D. R. Miller, D. J. Lemas, and Y.-R. Hong (2020) "COVID-19 Impacts Mental Health Outcomes and Ability/Desire to Participate in Research Among Current Research Participants," *Obesity*, **28**(12), pp. 2272–2281.

[144] Ford, D. H. and R. M. Lerner (1992) *Developmental systems theory: An integrative approach*, Sage Publications, Inc.

[145] Pépin, J. L., R. M. Bruno, R. Y. Yang, V. Vercamer, P. Jouhaud, P. Escourrou, and P. Boutouyrie (2020) "Wearable Activity Trackers for Monitoring Adherence to Home Confinement During the COVID-19 Pandemic Worldwide: Data Aggregation and Analysis," *Journal of Medical Internet Research*, **22**(6), p. e19787.

[146] Lathi, B. P. and R. A. Green (2005) *Linear systems and signals*, New York: Oxford University Press.

[147] Flanagan, E. W., R. A. Beyl, S. N. Fearnbach, A. D. Altazan, C. K. Martin, and L. M. Redman (2021) "The Impact of COVID-19 Stay-At-Home Orders on Health Behaviors in Adults," *Obesity*, **29**(2), pp. 438–445.

[148] Dunton, G. F., S. D. Wang, B. Do, and J. Courtney (2020) "Early Effects of the COVID-19 Pandemic on Physical Activity Locations and Behaviors in Adults Living in the United States," *Preventive Medicine Reports*, **20**, p. 101241.

[149] McCarthy, H., H. W. Potts, and A. Fisher (2021) "Physical Activity Behavior Before, During, and After COVID-19 Restrictions: Longitudinal Smartphone-Tracking Study of Adults in the United Kingdom," *Journal of Medical Internet Research*, **23**(2), p. e23701.

[150] Barkley, J. E., A. Lepp, E. Glickman, G. Farnell, J. Beiting, R. Wiet, and B. Dowdell (2020) "The Acute Effects of the COVID-19 Pandemic on Physical Activity and Sedentary Behavior in University Students and Employees," *International journal of exercise science*, **13**(5), pp. 1326–1339.

[151] Roche, M. J., A. L. Pincus, A. L. Rebar, D. E. Conroy, and N. Ram (2014) "Enriching Psychological Assessment Using a Person-Specific Analysis of Interpersonal Processes in Daily Life," *Assessment*, **21**(5), pp. 515–528.

[152] Heckman, B. W., A. R. Mathew, and M. J. Carpenter (2015) "Treatment Burden and Treatment Fatigue as Barriers to Health," *Current Opinion in Psychology*, **5**, pp. 31–36.

[153] Stevens, B. L., F. L. Lewis, and E. N. Johnson (2015) *Aircraft Control and Simulation: Dynamics, Controls Design, and Autonomous Systems*, Wiley.

[154] Hojjatinia, S., M. A. Shoorehdeli, Z. Fatahi, Z. Hojjatinia, and A. Haghparast (2020) "Improving the izhikevich model based on rat basolateral amygdala and hippocampus neurons, and recognizing their possible firing patterns," *Basic and Clinical Neuroscience*, **11**(1), pp. 79–90.

[155] Jackson, T. and A. Radunskaya (2015) *Applications of dynamical systems in biology and medicine*, vol. 158, Springer.

[156] Hojjatinia, S. and C. M. Lagoa (2019) "Comparison of different spike sorting subtechniques based on rat brain basolateral amygdala neuronal activity," in *2019 IEEE International Conference on Bioinformatics and Biomedicine (BIBM)*, IEEE, pp. 2251–2258.

[157] Cox, S. W. (1997) *Measurement and control in agriculture.*, Blackwell Science Ltd.

[158] Weber, T. A. (2011) *Optimal Control Theory with Applications in Economics*, vol. 1 of *MIT Press Books*, The MIT Press.

[159] Molenaar, P. C. M., R. M. Lerner, and K. M. Newell (eds.) (2014) *Handbook of developmental systems theory and methodology*, Guilford Press, New York, NY.

[160] Gottman, J. M., J. D. Murray, C. C. Swanson, R. Tyson, and K. R. Swanson (2005) *The mathematics of marriage: Dynamic nonlinear models*, MIT Press.

[161] Lathi, B. P. (2009) *Linear Systems and Signals*, 2nd ed., Oxford University Press, Inc., USA.

[162] MATLAB (2018) *9.7.0.1190202 (R2019b)*, The MathWorks Inc., Natick, Massachusetts.

[163] Grant, M. and S. Boyd (2014), "CVX: Matlab Software for Disciplined Convex Programming, version 2.1," `http://cvxr.com/cvx`.

[164] Selye, H. (1956) *The stress of life*.

[165] Lazarus, R. S. and S. Folkman (1984) *Stress, appraisal and coping*.

[166] Benowitz, N. L. (2008) "Clinical pharmacology of nicotine: implications for understanding, preventing, and treating tobacco addiction," *Clinical Pharmacology and Therapeutics*, **83**(4), pp. 531–541.

[167] Kassel, J. D., L. R. Stroud, and C. A. Paronis (2003) "Smoking, stress, and negative affect: correlation, causation, and context across stages of smoking," *Psychological Bulletin*, **129**(2), pp. 270–304.

[168] Khantzian, E. J. (1997) "The self-medication hypothesis of substance use disorders: a reconsideration and recent applications," *Harvard Review of Psychiatry*, **4**(5), pp. 231–244.

[169] Aronson, K. R., D. M. Almeida, R. S. Stawski, L. C. Klein, and L. T. Kozlowski (2008) "Smoking is associated with worse mood on stressful days: results from a national diary study," *Annals of Behavioral Medicine*, **36**(3), pp. 259–269.

[170] Devaux, M. and F. Sassi (2016) "Social disparities in hazardous alcohol use: self-report bias may lead to incorrect estimates," *European Journal of Public Health*, **26**(1), pp. 129–134.

[171] Pesko, M. F. (2014) "Stress and smoking: associations with terrorism and causal impact," *Contemporary Economic Policy*, **32**(2), pp. 351–371.

[172] Weinstein, S. M., R. Mermelstein, S. Shiffman, and B. Flay (2008) "Mood variability and cigarette smoking escalation among adolescents," *Psychology of Addictive Behaviors*, **22**(4), pp. 504–513.

[173] Cameron, A., K. P. Reed, and A. Ninnemann (2013) "Reactivity to negative affect in smokers: the role of implicit associations and distress tolerance in smoking cessation," *Addictive Behaviors*, **38**, pp. 2905–2912.

[174] Hughes, J. R. (1992) "Tobacco withdrawal in self-quitters," *Journal of Consulting and Clinical Psychology*, **60**(5), pp. 689–697.

[175] McKee, S. A., R. Sinha, A. H. Weinberger, M. Sofuoglu, E. L. Harrison, M. Lavery, and J. Wanzer (2011) "Stress decreases the ability to resist smoking and potentiates smoking intensity and reward," *Journal of Psychopharmacology*, **25**(4), pp. 490–502.

[176] Shiffman, S. (2005) "Dynamic influences on smoking relapse process," *Journal of Personality*, **73**(6), pp. 1715–1748.

[177] Hughes, J. R. (2007) "Effects of abstinence from tobacco: valid symptoms and time course," *Nicotine & tobacco research*, **9**(3), pp. 315–327.

[178] Dunton, G. F., A. J. Rothman, A. M. Leventhal, and S. S. Intille (2021) "How intensive longitudinal data can stimulate advances in health behavior maintenance theories and interventions," *Translational Behavioral Medicine*, **11**(1), pp. 281–286.

[179] Timms, K. P., D. E. Rivera, L. M. Collins, and M. E. Piper (2013) "Control systems engineering for understanding and optimizing smoking cessation interventions," *2013 American Control Conference (Acc)*, pp. 1964–1969.

[180] Lagoa, C. M., K. Bekiroglu, S. T. Lanza, and S. A. Murphy (2014) "Designing adaptive intensive interventions using methods from engineering," *Journal of Consulting and Clinical Psychology*, **82**(5), pp. 868–878.

[181] Rawlings, J. B. (2000) "Tutorial overview of model predictive control," *IEEE Control Systems Magazine*, **20**(3), pp. 38–52.

[182] Bekiroglu, K., M. A. Russell, C. M. Lagoa, S. T. Lanza, and M. E. Piper (2017) "Evaluating the effect of smoking cessation treatment on a complex dynamical system," *Drug and Alcohol Dependence*, **180**, pp. 215–222.

[183] Hovsepian, K., M. Al'absi, E. Ertin, T. Kamarck, M. Nakajima, and S. Kumar (2015) "cStress: towards a gold standard for continuous stress assessment in the mobile environment," *UbiComp 2015 - Proceedings of the 2015 ACM International Joint Conference on Pervasive and Ubiquitous Computing*, pp. 493–504.

[184] Saleheen, N., A. A. Ali, S. M. Hossain, H. Sarker, S. Chatterjee, B. Marlin, E. Ertin, M. Al'Absi, and S. Kumar (2015) "puffMarker: a multi-sensor approach for pinpointing the timing of first lapse in smoking cessation," *UbiComp 2015 - Proceedings of the 2015 ACM International Joint Conference on Pervasive and Ubiquitous Computing*, pp. 999–1010.

[185] Nakajima, M., A. M. Lemieux, M. Fiecas, S. Chatterjee, H. Sarker, N. Saleheen, E. Ertin, S. Kumar, and M. Al'Absi (2020) "Using novel mobile sensors to assess stress and smoking lapse," *International Journal of Psychophysiology*, **158**, pp. 411–418.

[186] Ertin, E., A. Raij, N. Stohs, M. Al'Absi, S. Kumar, and S. Mitra (2011) "AutoSense: unobtrusively wearable sensor suite for inferring the onset, causality, and consequences of stress in the field," *SenSys 2011 - Proceedings of the 9th ACM Conference on Embedded Networked Sensor Systems*, pp. 274–287.

[187] Holtyn, A. F., E. Bosworth, L. A. Marsch, B. McLeman, A. Meier, E. C. Saunders, E. Ertin, M. A. Ullah, S. A. Samiei, M. Hossain, S. Kumar, K. L. Preston, M. Vahabzadeh, D. Shmueli-Blumberg, J. Collins, J. McCormack, and U. E. Ghitza (2019) "Towards detecting cocaine use using smartwatches in the NIDA clinical trials network: design, rationale, and methodology," *Contemporary Clinical Trials Communications*, **15**, p. 100392.

[188] Hossain, S. M., T. Hnat, N. Saleheen, N. J. Nasrin, J. Noor, B. J. Ho, T. Condie, M. Srivastava, and S. Kumar (2017) "mCerebrum: a mobile sensing software platform for development and validation of digital biomarkers and interventions," *SenSys 2017 - Proceedings of the 15th ACM Conference on Embedded Networked Sensor Systems*, pp. 1–14.

[189] Battalio, S. L., D. E. Conroy, W. Dempsey, P. Liao, M. Menictas, S. Murphy, I. Nahum-Shani, T. Qian, S. Kumar, and B. Spring (2021) "Sense2Stop: A micro-randomized trial using wearable sensors to optimize a just-in-time-adaptive stress management intervention for smoking relapse prevention," *Contemporary Clinical Trials*, **109**, p. 106534.

[190] Shiffman, S. and T. A. Wills (1985) *Coping and substance use*, Academic Press; New York.

[191] Weinstein, S. M. and R. J. Mermelstein (2013) "Dynamic associations of negative mood and smoking across the development of smoking in adolescence," *Journal of Clinical Child and Adolescent Psychology*, **42**(5), pp. 629–642.

[192] Tan, X., M. P. Shiyko, R. Li, Y. Li, and L. Dierker (2012) "A time-varying effect model for intensive longitudinal data," *Psychological Methods*, **17**(1), pp. 61–77.

[193] Amaral, J. L., A. J. Lopes, J. M. Jansen, A. C. Faria, and P. L. Melo (2013) "An improved method of early diagnosis of smoking-induced respiratory changes using machine learning algorithms," *Computer Methods and Programs in Biomedicine*, **112**(3), pp. 441–454.

[194] Senyurek, V. Y., M. H. Imtiaz, P. Belsare, S. Tiffany, and E. Sazonov (2020) "A CNN-LSTM neural network for recognition of puffing in smoking episodes using wearable sensors," *Biomedical Engineering Letters*, **10**(2), pp. 195–203.

[195] Wang, S., R. Zhang, Y. Deng, K. Chen, D. Xiao, P. Peng, and T. Jiang (2018) "Discrimination of smoking status by MRI based on deep learning method," *Quantitative Imaging in Medicine and Surgery*, **8**(11), pp. 1113–1120.

[196] Nahum-Shani, I., E. B. Hekler, and D. Spruijt-Metz (2015) "Building health behavior models to guide the development of just-in-time adaptive interventions: a pragmatic framework," *Health Psychology*, **34**, pp. 1209–1219.

[197] Spruijt-Metz, D., E. Hekler, N. Saranummi, S. Intille, I. Korhonen, W. Nilsen, D. E. Rivera, B. Spring, S. Michie, D. A. Asch, A. Sanna, V. T. Salcedo, R. Kukakfa, and M. Pavel (2015) "Building new computational models to support health behavior change and maintenance: new opportunities in behavioral research," *Translational Behavioral Medicine*, **5**(3), pp. 335–346.

[198] Dallery, J., R. N. Cassidy, and B. R. Raiff (2013) "Single-case experimental designs to evaluate novel technology-based health interventions," *Journal of Medical Internet Research*, **15**(2), p. e22.

[199] McDonald, S., F. Quinn, R. Vieira, N. O'Brien, M. White, D. W. Johnston, and F. F. Sniehotta (2017) "The state of the art and future opportunities for using longitudinal n-of-1 methods in health behaviour research: a systematic literature overview," *Health Psychology Review*, **11**(4), pp. 307–323.

[200] Dumortier, A., E. Beckjord, S. Shiffman, and E. Sejdić (2016) "Classifying smoking urges via machine learning," *Computer Methods and Programs in Biomedicine*, **137**, pp. 203–213.

[201] Ye, L. and E. Keogh (2009) "Time series shapelets: a new primitive for data mining," *Proceedings of the ACM SIGKDD International Conference on Knowledge Discovery and Data Mining*, pp. 947–955.

[202] Muirhead, R. J. (2009) *Aspects of multivariate statistical theory*, John Wiley & Sons.

Vita

Sahar Hojjatinia

Education

- The Pennsylvania State University, University Park, PA
  PhD, Electrical Engineering and Computer Science, 2017-2022
- Islamic Azad University, Science & Research Branch, Tehran, Iran
  MS, Electrical Engineering, 2013-2015
- Jondi Shapour University of Technology, Dezful, Iran
  BS, Electrical Engineering, 2008-2012

Work and Teaching Experience

- Teaching Assistant, Pennsylvania State University, University Park, PA, 2018.
- R&D, Internship, Niroo Research Institute, Tehran, Iran, 2016-2017

Research Experience

- Research Assistant, Robust Machine Intelligence and Control Lab, The Pennsylvania State University, Advisor: Professor Constantino M. Lagoa, 2017-2022.
- Research Assistant, Fault Detection and Identification Lab, K.N. Toosi University of Technology, Advisor: Dr. Mahdi Aliyari Shoorehdeli, 2014-2015.
- Research Assistant, Neuroscience Research Lab, Shahid Beheshti University of Medical Sciences, Advisor: Professor Abbas Haghparast, 2014-2015.